Chapter 7

The Eocene-Oligocene boundary climate transition: an Antarctic perspective

Simone Galeotti[1,12], Peter Bijl[2], Henk Brinkuis[2,11], Robert M. DeConto[3,12], Carlota Escutia[4], Fabio Florindo[5,12], Edward G.W. Gasson[6], Jane Francis[7], David Hutchinson[8], Alan Kennedy-Asser[9], Luca Lanci[1,12], Isabel Sauermilch[2,10], Appy Sluijs[2,12] and Paolo Stocchi[11,12]

[1]Department of Pure and Applied Sciences, University of Urbino Carlo Bo, Urbino, Italy, [2]Laboratory of Palaeobotany and Palynology, Department of Earth Sciences, Marine Palynology and Paleoceanography, Utrecht University, Utrecht, the Netherlands, [3]Department of Geosciences, University of Massachusetts, Amherst, Amherst, MA, United States, [4]Andalusian Institute of Earth Sciences, CSIC and Universidad de Granada, Armilla, Spain, [5]National Institute of Geophysics and Volcanology, Rome, Italy, [6]Centre for Geography and Environmental Science, University of Exeter, Cornwall Campus, Penryn, United Kingdom, [7]British Antarctic Survey, Cambridge, United Kingdom, [8]Department of Geological Sciences and Bolin Centre for Climate Research, Stockholm University, Stockholm, Sweden, [9]BRIDGE, School of Geographical Sciences, University of Bristol, Bristol, United Kingdom, [10]Institute for Marine and Antarctic Studies, University of Tasmania, Hobart, TAS, Australia, [11]Coastal Systems Department, Royal Netherlands Institute for Sea Research, Utrecht University, Den Burg, the Netherlands, [12]Institute for Climate Change Solutions, Frontone, Italy

7.1 Introduction

The Eocene-Oligocene transition (EOT), defined as a 500-kyr long phase of accelerated climatic and biotic change that began before and ended after the Eocene-Oligocene boundary (EOB) about 34 million years ago (Ma), marks a fundamental change in the climate of our planet from a warm, ice-free greenhouse state to an icehouse state (Westerhold et al., 2020). This climatic transition is associated with an ~1.5‰ increase in benthic foraminiferal oxygen isotopic ($\delta^{18}O$) values corresponding to the 'earliest Oligocene oxygen isotope shift' (EOIS) (Hutchinson et al., 2021). Mass-balance equations, deconvolving temperature and ice volume effects, demonstrate that the EOIS cannot be caused by either deep-sea temperature or ice volume change alone; both must have contributed (Bohaty et al., 2012; Coxall et al., 2005; Lear et al., 2008;

Antarctic Climate Evolution. DOI: https://doi.org/10.1016/B978-0-12-819109-5.00009-8

Shackleton and Kennett, 1975; Zachos et al., 1996). From various high-resolution isotope records, it was shown that the $\delta^{18}O$ shift associated with the Eocene-Oligocene transition (EOT) is a stepwise event, involving several inflections in the $\delta^{18}O$ records which each represents varying contributions of deep-sea temperature and ice volume change (e.g., Bohaty et al., 2012; Lear et al., 2008). These different phases in the EOT have been given different names by a number of authors. For the sake of consistency, we use the terminology of Hutchinson et al. (2021) as presented in Fig. 7.1.

High-resolution proxy records and coupled climate–ice sheet modelling suggest that the ultimate driver for initiating large-scale Antarctic glaciation came from radiative forcing: the Antarctic Ice Sheet (AIS) formed as the

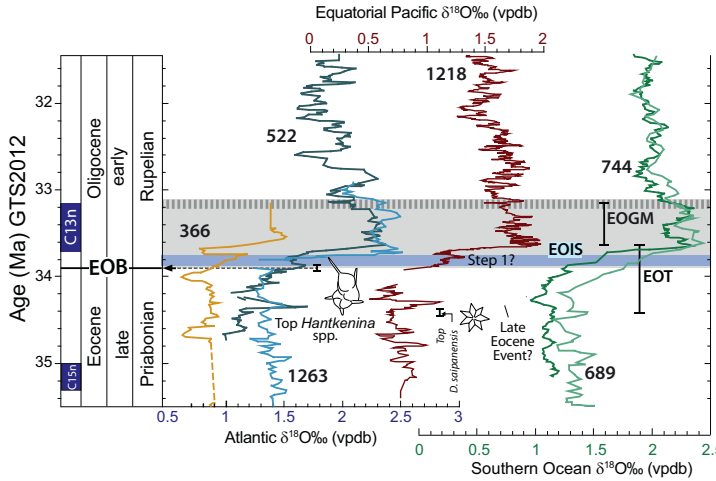

FIGURE 7.1 Oxygen stable isotope and chronostratigraphic characteristics of the Eocene-Oligocene transition (EOT) from deep marine records and EOT terminology on the Geological Time Scale 2012 (Vandenberghe et al., 2012) Benthic foraminiferal $\delta^{18}O$ from six deep sea drill holes are shown: Atlantic Sites DSDP 366, 145 522 and ODP 1263 (Langton et al., 2016; Zachos et al., 1996); Southern Ocean Sites ODP 744 and 689 (Diester-Haass and Zahn, 1996; Zachos et al., 1996) and the Equatorial Pacific Site ODP 1218 (Coxall and Wilson, 2011). Due to different sample resolutions, running means are applied using a 3-point filter for Sites DSDP 522 and ODP 689 and 1263, 5-point filter for Sites DSDP 366 and ODP 744 and a 7-point filter for Site ODP 1218. Time scale conversions were made by aligning common magneto-stratigraphic tie points. The EOT is defined as a 500-kyr long phase of accelerated climatic and biotic change that began before and ended after the Eocene-Oligocene boundary (EOB) (after Coxall and Pearson, 2007). Benthic data are 150 all *Cibicidoides* spp. or 'Cibs. Equivalent' and have not been adjusted to sea water equilibrium values. 'Step-1' comprises a modest $\delta^{18}O$ increase linked to ocean cooling (Bohaty et al., 2012; Lear et al., 2008). 'Step-2' corresponds to the Early Oligocene oxygen Isotope Step (EOIS), defined herein. The 'Top (T) *Hantkenina* spp.' marker corresponds to the position of this extinction event at DSDP Site 522 (including sampling bracket) with respect to the corresponding Site DSDP 522 $\delta^{18}O$ curve, which coincides with the published calibrated age of this event (33.9 Ma). The 'Late Eocene Event' $\delta^{18}O$ maximum (after Katz et al., 2008) may represent a failed glaciation. *From Hutchinson et al. (2021).*

system crossed a climatic threshold following a gradual decrease of atmospheric CO_2 levels under favourable orbital conditions for ice sheet expansion (DeConto and Pollard, 2003; DeConto et al., 2008; Pearson et al., 2009). However, many uncertainties remain. Ice sheet model simulations are sensitive to poorly-constrained boundary conditions, such as paleotopography, paleoceanographic conditions and indirect coupling to climate models, all of which affect the simulated timing, amplitude and volume of ice formation across the EOT (Paxman et al., 2019). Also, uncertainty exists as to the volume of ice already present prior to the EOT (Carter et al., 2017; Scher et al., 2014). Although the prevailing view is that tectonic opening of Southern Ocean gateways was not the direct cause of Antarctic glaciation (Huber et al., 2004), questions remain about what the impact of evolving oceanographic changes was on the inception of the ice sheet and its subsequent history (Houben, 2019; Sijp et al., 2011). Further questions remain about the response of regional climate and oceanography to the ice sheet's early growth (e.g., DeConto et al., 2007; Goldner et al., 2013). Reconstruction of the Cenozoic continental environmental history of Antarctica is, therefore, crucial to a thorough understanding of the role of high-latitude physical and biogeochemical processes in the global ocean and climate system and across the EOT. Precise stratigraphic correlation between the Antarctic continental margin and global marginal and open ocean records provides clues on the evolution of global climate. This global perspective is key to constraining the sensitivity of the AIS to changing global boundary conditions. Recently, major advancements have been made in reconstructing the paleogeographic, oceanographic and climatologic framework under which Antarctica became fully glaciated, as well as the response of regional climate, ocean and sea level to that glaciation.

This chapter reviews our current understanding of the greenhouse-icehouse transition from an Antarctic perspective. Before we present a summary of the evidence for the environmental evolution on the continent and marginal marine settings derived from land-based sections and drill-holes, we first lay out some crucial concepts necessary to interpret or reinterpret these observations. Although many of these concepts are not new, their importance has become appreciated in climate and ice sheet reconstructions across the EOT.

7.2 Background

7.2.1 Plate tectonic setting

Crucial boundary conditions for EOT glaciation relate to the plate tectonic setting, as it determines the solar energy on, and oceanographic conditions around, Antarctica. We distinguish here two important aspects: the relative and the absolute position of Antarctica and surrounding tectonic plates.

1. Relative plate position: This involves plate motions relative to one another (the plate circuit) and is reconstructed through stripping back ocean crust based on its age, and restoring intraplate and plate-boundary kinematics. Complex but critical areas involve the relative plate motions between the East Antarctic, West Antarctic and Antarctic Peninsula plates, which may have influenced the paleotopography of Antarctica at the EOT. Relative plate motions within Antarctica are poorly constrained, but Dalziel (2006) suggests that the West Antarctic Rift System (from the Ross Sea to the Ferrigno Rift) may have continued until the Miocene, with a total displacement of ~200 km. The opening of the Drake Passage/Scotia Sea and the Australian-Antarctic separation have implications for the paleoceanographic setting around Antarctica, the presence of circum-Antarctic ocean circulation and heat transport. Of these, the opening of the Tasman Gateway is stratigraphically more tightly correlated with the EOT. Slow seafloor spreading between Antarctica and Australia started in the Late Cretaceous (~94 Ma along the western part; Cande and Mutter, 1982), the breakup of the final continental connection (between the South Tasman Rise and Terre Adelie) occurred no earlier than 33.5 ± 1.5 Ma (ref; e.g., Cande and Stock, 2004; Williams et al., 2019), quasi-synchronous with the EOT and concomitant to strong subsidence of continental margins in the Tasman region (Stickley et al., 2004). The shallowly open gateway allows initial westward countercurrent flow from 50 Ma onwards (Bijl et al., 2013), but with continuous gateway deepening, intensified atmospheric circulation (Houben, 2019) and northward tectonic drift into the strong westerlies wind system. The eastward flowing proto-Antarctic circumpolar current (ACC) establishes slightly after the EOT, around 30 Ma (Scher et al., 2015). In addition to the direct effect of gateway opening on the Antarctic climate, an indirect role has also been proposed through the ocean circulation reorganisation causing atmospheric CO_2 drawdown (Scher et al., 2015). The plate tectonic reconstruction of Drake Passage is extremely complex due to the abundance of sub-continents, various rift basins and complex absolute motions (e.g., Pérez et al., 2019). The timing of deepening of the tectonically complex Drake Passage is strongly debated, with proposed opening ranging from 49 Ma (Eagles et al., 2006; Livermore et al., 2007) to ~17 Ma (Barker, 2001). Particularly, the motions of continental blocks within the Drake Passage are believed to restrict the gateway from being deeply open (Barker, 2001; Pérez et al., 2019) and uplift processes may have closed the DP region again around 21 Ma, after its initial opening (Lagabrielle et al., 2009). Recent palaeogeography reconstructions characterise the Drake Passage as narrow and shallow in both the late Eocene and early Oligocene, with minimal widening or deepening in a ~5–10 Ma window around the EOT (e.g., Scotese and Wright, 2018). Therefore, even if opening Drake Passage has a long-term cooling effect

on Antarctic climate, there is no clear evidence that a significant opening occurred at the EOT.

2. Absolute plate position: The absolute position of continents involves the position of the spin axis of the Earth on the plate circuit. This changes through time as a result of true polar wander. It determines the absolute latitudinal coordinates, and thereby determines the amount of incoming sunlight and height of the snow line on Antarctica. The south polar position of Antarctica makes it extremely sensitive to changes in true polar wander. It makes true polar wander changes act as an antagonist: a change in true polar wander yields opposing latitude changes on either side of a longitudinal line. This becomes important when one compares paleoclimate reconstructions from East and West Antarctica. It is also important for the absolute position of Southern Ocean gateways. With their paleolatitude around 60°S, these gateways are at the boundary of prevailing easterly winds in the South and westerly winds in the North. A gateway position change of a couple of degrees relative to the spin axis of the Earth thus may have consequences for its throughflow. Conventional paleogeographic grids (e.g., for modelling studies) use (moving) hotspot reference frames (see discussion in Baatsen et al., 2016), that do not account for true polar wander. Using a paleomagnetic reference frame to determine the absolute position of the place circuit relative to the spin axis of the Earth does take true polar wander into account. This changes the paleo-position of Antarctica by ~2° towards the Pacific side in the Eocene (van Hinsbergen et al., 2015), when true polar wander was particularly strong. While in hotspot reference frames, Wilkes Land and Seymour Island appear at ~equal paleolatitudes in the Eocene, in paleomagnetic reference frames their latitudinal difference is up to 4°. Although absolute paleolatitude reconstructions using paleomagnetic reference frames come with error margins, they illustrate the importance of accurate absolute plate positions and motions for paleoclimate reconstructions.

7.2.2 Antarctic paleotopography

The Antarctic topography on which the ice sheet formed at the EOT was different from the modern-day topography. The onset of Antarctic glaciation and subsequent ice flow caused extensive glacial weathering and sediment transport towards the continental margin. Thermal subsidence, tectonic processes and isostatic loading also altered the landscape, and each needs to be considered when reconstructing the past Antarctic topography. Earlier reconstructions of Antarctic paleotopography (Wilson and Luyendyk, 2009) resulted in vast areas of west Antarctica being restored to above sea level. Subsequent reconstructions by Wilson et al. (2012) restored sediment packages back onto the whole continent, which resulted in higher paleotopographies and a vastly larger landmass than earlier reconstructions and than today. Ice sheet model simulations using this reconstruction suggested that

the continent could have supported the growth of ice sheet with a volume 1.4 times larger at the EOT than when using a modern-day topography (Wilson et al., 2013). The growth of an ice sheet of this size would have caused an increase in benthic $\delta^{18}O$ of up to 1‰ (Wilson et al., 2013).

Continued improvements to the reconstruction technique, and more data constraining the modern-day Antarctic topography, have led to a new suite of reconstructions of the past Antarctic topography for the Oligocene-Miocene transition, mid-Miocene and mid-Pliocene, in addition to the EOT (Paxman et al., 2018, 2019). All this work has shown that the evolution of the Antarctic landscape since the EOT, and the erosion of deep subglacial basins, has continually increased the sensitivity of the ice sheet to ocean warming (Colleoni et al., 2018; Gasson and Keisling, 2020; Paxman et al., 2021).

7.2.3 Paleoceanographic setting

The Tasmanian Gateway was deeply open by the EOT (Cande and Stock, 2004; Stickley et al., 2004), and the Drake Passage allowed throughflow from the Pacific into the Atlantic (Scher and Martin, 2008). Although this must have initiated the onset of circumpolar flow, both numerical modelling (Hill et al., 2013) and field data (e.g., Bijl et al., 2018; Salabarnada et al., 2018) suggest that this proto-ACC was far from present-day flow strengths. How the proto-ACC oceanographic setting influenced poleward ocean heat transport remains under debate (Baatsen et al., 2020; Huber and Nof, 2006). Instead of a strong ACC, and particularly with restricted or closed gateways in the Eocene, Southern Ocean circulation featured strong, clockwise circulating gyres: one in the Pacific Ocean and another in the Atlantic-Indian ocean (Huber et al., 2004; Sloan and Rea, 1995). Arguably the onset of a Proto-ACC influenced this gyral circulation (Houben, 2019), but to what extent is as yet unknown.

7.2.4 Global average and regional sea level response

Over the past few years, the paleoclimate community has started to appreciate the complexity of sea level reconstructions from a geodynamic perspective. Previously, a conceptual model of glacio-eustatic sea level change was applied (e.g., Miller et al., 2008), which assumes that extraction of water from ocean basins and its storage in continental ice sheets causes a globally quasi-uniform sea level change. Connections with the geodynamic community since $\sim$2010 led to significant reinterpretation, however. Geodynamic principles prescribe that any relocation of mass (in the case of the EOT relocation of water from the ocean basins onto the Antarctic continent) creates a redistribution of both gravitational forces and loading of the lithosphere. The first induces a displacement of the leftover, deformable ocean water, towards the more rigid ice mass. The overall relative sea level (RSL) pattern, as a result of ice formation, is

consistent with the typical wave-like deformation that is induced by glacial- and hydro-isostatic adjustment (hereafter GIA). GIA consists of the response of solid Earth and gravity potential to redistributions in surface mass (from ocean water to continental ice). GIA can be modelled by solving the so-called sea level equation (SLE, Farrell and Clark, 1976; Spada and Stocchi, 2007). The SLE is a linear integral equation that yields the regionally varying RSL change for a prescribed ice sheet thickness chronology and solid Earth rheological model (the latter prescribes the deformation of the lithosphere). The area that deforms and subsides as a result of ice sheet growth is not limited to the ice-covered area, but extends further outside the glaciated area, thanks to the flexure of the underlying lithosphere. Lithospheric deformation can be rheologically described as purely elastic, thus providing an instantaneous response to any incremental surface loading. The areal extent and depth of the subsidence directly depends on the thickness of the lithosphere. Underneath the deformed lithosphere, the viscous upper mantle starts to flow, causing a further subsidence that is delayed by the viscosity. The upper mantle material flows outwards and upwards, forming the so-called uplifting peripheral forebulge that surrounds the ice sheet. As the ice sheet grows thicker and extends further offshore across the inner shelf, the forebulge is pushed outward. As a result, the offshore areas that were initially shoaling as upper mantle material upwelled, and a peripheral forebulge developed, now subside rapidly in response to the lithospheric flexure extending outwards from the ice-sheet margins. Both act to restore equilibrium. As a result, the magnitude and even the sign of sea level change as a result of ice sheet installation might be different per place on Earth. These geodynamical principles have most profound effects for sea level reconstructions close to the locus of ice sheet formation. Further away from the ice sheet sea level change will approach the eustatic value. We will further discuss the implications of these concepts below.

7.2.5 Proxies to reconstruct past Antarctic climatic and environmental evolution

Over the past years, proxies to reconstruct past climatic, oceanographic and environmental conditions around Antarctica have become more quantitative.

The most reliable atmospheric CO_2 reconstructions for the EOT interval are based on stable carbon isotopic composition of organic phytoplankton biomarkers (e.g., Pagani et al., 2005; Zhang et al., 2013) and boron isotopes in calcium carbonate microfossils (Anagnostou et al., 2020; Pearson et al., 2009). Absolute, quantitative proxies for sea surface temperature (SST) come from organic biomarkers (TEX_{86} and $U^{K'}_{37}$) (Douglas et al., 2014; Liu et al., 2009) and clumped isotopes on bivalves and planktonic foraminifera (Judd et al., 2019; Petersen and Schrag, 2015).

Mean annual air temperature (MAT) reconstructions come from a suite of proxies, based on vegetation (pollen or leaf assemblages) nearest living

relative approaches (e.g., Francis et al., 2009), soil-derived organic biomarkers (MBT) (Pross et al., 2012) and the chemical index of alteration measured on detrital material (e.g., Passchier et al., 2013, 2017). The last of these is specifically a quantitative proxy for air temperature at the site of chemical weathering. The vegetation composition, as well as plant-derived organic biomarkers (n-alkanes) and weathering indices provide mostly qualitative information on hydrological conditions on the continent.

Qualitative reconstructions come from calcareous nannofossil, dinoflagellate cyst and diatom assemblages (Houben et al., 2013; Villa et al., 2013).

Independent reconstructions of deep-sea temperature come from Mg/Ca ratios in benthic foraminifera (e.g., Bohaty et al., 2012). These are then used to deconvolve temperature and ice volume effects on $\delta^{18}O$ for ice volume reconstructions. This exercise requires assumptions on the isotopic composition of the ice sheet.

Qualitative evidence for marine-terminating glaciers come from the presence of iceberg-rafted debris (IRD) in marine sediments (e.g., Ehrmann and Mackensen, 1992; Zachos et al., 1992).

All of these proxies come with underlying assumptions, uncertainties, error margins and quantified confidence intervals. The relationship between the measured parameter in the proxy carrier and the environmental parameter of interest is sometimes poorly understood mechanistically. These proxies are still very much in development while being applied to reconstruct past Antarctic climate and environmental conditions.

7.2.6 Far-field proxies

In marine geochemical records, the primary evidence for climate change leading to the establishment of the AIS is a relatively rapid ($\sim$200 kyr) $\sim$1.5‰ increase in $\delta^{18}O$ values of deep-sea benthic foraminifera (Coxall et al., 2005; Diester-Haass and Zahn, 1996, 2001; Miller et al., 1987; Zachos et al., 1992, 1996). This EOIS captured by marine carbonates has been well documented from deep-sea cores (Kennett and Shackleton, 1976; Savin, 1977; Savin et al., 1975; Shackleton and Kennett, 1975) as well as outcrop sections (e.g., Devereux, 1967). The isotope shift was initially attributed to 4°C–6°C of marine cooling. Later studies confirmed the occurrence of the climate shift and interpreted it to partly reflect the emplacement of a minor-to-moderate (e.g., Keigwin, 1980; Keigwin and Corliss, 1986; Miller and Curry, 1982; Murphy and Kennett, 1986; Shackleton et al., 1984) or major (Matthews and Poore, 1980; Poore and Matthews, 1984; Prentice and Matthews, 1988) ice volume in the earliest Oligocene. The discovery of Oligocene proximal glaciomarine sediments from the Ross Sea and Prydz Bay (Hambrey and Barrett, 1993; Hambrey et al., 1991) and IRD associated with the oxygen isotope shift at Ocean Drilling Programme (ODP) Site 748 near Antarctica confirmed this interpretation (Zachos et al., 1994).

The acquisition of high-resolution records has later shown that the EOIS and the preceding cooling trend were not monotonic. A detailed record from the equatorial Pacific ODP Site 1218 revealed that the EOIS is actually made of two steps separated by ~200 kyr (Coxall et al., 2005). The first step, 'Step 1' of Pearson et al. (2008) or EOT-1 of Coxall and Wilson (2011), which occurs between 34.2 and 33.8 Ma, is not readily identified at all sites. The use of independent temperature proxies such as Mg/Ca and TEX_{86} has improved estimates of ice volume from oxygen isotope records. The first step, starting at ca. 34.2 Ma, is thought to primarily reflect a temperature decrease while the second, which unravels between 33.7 and 33.6 Ma, has been interpreted as the onset of a prolonged interval of maximum ice extent often referred to as the Earliest Oligocene Glacial Maximum (EOGM) between 33.6 and 33.2 Ma (Bohaty et al., 2012; Katz et al., 2008; Lear et al., 2008). Other oxygen isotope maxima in the late Eocene have been interpreted to reflect ephemeral precursor glaciations during the late Eocene (Houben et al., 2012; Katz et al., 2008; Scher et al., 2011, 2014). Among these, the oldest and most prominent one is reported to have occurred at 37.3 Ma (Scher et al., 2014). Another event of hypothesised transient glaciation occurred at about 34.15 Ma (Katz et al., 2008). As recently reviewed by Hutchinson et al. (2021), inter-site correlation for some of these features in the oxygen isotope record is not straightforward and the usage of certain terms has changed through time, which make it difficult to settle a consistent terminology for all of them.

However, benthic foraminiferal $\delta^{18}O$ values are influenced by both deep-sea temperature and the volume of continental ice, and the exact magnitude of deep-sea temperature decrease across the EOT is far from clear. Progress in paleotemperature proxies, including Mg/Ca, clumped isotopes and TEX_{86}, have led to independent means of quantifying changes in bottom and surface waters across the EOT (Bohaty et al., 2012; Evans et al., 2016; Lear et al., 2008; Liu et al., 2009).

These records suggest that deep-water temperature cooled by 3°C–5°C across the EOT (Liu et al., 2009). Global average sea-surface temperature dropped by approximately 2.9°C although with large inter-site differences (Hutchinson et al., 2021). The associated estimated volume of Antarctic ice depends upon the assumed isotopic composition of the ice sheet but was likely between 70% and 110% of the size of the modern-day AIS (Bohaty et al., 2012; Lear et al., 2008). Accordingly, a ca. 70 m sea-level fall is estimated from low-latitude shallow marine sequences (Katz et al., 2008; Miller et al., 2008).

7.3 Antarctic Sedimentary Archives

7.3.1 Land-based outcrops

Documenting the evolution of continental environmental conditions across the EOT is crucial to our understanding of the transition from greenhouse to

icehouse. Extensive ice cover and erosion hinders access to land-based sedimentary archives, which are confined to locations along the continental margin. Sedimentary successions outcropping on the continental margin are known from the Antarctic Peninsula and King George Island (Fig. 7.2). Information is also obtained from glacial erratics, known as the McMurdo erratics, from the Ross Sea margin. Although not capturing the EOT, these sedimentary archives record the longer-term evolution of climate leading up to and following this transition. A summary of important outcrops and the environmental signal obtained from them is presented below.

7.3.1.1 *Antarctic Peninsula Region*

Eocene sediments comprising the La Meseta Formation (Elliot and Trautman, 1982) are exposed on Seymour Island, Antarctica (~64°S, 54°W), located approximately 100 km east of the Antarctic Peninsula (Fig. 7.2). Based on magnetostratigraphic studies (Beamud et al., 2015) and Sr isotopes (Ivany et al., 2008), the La Meseta Formation was attributed an age of ~56.2 to ~58.8 Ma. However, dinoflagellate cyst biostratigraphy (Amenábar et al., 2020; Douglas et al., 2014) correlated to the zonation described in Bijl et al. (2013) provides a younger age (Lutetian-Priabonian; ~45 to ~34 Ma) for these strata, which we follow here.

The La Meseta Formation has been originally subdivided into seven informal mapping units 'Tertiary Eocene La Meseta' (Telms 1 to 7) (Sadler, 1988) and later refined into six erosional-based units, or allomembers (Marenssi et al., 1998). The formation consists of mudstones and sandstones with interbedded conglomerates with horizons characterised by an accumulation of molluscs, which were deposited in deltaic, estuarine and shallow

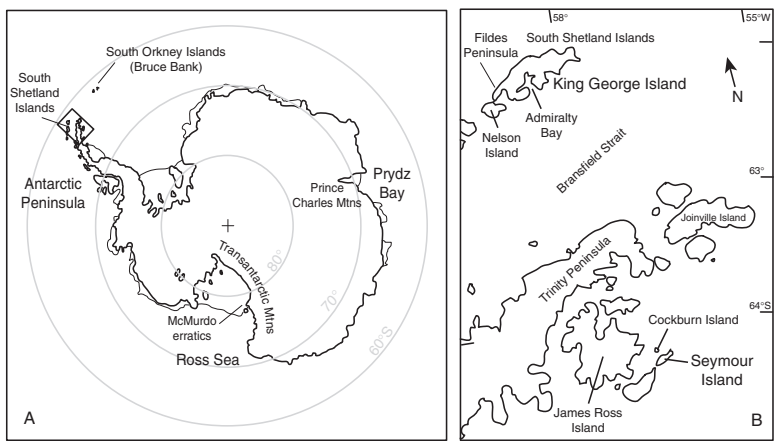

FIGURE 7.2 Map of the Antarctic continent (A) and the Antarctic Peninsula (B) showing some of the locations mentioned in the text. *From Francis et al., 2009.*

marine environments as part of a tectonically-controlled incised valley system (Marenssi et al., 1998; Porebski, 1995). Provenance studies on sandstones of the La Meseta Formation demonstrate that the source rock was located west-northwest along the present-day Antarctic Peninsula. The formation provides high diversity and abundance of fossil remains (Marenssi, 2006), including the only land mammal fossil findings of the entire continent of Antarctica (Davis et al., 2020; Gelfo et al., 2019; Reguero et al., 2002) along with marine vertebrates (including giant penguins) and invertebrates, fossil wood, fossil leaves and a rare flower (Acosta Hospitaleche, 2014; Acosta Hospitaleche and Reguero, 2014; Davis et al., 2020; Francis et al., 2004; Gandolfo et al., 1998a,b,c; Jadwiszczak and Mörs, 2019; Stilwell and Zinsmeister, 1992; Tambussi et al., 2006). While detailed correlation of the Eocene open ocean paleoclimate record with that of the Seymour Island continental margin sequence has always proved problematic, sedimentological, palaeontological and geochemical proxy records from the latter provide significant insights into the Antarctic environmental and climate evolution of this area across the middle to latest Eocene.

The Ypresian *Cucullaea* shell bed of La Meseta Formation (Telm 4 of Sadler, 1988; ~42 Ma) contains a remarkably diverse assemblage of plants, invertebrates and vertebrates that have provided a valuable record of both continental and marginal settings, which indicate an environment completely different to the present-day Antarctica (Reguero et al., 2012). Seasonally-resolved proxy data derived from bivalves estimate winter SSTs near 9°C and summer SSTs around 17°C, indicating that the Antarctic Peninsula was far too warm to support significant ice accumulation, at least at low elevation (Telm 5 ~41–38 Ma; Judd et al., 2019). Isotope-derived mean-annual temperature (MAT) is in good agreement with previous estimates from clumped isotopes (12.6°C; Douglas et al., 2014) TEX_{86} (15.4°C; Douglas et al., 2014) and bulk oxygen isotope analyses of Telm 5 carbonates (~10°C–14.5°C; Dutton et al., 2002; Ivany et al., 2008, and references therein). A stepwise increase in the oxygen isotopic composition ($\delta^{18}O$) of bivalve shells from Telm 6 (~38–36 Ma) suggests ~10°C of cooling (Ivany et al., 2008). Much of the recorded increase of oxygen isotope values took place across a short interval centred at ~37 Ma (Douglas et al., 2014). TEX_{86} and clumped isotope data from Douglas et al. (2014) do not show such an abrupt temperature decrease although they indicate a generally warmer temperature from Telms 2, 3 and 4 (45–41 Ma) compared to Telms 5, 6 and 7 (41–34 Ma). Yet, the occurrence of ice-rafted debris has been reported from the upper part of the La Meseta Formation (Telm 6 or 7) (Doktor et al., 1988) and paleoclimatic evidence of a severe climatic deterioration towards the end of the Eocene. It is possible that by the end of the Eocene, limited ice, perhaps as valley glaciers, was already present in the area. The presence of local glaciers and ice caps at the northern Antarctic Peninsula during the

middle Eocene-early Oligocene (49–32 Ma) was also argued by Anderson et al. (2011). Accordingly, high diversity Neogastropoda populations indicative of warm conditions in the lower Telms terminate abruptly in the upper La Meseta Formation with an extinction event that most likely heralds the onset of global cooling (Crame et al., 2014). Other signals of cooling are provided by a swift decrease of the Chemical Alteration Index (CIA) values and a concomitant inception of illite-dominated clay mineral associations at the top of the La Meseta Formation, suggestive of a transition to cold, frost-prone and relatively dry conditions during the late Eocene.

Further evidence for a climatic deterioration on Seymour Island during the late Eocene comes from floral records. Leaves and wood of both angiosperm and conifer affinity occur with fern fossils and a flower (Case, 1988; Francis et al., 2004; Reguero et al., 2002). *Nothofagus* leaves were found to be notophyllous (a leaf-size category 7.5–12.5 cm long). Angiosperm fossils affiliated to families including Nothofagaceae, Dilleniaceae, Myricaceae, Myrtaceae, Elaeocarpaceae, Moraceae, Cunoniaceae, Winteraceae and Lauraceae have been described (Francis et al., 2004; Gandolfo et al., 1998a,b; Reguero et al., 2002). Doktor et al. (1996) also described leaves affiliated with Podocarpaceae, Araucariaceae, Nothofagaceae and Proteaceae. Gothan (1908) was the first to describe fossil wood from Seymour Island, which has subsequently been reexamined by several authors and identified as having both angiosperm and coniferous affinities (Brea, 1996, 1998; Francis, 1991; Francis and Poole, 2002; Reguero et al., 2002; Torres et al., 1994).

A decrease in leaf sizes in the upper Telms suggests that the climate deteriorated towards the end of the Eocene, as observed in studies of the La Meseta Formation by Case (1988) and Reguero et al. (2002). Gandolfo et al. (1998a,b) suggested a temperate MAT of 11°C–13°C for the Cucullaea I Allomember during the early late Eocene. Further climate data were provided by leaf margin analyses of a late Palaeocene flora (Cross Valley Formation) and of the early late Eocene Cucullaea 1 flora, which indicate a decrease in floral diversity and a change from MATs of 14°C during the late Palaeocene to 11°C during the early late Eocene, with signs of freezing winters in the late Eocene (Francis et al., 2004). The shift from cool temperate, humid Valdivian-type forest to a more depauperate vegetation was accompanied by a decrease in typical Eocene dinoflagellate cysts, an increase in sea ice–indicative marine phytoplankton, and an increase in reworked palynomorphs, suggesting the onset of periglacial conditions and a subpolar climate just before the EOT boundary in the back-arc James Ross Basin (Warny et al., 2018).

All in all, the persistence of vegetation and geochemical evidence suggest that if some ice developed during the latest Eocene its distribution was limited to elevated areas.

7.3.1.2 King George (25 de Mayo) Island, South Shetland Islands

King George Island and neighbouring Nelson Island consist of several tectonic blocks bounded by two systems of strike-slip faults of Paleogene-early Neogene (54–21 Ma) age (Birkenmajer, 1989). Thus, considerable differences in stratigraphic succession, age and character of the rocks occur between particular blocks. The stratigraphic sequence includes mainly Late Cretaceous to early Miocene island-arc extrusive and intrusive rocks comprising mainly terrestrial lavas, pyroclastic and volcaniclastic sediments often with terrestrial plant fossils. Fossiliferous marine and glaciomarine sediments are also represented, and provide clues to paleoenvironmental conditions during the early-middle Oligocene.

Several sequences of tillites crop out within these complicated sequences, representing glacial and interglacial events. Initial reports of supposed Eocene-age tillites at Magda Nunatak (Birkenmajer, 1980a,b), named the Krakow Glaciation and dated at 49 Ma, have been disproved by Sr dating (Dingle and Lavelle, 1998). Tillites on King George Island have been reported from the Point Thomas Formation in Admiralty Bay, which would provide evidence for the presence of alpine glaciers during the middle Eocene (Birkenmajer et al., 2005). However, age control is poor and the potential extent of glaciers and their drainage pattern on the eastern side of the peninsula is unconstrained.

The earliest clear evidence for glacial activity from the King George Island are diamictites and ice-rafted deposits from the Krakowiak Glacial Member of the Polonez Cove Formation, which are dated to a mid-Oligocene age (30–26 Ma) (Troedson and Smellie, 2002). At its maximum extent, ice was grounded on a shallow marine shelf. Interestingly, exotic clasts within this sequence may represent ice-rafted debris that was derived from as far away as the Transantarctic Mountains, suggesting marine-based glaciation in the Weddell Sea region. As reported by Warny et al. (2018), however, unpublished strontium isotope results point to older geological ages (early Oligocene, ca. 32–30 Ma) for parts of the glacio-marine deposits of the Krakowiak Glacier Member. The only other terrestrial evidence for Oligocene ice, possibly representing local alpine glaciation, is from Mount Petras in Marie Byrd Land, West Antarctica, where deposits indicate volcanic eruptions beneath ice (Wilch and McIntosh, 2000).

Many macrofloras have been discovered on King George Island in the South Shetland Island group, north of the Bransfield Strait in the Antarctic Peninsula region, currently dated between late Palaeocene and late Eocene. The floras may have lived at a paleolatitude of ~67°S (Van Hinsbergen et al., 2015). The stratigraphy is complex: Birkenmajer (1981, 1989, 1990) and Birkenmajer et al. (1986) erected many local formations, but a simpler scheme was created by Smellie et al. (1984). No single stratigraphic scheme

exists and so the stratigraphic context of the floras remains unclear. The stratigraphic framework used here includes both schemes (also reviewed by Hunt, 2001).

Leaf macrofloras, currently understood to be of late Palaeocene to middle Eocene age, have been described in varying completeness from the Admiralty Bay and Fildes Peninsula areas of the island. In the Admiralty Bay area, the Mt. Wawel Formation (Point Hennequin Group), attributed to the middle Eocene based on U-Pb and ^{40}Ar-^{39}Ar analyses (Nawrocki et al., 2011), contains the macroflora deposits collectively known as the Point Hennequin Flora with individual localities named Mount Wawel and Dragon Glacier Moraine floras (Askin, 1992; Birkenmajer and Zastawniak, 1989a; Hunt, 2001; Hunt and Poole, 2003; Zastawniak et al., 1985). The Mount Wawel flora comprises macrofossils of *Equisetum* (horsetail), ferns and several *Nothofagus* species as microphyllous leaves (a leaf-size category of 2.5–7.5 cm long), in addition to a few other angiosperms and Podocarpaceae. The Dragon Glacier Moraine flora is similar; the angiosperm leaves being dominated by *Nothofagus* and the conifers including Araucariaceae and Cupressaceae, in addition to Podocarpaceae. The middle Eocene Petrified Forest Creek flora from the Arctowski Cove Formation and the late Eocene *Cytadela* flora from the Point Thomas Formation are both within the Ezcurra Inlet Group. The middle Eocene Petrified Forest Creek flora is a wood flora requiring revision, but intermediate *Fagus–Nothofagus*-type species are recorded. The *Cytadela* leaf flora includes ferns (including a *Blechnum*-affinity species), mostly small *Nothofagus*-type leaves with pinnately veined leaves of other dicotyledonous types and possible Podocarpaceae (Askin, 1992; Birkenmajer, 1997; Birkenmajer and Zastawniak, 1989a). Birkenmajer and Zastawniak (1989a) considered this flora of an age close to the E/O transition.

In this region, therefore, *Nothofagus*-dominated forests were the norm in the middle to late Eocene with ferns and tree ferns becoming increasingly important. Estimated MATs of 5°C–8°C are slightly cooler than those on Seymour Island to the east during the middle Eocene, and the vegetation was similar to the southernmost Patagonian–Magellanic forests of southern Chile (Askin, 1992; Birkenmajer and Zastawniak, 1989a; Hunt, 2001; Zastawniak et al., 1985). By the late Eocene, vegetation was more comparable to the recent fern-bush communities of southern oceanic islands (e.g., the Auckland Islands), interpreted from the *Cytadela* and Petrified Forest Creek floras (Askin, 1992; Birkenmajer, 1997; Birkenmajer and Zastawniak, 1989a). However, this observation entails MAT estimates of 11.7°C–15°C, which appear too high especially considering the small size of the leaves (Francis, 1999).

In the Fildes Peninsula area in the southwest of King George Island, the Fildes Peninsula Group contains the contemporary middle Eocene Collins Glacier and Rocky Cove floras within the Fildes Formation, and

the diverse late Palaeocene–middle Eocene Fossil Hill flora (Fossil Hill Formation). The latter is a leaf flora containing 40 recognised taxa, including mixed broadleaf angiosperms (with large-leaved *Nothofagus* species), conifers (podocarp, araucarian and cupressacean) and ferns (Birkenmajer and Zastawniak, 1989a,b; Francis, 1999; Haomin, 1994; Li, 1992; Reguero et al., 2002). Neotropical and sub-Antarctic elements appear to be mixed perhaps indicating a collection derived from communities at different altitudes (Li, 1992), although this mixed signature may be a feature of Paleogene polar biomes (Francis et al., 2004). The *Nothofagus* leaves are much larger than their modern relatives, suggesting warm and humid climate conditions during the early part of the Eocene. Estimates of MAT suggest >10°C (from 40% entire-margined leaves) and a small annual temperature range (Li, 1992).

Fossil leaves remain undescribed from the Rocky Cove flora; however, wood from this locality has been identified as *Nothofagoxylon antarcticus* (Hunt, 2001; Shen, 1994). The Collins Glacier deposit is primarily a wood flora that includes wood of both coniferous (*Cupressinoxylon* sp. and *Podocarpoxylon fildesense*) and angiospermous (*Nothofagoxylon* spp., *Weinmannioxylon eucryphioides* (Cunoniaceae) and *Myceugenelloxylon antarcticus* (Myrtaceae) affinity (Hunt, 2001; Poole et al., 2001, 2005). Changes in the vegetation suggest that MAT had dropped to ~9°C by the middle Eocene, which compares well with an estimate of ca. 8°C derived from leaf analysis of the same flora. This temperature drop was accompanied by a concomitant increase in precipitation. However, the absence of a change from a semiring to ring porous condition in angiosperm wood indicates that seasonality had not greatly intensified (Poole et al., 2005).

7.3.1.3 The Ross Sea Region

Several hundred glacial erratic boulders and cobbles recovered from coastal moraines around the shores of Mount Discovery, Brown Peninsula and Minna Bluff provide a window on Eocene environmental conditions in the Ross Region. This ensemble, collectively known as the McMurdo Erratics, is most likely derived from sub-glacial basins, such as Discovery Deep, that lie along the coast of the Transantarctic Mountains or basement highs situated to the east of the discovery accommodation zone (Wilson, 1999; Wilson et al., 2006). The erratics were distributed into their distinctive pattern of terminal and lateral retreat moraines during relatively recent advance and retreat of grounded ice into southern McMurdo Sound (Wilson, 2000). Subsequent basal adfreezing and surface ablation has transported the erratics to the surface of the McMurdo Ice Shelf. Although currently out of their original stratigraphic position, this suite of erratics provides a means to obtain geologic data that are otherwise buried beneath the AIS and fringing ice shelves.

The McMurdo Erratics comprise a range of lithotypes and ages. Eocene rocks contain a rich suite of fossil flora and fauna including marine and terrestrial palynomorphs, diatoms, ebridians, marine vertebrates and invertebrates, terrestrial plant remains and a bird humerus. Biostratigraphic data from dinoflagellate cyst (dinocyst), ebridian and mollusc assemblages recovered from many of the erratics indicate that the majority of fossiliferous rocks range from middle to late Eocene, 43–34 Ma. Erratics collected between 1993 and 1996 (Stilwell and Feldmann, 2000) include several hundred samples of Oligocene, Miocene and Pliocene sediment. Although relatively rich dinoflagellate cyst (dinocyst) assemblages have been described from Oligocene-Miocene Sequences from the Cape Roberts Cores, assemblages in post-Eocene erratics comprise few taxa (typically of five species), which may be because of the proximal paleo-depositional setting of the sediments that the erratics represent.

The majority of the Eocene erratics record a suite of lithofacies that were deposited in coastal–terrestrial to inner shelf marine environments (Levy and Harwood, 2000a,b). These sediments were probably deposited within fan deltas that formed along the rugged coastline of the rapidly rising Transantarctic Mountains. Abundant macroinvertebrate faunas, including bivalves, gastropods, scaphopods, cirripeds, bryzoans, decapods and brachiopods, indicate that many of these sediments were deposited in a spectrum of predominantly shallow marine environments. The presence of terrestrial plant material and palynomorphs also suggests that the majority of the rocks were formed in nearshore environments. However, the occurrence of outer shelf dinocyst species and the absence of benthic diatom taxa in many of the fine-grained lithofacies indicate that outer shelf environments were also present in the source region. The Eocene erratics contain no direct or unequivocal sedimentological evidence for the presence of ice close to the basins in which the sediments were originally deposited. It is notable that erratics composed of diamictites recovered from the coastal moraines are all Oligocene and younger in age.

Although rare, fossil leaves, wood and pollen recovered from several erratics provide a glimpse of the Eocene climate for the region. One erratic contains wood and leaves from *Araucaria* and *Nothofagus* trees, which suggests cool temperate conditions with some winter snow, but temperatures were probably not cold enough to allow extensive ice at sea level (Francis, 2000; Pole et al., 2000). Spore and pollen assemblages recovered from the erratics reflect *Nothofagus*-podocarpaceous conifer-Proteaceae vegetation with other angiosperms growing in temperate climate conditions (Askin, 2000). Oligocene and younger erratics show a major drop in species richness, which is also noted in sequences recovered in CIROS-1 and the Cape Roberts Project (CRP) cores (Mildenhall, 1989; Raine and Askin, 2001).

Fossil invertebrate remains recovered from the erratics include a humerus shaft from a pseudodontorn (giant bony-toothed sea bird) (Jones, 2000), a

probable crocodile tooth (Willis and Stilwell, 2000) and teeth from two species of shark (Long and Stilwell, 2000). The small but significant record of East Antarctic invertebrate fauna indicates a temperate to cool-temperate marine environment.

The n-alkane distributions from the Eocene McMurdo erratics are different from those from the Oligocene and Miocene, specifically in the prominence of the n-C29 as opposed to the n-C27 (Duncan et al., 2019). According to these authors, this observation can be explained by a combination of climate cooling as the AIS developed, and a shift in plant community towards low diversity tundra: *Nothofagus*, podocarpidites and bryophytes (Askin, 2000; Askin and Raine, 2000; Lewis et al., 2008; Prebble et al., 2006).

7.3.2 Sedimentary archives from drilling on the Antarctic Margin

Over the last decades, much effort has been put into the search for continuous sedimentary records of the EOT through drilling on the Antarctic margin. Yet, there are very few ice sheet−proximal records through this interval mainly because marine sedimentary successions on the Antarctic margin are exposed to glacial erosion, similarly to land-based successions and because the age models developed for high latitude settings might be difficult to correlate to lower latitude chronologies.

7.3.2.1 Drill cores in the western Ross Sea

Two drill holes have recovered sediment sequences that approach or span the E/O boundary with exceptionally high recovery in the western Ross Sea area: the CIROS-1 and CRP-3 drillholes (Fig. 7.3). In the 702-m-deep CIROS-1 hole (Barrett, 1989; Barrett et al., 1991), the lower part of the core was originally regarded as late Eocene, with a breccia passing up into mudstone and sandstone. The boundary with the Oligocene was originally placed at about 570 m (Barrett et al., 1989), but magnetobiostratigraphic data (Wilson et al., 1998) suggest that the EOB is much higher, at about 410−420 m. In either case, there is no obvious lithological transition, and finer grained facies include alternations of weakly stratified sand and mud, with intraformational conglomerate and occasional diamictite. Moving up core, a major hiatus exists at 366 m, which coincides with the early/late Oligocene boundary (around 28.1 Ma).

The CIROS-1 core was originally interpreted in terms of depositional setting, ice proximity and water depth (Barrett, 1996; Hambrey and Barrett, 1993; Hambrey et al., 1989). The breccia at the base of the hole is interpreted as a fault-brecciated conglomerate. The overlying sandstone/mudstone/diamictite succession is marine, influenced to varying degrees by resedimentation and iceberg-rafting. Above the major hiatus at 366 m, the

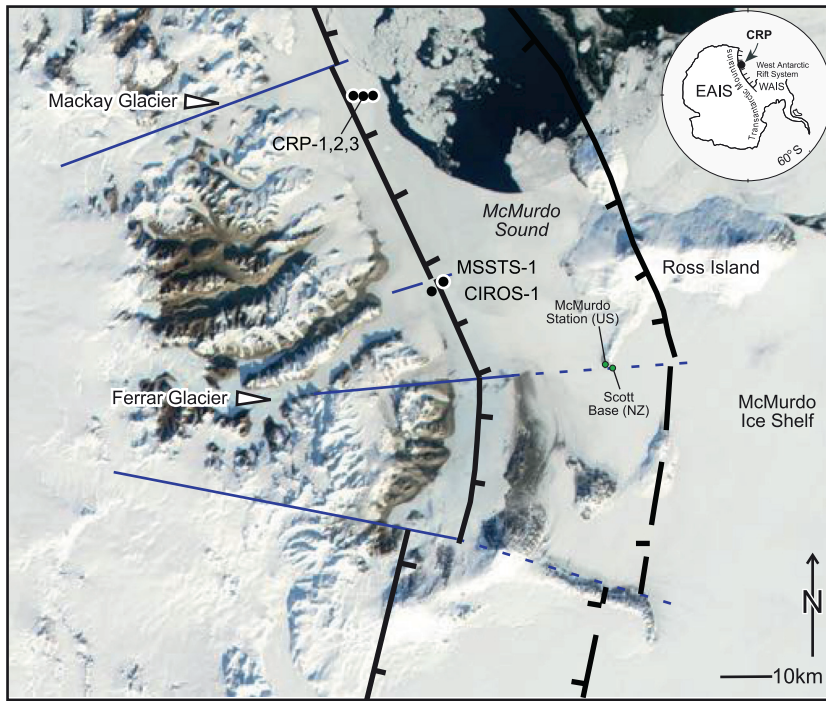

FIGURE 7.3 Satellite image with the location of the CRP, MSSTS-1 and CIROS-1 drill sites in the Southern McMurdo Sound. Key geographical and geological features of the area, including the boundary faults of the southern extension of Terror Rift, are shown. *From Galeotti et al. (2016).*

sandstones were regarded as fluvial, and the diamictites as basal glacial deposits, indicating ice overriding the site. However, Fielding et al. (1997) argued, based on a sequence stratigraphic analysis, that the late Oligocene diamictite was also glaciomarine. In contrast, Hiemstra (1999) reverted in part to the original view of grounded ice on the basis of microstructural studies. Whichever solution is the correct one, there is no clear evidence for a major environmental shift at the EOB, but there is evidence for more ice-proximal conditions at the early/late Oligocene transition.

A record of climate change through the EOT has also been determined from the environmental magnetic record in the CIROS-1 core (Sagnotti et al., 1998). Variations in magnetite were related to the concentration of detrital material transported into the Victoria Land Basin, influenced by climate and weathering rates on the Antarctic continent (especially of the Ferrar Group). Sagnotti et al. (1998) determined, from changes in the abundance of magnetite, that although there were some cold dry intervals (35–36 Ma) alternating with warm humid climates during the late Eocene, a stable cold dry climate was not established in Antarctica until the EOB, with major ice-sheet growth occurring at the early/late Oligocene boundary. This

pattern matches the clay mineral history, which shows a shift from smectite-rich to smectite-poor assemblages in Antarctica at the EOB (Ehrmann, 1997; Ehrmann and Mackensen, 1992). A single *Nothofagus* leaf was found in the CIROS-1 core, originally thought to be Oligocene in age (Hill, 1989), but after recent refinement of the age model, it is now considered early Miocene (Roberts et al., 2003). Terrestrial temperature estimates for the CIROS-1 core suggest the temperature in the late Eocene was ca. 9°C (Passchier et al., 2013), broadly in agreement with fossil wood from a McMurdo glacial erratic that puts the maximum seasonal temperature at 13°C (Francis, 2000).

The second core that contains the EOT is the Cape Roberts Project Core CRP-3. Drilling at CRP-3, ~12 km east of Cape Roberts provided an almost continuous core through 823 m of Cenozoic sedimentary strata on the western edge of the Victoria Land Basin (VLB), at the Western margin of the Ross Sea continental shelf (CRP Science Team, 2000). At 823 m below the sea floor (mbsf), the basement of the VLB was penetrated and a further 133 m of basement rocks was recovered and correlated with the Devonian-age, Arena Sandstone of the Beacon Supergroup.

The CRP-3 succession contains an array of lithofacies comprising fine-grained mudrocks, interlaminated and interbedded mudrocks/sandstones, mud-rich and mud-poor sandstones, conglomerates and diamictites that are together interpreted as the products of shallow marine to possibly non-marine environments of deposition, affected by the periodic advance and retreat of a land-terminating and tidewater glacier (Fielding et al., 2001; Powell et al., 2001).

The uppermost 330 mbsf shows a cyclical arrangement of lithofacies and is interpreted to reflect cyclical variations in relative sea level (>20 m) in concert with variations in the proximity of a marine-terminating glacier, ultimately regulated by fluctuations in the volume of the AIS (Naish et al., 2001). A conceptual depositional model for the late Oligocene-Miocene interval was developed by Powell et al. (2000), based on facies associations and comparison with modern glaciomarine environments, such as those in Alaska and Greenland. This shows that during an advance and still-stand, a grounding-line fan develops, and this is followed by rapid recession until another fan develops. The sequence becomes even more complex when the glacier overrides previously formed fans. Fig. 7.4 is a simplified version of this model.

Between 330 and 780 mbsf, cyclical units generally characterised by fining-upward successions from conglomerate above a sharp boundary passing into sandstone facies were interpreted as fluvial to shallow-marine deltaic depositional sequences recording cyclical variations of relative sea level (<20 m) in concert with a more 'indirect' record of the proximity of an advancing and retreating land-terminating ice margin (Fielding et al., 2001). The early Oligocene landscape was characterised by temperate glaciers

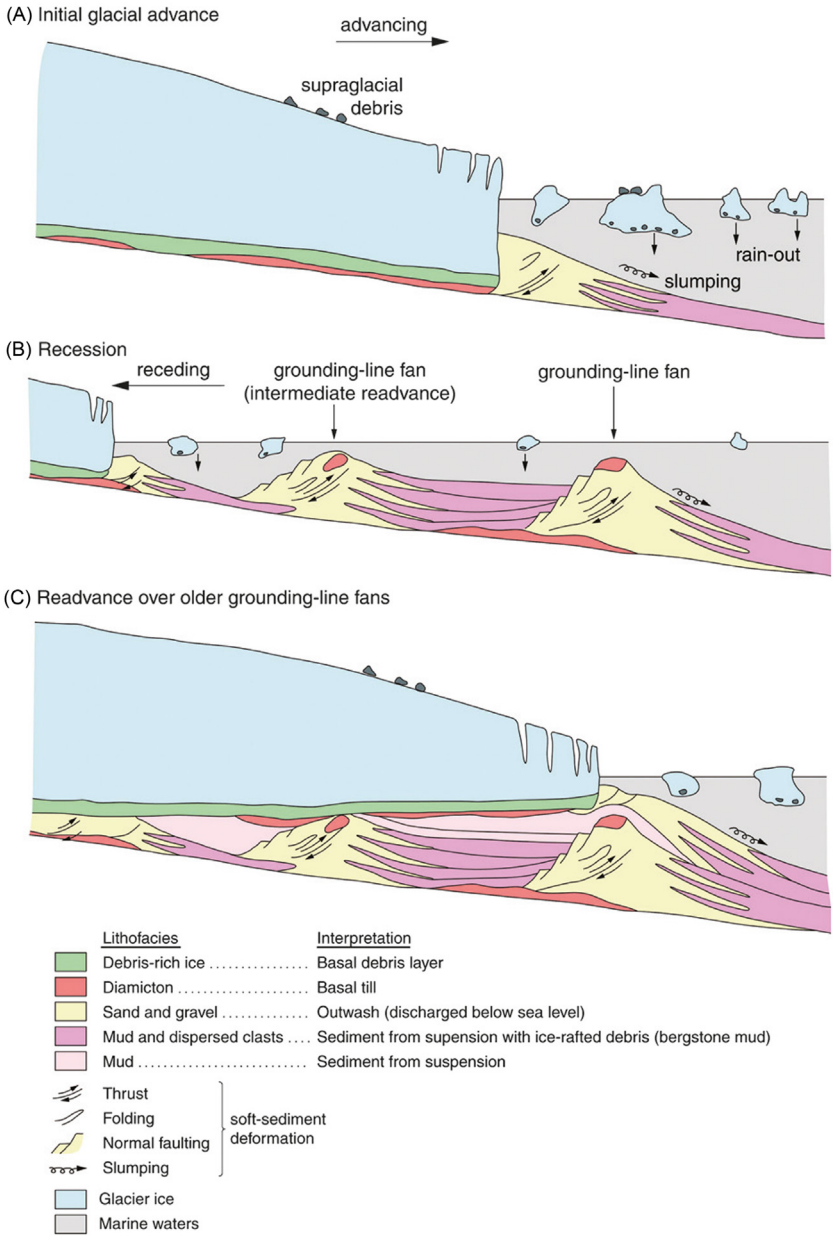

FIGURE 7.4 Grounding-line fan model of glaciomarine sedimentation for late Oligocene/early Miocene time. *From Hambrey et al. (2002); Simplified from Powell et al. (2000). Reproduced with permission of The Geological Society Publishing House, Bath, UK.*

flowing from the early East Antarctic Ice Sheet (EAIS), some terminating in the sea, and others on braided outwash plains (Fig. 7.5).

A total of thirty-seven sedimentary cycles occur below 300 mbsf and are associated with <20 m oscillations in relative sea level (Galeotti et al., 2012; Naish et al., 2001). At about 300 mbsf, the first diamictites occur recording the development of a more expansive marine-terminating ice sheet on the western Ross Sea continental shelf for the first time. Above this level, eleven glaciomarine sedimentary cycles associated with larger sea-level fluctuations of >20 m are bounded by glacial surfaces of erosion, which implies the loss of part of the sedimentary record (Fielding et al., 2001). Water depth changes across these cycles represent oscillations between innermost shelf ($\sim$5 m) and the offshore low-energy shelf below wave base (up to $\sim$50 m) (Dunbar et al., 2008). Accommodation space for the preservation of such a remarkably complete sedimentary record was provided by high rates of tectonic subsidence during the initial stages of rift extension beginning in the latest Eocene (Fielding et al., 2008; Henrys et al., 2007).

Based on spectral analysis of the clast abundance in the lower part of the CRP-3 drillhole and using the available magnetostratigraphic correlation (Florindo et al., 2005), Galeotti et al. (2012) showed that the facies fluctuations in the lower part of CRP-3 reflect astronomically forced cycles of

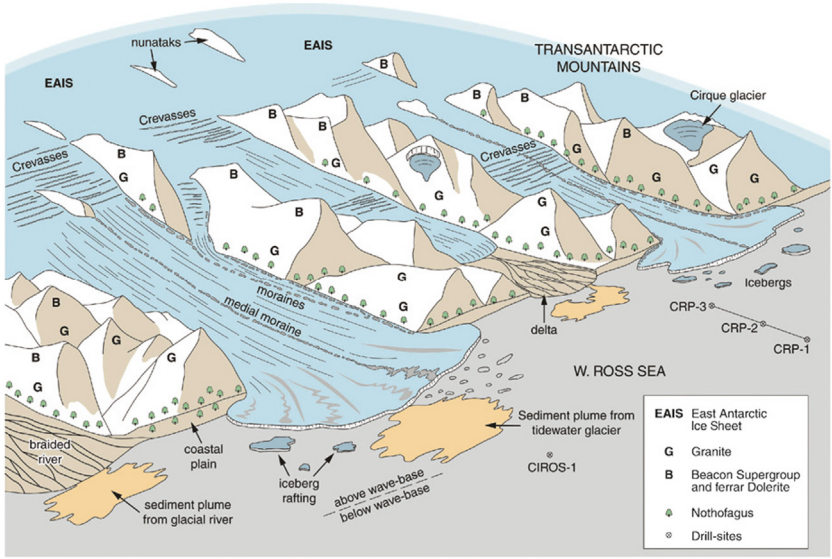

FIGURE 7.5 Cartoon depicting the Victoria Land coast in early/late Oligocene time, with glacier- and river-influenced coast, and vegetated mountainsides and lowlands. This scenario is based on a combination of sedimentological evidence and floral data from CIROS-1 and Cape Roberts cores. *From Hambrey et al. (2002). Reproduced with permission of The Geological Society Publishing House, Bath, UK.*

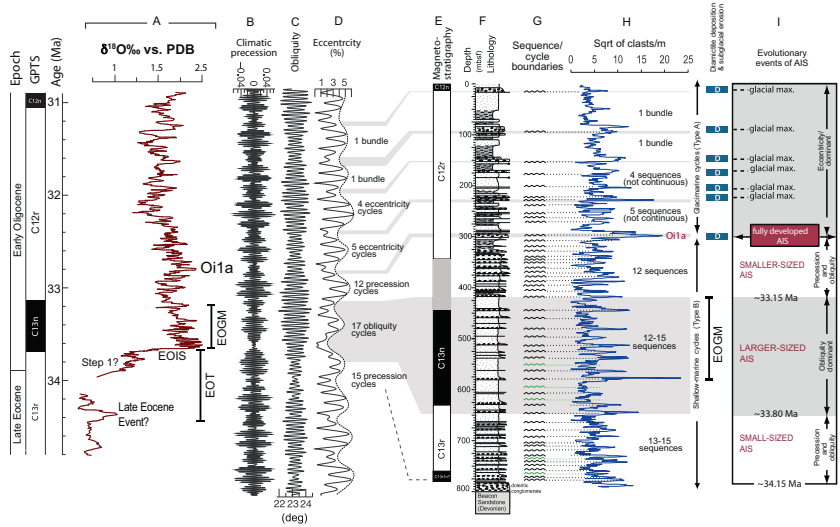

FIGURE 7.6 (A) Deep-sea oxygen isotopic record from ODP Site 1218 (Coxall and Wilson, 2011; Coxall et al., 2005), and time series for (B) climatic precession, (C) obliquity and (D) eccentricity correlated with the (E, F, and G) magnetostratigraphy, lithostratigraphy and sequence stratigraphy (Fielding et al., 2001; Florindo et al., 2005), and (H) square root of clast abundance (Sandroni and Talarico, 2001) for the late Eocene–early Oligocene CRP-3 drill core. (G) Thirty-seven shallow-marine sedimentary cycles (sequences; Type B) occur in the lower 500 m of the core record, controlled by advances and retreats of land-terminating glaciers associated with <20 m sea-level oscillations. Eleven overlying glaciomarine sedimentary cycles (sequences; Type A), each bounded by glacial surfaces of erosion, occur in the upper 300 m of the CRP-3 core, and record oscillations in the extent of a more expansive marine-terminating ice sheet in Ross Embayment. (I) Inferred stages and events in the development of the AIS across the E-O boundary and the relationship to orbital forcing are summarised. *From Galeotti et al. (2016), modified.*

glacial advancement and retreat. The resulting astrochronology provides an independently-derived age model for CRP-3, which enabled a precise definition of the E/O boundary and the first one-to-one correlation of direct physical evidence of astronomically-controlled glaciation from the Antarctic margin to the highly-resolved, orbitally tuned $\delta^{18}O$ record of paleoclimate changes across the E/O boundary climate from the deep sea (Coxall and Wilson, 2011; Coxall et al., 2005) (Fig. 7.6).

Extension of the astrochronological interpretation to the upper part of the drillhole (Galeotti et al., 2016) further constrained the age of the first marine calving ice at 32.8 Ma, coinciding with the Oi1a glacial episode of Miller et al. (1991) (Fig. 7.6).

7.3.2.2 *The Prydz Bay Region*

Drilling in Prydz Bay was undertaken by two ODP legs (Fig. 7.7). In contrast to the western Ross Sea cores, core-recovery rates here were much

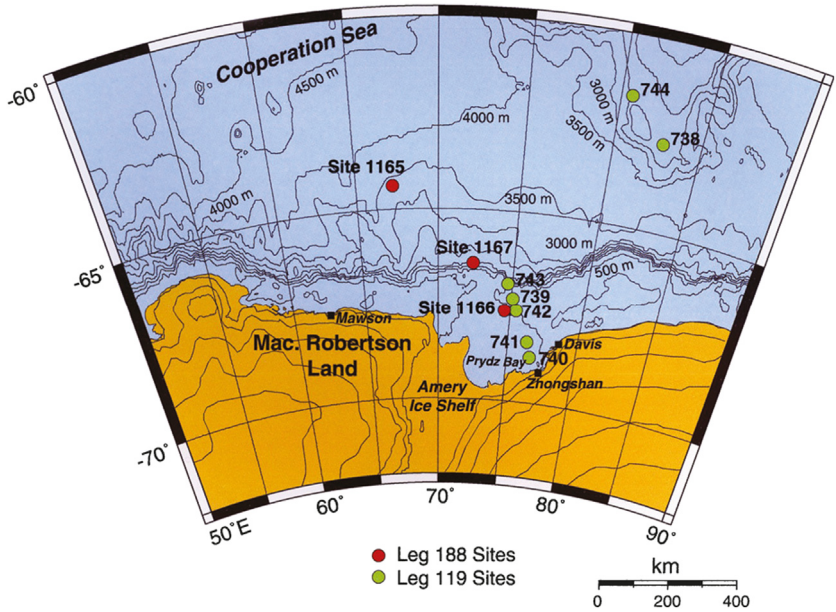

FIGURE 7.7 Location of drill sites in Prydz Bay, East Antarctica, from ODP legs 119 and 188. Continental shelf sites 742 and 1166 include strata that cross the E-O transition. *From Shipboard Scientific Party (2001a). Reproduced with permission of the Ocean Drilling Program, College Station, Texas.*

less satisfactory; hence, interpreting depositional processes is more questionable. Nevertheless, plausible paleoenvironmental scenarios have been derived, albeit lacking precise constraints owing to core loss. Prydz Bay represents the continuation of the Lambert Graben, which contains the Lambert Glacier–Amery Ice Shelf System, an ice drainage basin covering approximately 1 M km^2, draining 13% of the EAIS by surface area. Thus, the record in Prydz Bay provides a signal of the interior of the ice sheet since its inception and complements the Oligocene to Pliocene uplifted glaciomarine record in the Prince Charles Mountains (see Haywood et al., 2008). Prydz Bay itself is dominated by a trough-mouth fan that prograded during phases of glacier advance to the shelf break. Like the western Ross Sea, large data sets are available covering all aspects of core analysis from ODP Legs 119 and 188 (Barron et al., 1991; Cooper and O'Brien, 2004; Cooper et al., 2004; O'Brien et al., 2001) and a convenient summary has been provided by Whitehead et al. (2006) and McKay et al. (2021).

ODP Leg 119 drilled at two sites, 739 (480 mbsf) and 742 (316 mbsf), the lower parts of both were loosely dated shipboard as middle Eocene to early Oligocene. The dominant facies recovered was massive diamictite,

with minor stratified diamictite and sand (Hambrey et al., 1991, 1992). Poorly consolidated fine-grained facies may well have been washed away during the drilling, since core-recovery rates were less than 50%. A few broken shell fragments are present, but there was a dearth of material suitable for precise dating. The base of Site 742 is represented by a zone of soft-sediment deformation. The Oligocene succession forms part of a prograding unit as defined in seismic profiles but is truncated by a regional unconformity. Above lies a flat-lying sequence of more diamictite, some with preferred clast orientation and overcompaction, of late Miocene to Pliocene age (Cooper et al., 1991).

The interpretation of the Leg 119 facies is as follows: the deformed bed at the base of Site 742 may represent the first stages of glaciation, with the ancestral Lambert Glacier extending across the continental shelf for the first time. Then the bulk of the recovered facies in Sites 739 and 742 (diamictite) records deposition from the grounding-line of a tidewater glacier margin, by debris rain-out and submarine sediment gravity flow beyond the shelf break, conditions which characterise much of early Oligocene time.

Leg 188 drilled Site 1166 on the continental shelf near Sites 739 and 742 in order to obtain a more complete record of the EOT, but again core recovery was poor (19%). From the base upwards, late Eocene matrix-supported sand was followed by a transgressive surface and the late Eocene to early Oligocene graded sand and diatom-bearing claystone with dispersed granules. These facies are capped by an unconformity and 'clast-rich clayey sandy silt' (diamicton/ite) of Neogene age (Shipboard Scientific Party, 2001a,b,c,d).

Site 1166 begins at the base with late Eocene fluvio-deltaic sands, which are inferred to be pre-glacial. The overlying late Eocene to early Oligocene sand and claystone represent shallow marine and open marine conditions, respectively, but in a proglacial setting as indicated by ice-rafted granule-sized material. The Neogene strata that lie unconformably above represent full glacial conditions.

A revised biostratigraphic age model based on dinocysts, calcareous nannofossils and diatoms (Houben et al., 2013) allowed the EOT to be identified within Site 739. The first common occurrence of the calcareous nannofossil *Reticulofenestra daviesii* in Core 739C-38R at ~300 mbsf (Wei and Thierstein, 1991) likely correlates with the onset of an early Oligocene acme documented for this species, which has been dated to 33.7 Ma (Persico et al., 2012). At nearby Site 744, the onset of this acme is calibrated to the base of subchron C13n in the earliest Oligocene (~33.7 Ma) (Fioroni et al., 2012). The first occurrence of the dinoflagellate *Malvinia escutiana* in Core 739C-39R at 310.73 mbsf is correlated to the Oi-1 excursion (Houben et al., 2011). These datums constrain the age for the upper 310 m of strata drilled in Hole 739 C to early Oligocene and younger. A late Eocene dinoflagellate assemblage, which includes *Deflandrea* sp. A sensu Brinkhuis et al. (2003) and *Vozzhennikovia* sp., is present from the base of the section up to Core 739C-41R

(∼330 mbsf) (Houben et al., 2013; Truswell, 1997). At ODP Site 1172 on the East Tasman Plateau *Vozzhennikovia* sp. has a last occurrence in Chron C13r (Brinkhuis et al., 2003; Houben, 2019). Houben et al. (2013) documented the onset of typical sea ice–associated dinocyst assemblages at the Oi-1 equivalent stratigraphic level at Site 739.

The revised stratigraphies of ODP Sites 739, 742 and 1166 were put into context of the seismostratigraphy in Passchier et al. (2016), and geochemical weathering data provide a well-resolved near-field record of Antarctic continental ice growth, temperature and weathering changes from Prydz Bay. Variations in CIA and the S-index suggest the presence of ephemeral mountain glaciers on East Antarctica during the late Eocene between 35.9 and 34.4 Ma. The onset of diamict deposition, the prograding clinoforms in seismic data, the declining values of the CIA, and enhanced erosion and glacial weathering rates (Scher et al., 2011; Tochilin et al., 2012) all suggest that high-latitude climate deterioration and ice growth in the hinterland of Prydz Bay intensified 0.5 Myr prior to the EOIS with major ice growth coincident with Eocene-Oligocene precursor glaciation. Glacial microtextures are present on sand grains at ∼240 mbsf in Core 1166A-26R (Strand et al., 2003), which date the onset of some glaciation to ∼35.9 Ma. However, in contrast to the glaciation episodes associated with the EOIS, evidence from Holes 742A and 1166A points to ephemeral, partial, glaciation prior to EOT. A stepwise climate cooling of the hinterland is documented at Prydz Bay starting from 34.4 Ma as the ice sheet advanced towards the edges of the continent during the Eocene-Oligocene precursor interval (Passchier et al., 2016). Different than records in the Ross Sea, sedimentary archives from Prydz Bay provide evidence for full glacial development at the EOT when the ice sheet reached the continental margin.

7.3.2.3 Weddell Sea

ODP Leg 113 recovered the EOB at Sites 689 on the Maud Rise and 696 on the South Orkney Microcontinent (SOM) (Fig. 7.8). Maud Rise lies 100 km south of the present-day Polar Front, 100 km north of the Antarctic Divergence and ∼700 km from the Antarctic continent (Barker et al., 1988, 2007). Although at a more distal position, the open-ocean pelagic sedimentary succession that includes the EOB cored at ODP Site 689 provides evidence for iceberg calving from both West and East Antarctica from ca. 36.5 Ma (Carter et al., 2017; Ehrmann and Mackensen, 1992).

Site 696 was drilled at 650 m water depth in the southeastern margin of the SOM, northern Weddell Sea (Barker et al., 1988). A revised age model suggests that the EOT was well recovered at this site (Houben, 2019; Houben et al., 2013). The late Eocene section is characterised by a change from organic-rich sandy mudstone facies to glaucony-bearing packstone facies (Barker et al., 1988). Mature glauconitic sediments formed in open

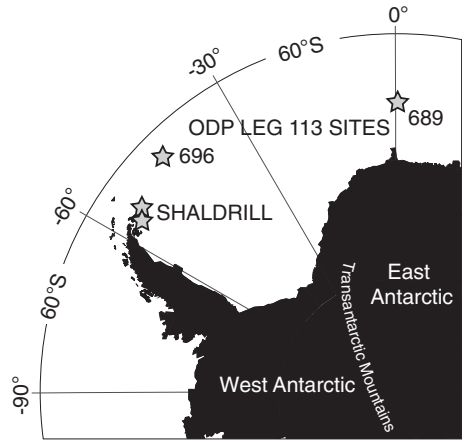

FIGURE 7.8 Location of drill sites in the Weddell Sea, East Antarctica, from ODP legs 113.

marine, shelf-slope transition under sub-oxic conditions are interpreted to record a transgressive condensed sequence deposited at the SOM prior to the EOT (López-Quirós et al., 2019). A change in environmental conditions is also recorded by a relatively diverse dinocyst Eocene assemblage, interpreted to result from temperate or warmer conditions in the northern Antarctic Peninsula area, followed by cooling shown by a decrease in diversity (Mohr, 1990). Crucial was the finding of dinocysts closely resembling the modern species *Selenopemphix antarctica* at ODP Site 696 and other circum-Antarctic sites corresponding closely to the Oi-1 event (Houben et al., 2013). *S. antarctica* is the dominant dinocyst in the modern seasonal Southern Ocean sea-ice zone and derives from a heterotrophic dinoflagellate that primarily feeds on diatoms (e.g., Houben et al., 2013). Its first occurrence and moderate abundance immediately following Antarctic glacial expansion was therefore interpreted to reflect the inception of seasonal sea ice (Houben et al., 2013). Following modelling simulations, this is likely associated with glacial expansion to the coastline (DeConto et al., 2007), consistent with time-equivalent ice rafted debris (Salamy and Zachos, 1999).

Evidence for cool but not polar conditions in the late Eocene are derived from the analysis of marine and terrestrial taxa from the SHALDRIL site 3 Hole C off James Ross Island, which also provides evidence for increased physical weathering towards the end of the Eocene (Anderson et al., 2011). In line with observations at Ste 689, the presence of algae species associated with modern-day Arctic sea ice at the SHALDRIL 3-C site provides evidence for further cooling across the EOT (Anderson et al., 2011).

Seismic reflection profiles in the Weddell Sea region, constrained by sediment ages (ODP Sites 693, 694 and 697; and SHALDRIL 3C), and magnetic anomalies indicate that after the EOIS there is an approximate doubling

in sedimentation rates suggesting increased erosion, but not enough to suggest the West Antarctic Ice Sheet (WAIS) was expanded to modern proportions (Huang et al., 2014).

7.3.2.4 Wilkes Land

The Integrated Ocean Drilling Program (IODP) Expedition 318 drilled the eastern segment of the Wilkes Land margin and recovered sediments from the early-middle Eocene and Oligocene at Site U1356 located on the lower continental rise, and earliest Oligocene sediments at Site U1360 located on the continental shelf (Escutia et al., 2011, Tauxe et al., 2012) (Fig. 7.9).

Today, Site U1356 lies offshore the Wilkes Subglacial Basin (WSB), where the EAIS is marine-based (i.e., grounded on a bed that is below sea level), and is close to the southern boundary of the ACC, near the Antarctic Divergence at 63°S (Bindoff et al., 2000p; Orsi et al., 1995). During the Eocene and early Oligocene, topographic reconstructions show the WSB to be mostly emerged and occupied by low-lying lands (Paxman et al., 2018, 2019; Wilson and Luyendyk, 2009). Reconstructions of the position of the Antarctic Divergence during the early Oligocene, based on a bed the distribution of terrigenous and biogenic (calcareous and siliceous microfossils) sedimentation, Nd isotopes and Al/Ti ratios through a core transect across the Australian–Antarctic basin in the Southern Ocean, place it north of Site U1356 at around 60°S, (Scher and Martin, 2008; Scher et al., 2015). Paleogeographic reconstructions place Site U1356 during the early and middle Eocene to the south of the Antarctic Divergence at paleolatitudes of 70 and 65°S, respectively (Bijl et al., 2013; Pross et al., 2012).

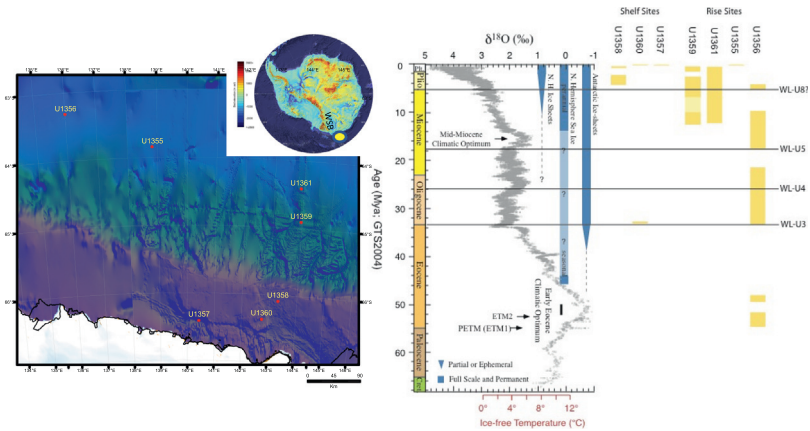

FIGURE 7.9 Location map and chronostratigraphic extent of drill sites in Wilkes Land, from Integrated Ocean Drilling Program (IODP) Expedition 318. *Adapted from Escutia and Brinkhuis (2014).*

Pollen and spores preserved in early Eocene sediments (~55 Ma) reveal that climates along the Wilkes Land coast during peak greenhouse conditions supported the growth of highly diverse, near-tropical (including palms and Bombacoideae) and temperate forests (Contreras et al., 2013; Pross et al., 2012). Using the nearest living relative approach on pollen and spore assemblages to reconstruct paleotemperatures, the paratropical rainforest biome yields winters that were frost-free and mild, with cold monthly mean winter temperatures (MWT) above 10°C, despite polar darkness during winter. Most samples indicated MATs of 16°C ± 5°C with mean summer temperatures (MST) of 21°C ± 5°C and MWT of 11°C ± 5°C. The temperate rainforest biome yields cooler climates with values for MAT and MWT of 9°C ± 3°C and 5°C ± 2°C, respectively, and MST between 14°C ± 1°C and 18°C ± 3°C (Pross et al., 2012). For both biomes, the mean annual precipitation was more than 100 cm/yr. The temperatures indicated by the palynomorphs are similar to those obtained with independent organic geochemical paleotemperature proxies [i.e., branched tetraether lipids, TEX86 and methylation of branched tetraether (MBT)−cyclisation of branched tetraether (CBT) ratios]. MBT/CBT data yield soil temperatures of 24°C−27°C similar to the MSTs derived for the paratropical forest biome, suggesting a common source.

Paratropical conditions persisted in the lowlands of this segment of the Wilkes Land margin at least until 53.9−51.9 Myr ago (Contreras et al., 2013; Pross et al., 2012). The palynological content of the middle Eocene section (49−47 Ma), above a 2 m.y. hiatus, reflects 2°C−3°C cooler temperatures for both winter and summer. MBT/CBT data also record cooling in the middle Eocene with soil temperatures of 17°C−20°C (Pross et al., 2012). Pollen and spore assemblages lacking the megathermal flora were dominated by *Nothofagus*.

In addition to the insights into continental climates, the Eocene succession from Site U1356 allows assessment of the biogeographic patterns resulting from throughflow of surface waters as the Tasmanian Gateway opened (Bijl et al., 2013). Dinocyst analyses from Site U1356, compared to ODP Leg 189 sites around Tasmania, the Australian Bight (ODP Leg 182) and sections in the southeast Australian Margin suggest the earliest throughflow of South Pacific Antarctic waters through the Tasmanian Gateway to be coeval with the shift in rifting direction from SE−NW to S−N (Cande and Stock, 2004) and the onset of a gradual deepening of the South Tasman Rise (Hill and Exon, 2004). Moreover, the onset of throughflow coincides with the earliest signs of cooling following the Early Eocene Climatic Optimum (EECO) (Bijl et al., 2013; Pross et al., 2012). The tectonic opening of the Tasmanian Gateway provides a plausible explanation of southern high latitude cooling following the EECO in the absence of significant equatorial cooling in the middle Eocene (Bijl et al., 2013, 2009). However, more recent work has indicated that tropical cooling did occur in correspondence with

Southern Ocean cooling, pointing to greenhouse gas forcing as the main cause (Cramwinckel et al., 2018).

At Site U1356, the upper middle Eocene to the late Eocene is conspicuously missing in a ~13 m.y. hiatus (~47–33.6 Ma) associated with the unconformity WL-U3 (Escutia et al., 2011; Tauxe et al., 2012). Sediments directly overlying WL-U3 at Site U1356 are dated earliest Oligocene (33.6 Ma) based on the presence of the dinocyst species *Malvinia escutiana* (Houben et al., 2011), the calcareous nannofossil assemblage suggesting an age older than 31.5 Ma (Escutia et al., 2011; Tauxe et al., 2012) and a normal polarity interval interpreted to correspond to Chron C13n (Tauxe et al., 2012). Across the hiatus, environments changed from non-glacial shallow-water depositional environments below to glaciomarine deep-water settings above WL-U3 (Escutia et al., 2011).

These findings imply significant crustal stretching, subsidence of the outer margin and deepening of the Tasman Rise and the Adélie Rift Block some time between 47 and 33.6 Ma (Escutia et al., 2011). Indeed, final loss of a continental connection between Tasmania and Antarctica occurred around 34 Ma, between the South Tasman Rise and Adélie Land (Cande and Stock, 2004). Despite ongoing subsidence, it has been interpreted that the erosive nature of unconformity WL-U3 is related to the early stages of EAIS development. The impact of ice sheet growth, including crustal and sea level response is proposed as the principal mechanism that formed unconformity WL-U3 (Escutia et al., 2011; Stocchi et al., 2013). Microfossils, sedimentology and geochemistry of the early Oligocene sediments immediately above unconformity WL-U3 unequivocally reflect ice-house environments with evidence of iceberg activity (dropstones) and seasonal sea ice cover (Escutia et al., 2011; Houben et al., 2013). In addition, clay mineralogy suggests a shift from chemical weathering to physical weathering, suggestive of much colder/arid weathering regimes (Escutia et al., 2011; Passchier et al., 2013).

In addition to the ice-distal record, the stratigraphic marker for the Oi-1, *M. escutiana* allowed an earliest Oligocene age to be assigned to lowermost sediments recovered from Wilkes Land continental shelf Site U1360 (Escutia et al., 2011; Houben et al., 2013). Glacial diamicton characterises earliest Oligocene sedimentation at Site U1360, indicating an ice proximal to ice distal environment (Escutia et al., 2011). At Site U1360, however, earliest Oligocene glacimarine sediments lie at around 90 m above unconformity WL-U3. This suggests that progressive tectonic subsidence, the large accommodation space created by erosion in the margin (300–600 m of missing strata on the shelf; Eittreim et al., 1995), and partial eustatic recovery (Stocchi et al., 2013) allowed Eocene sediments, in addition to those from the early Oligocene, to accumulate above unconformity WL-U3 on the continental shelf while a hiatus formed at the distal U1356 (Escutia and Brinkhuis, 2014). The continuous presence of reworked middle-late

Eocene dinocyst species in Oligocene sediments from Site U1356 supports unabated submarine erosion of the Antarctic shelf late Eocene strata (Houben et al., 2013).

Early Oligocene dinoflagellate cyst records from U1356 and U1360, combined with those from other locations across the Antarctic Margin, suggest a major restructuring of the Southern Ocean plankton ecosystem, which occurred abruptly and concomitant with the first major Antarctic glaciation in the earliest Oligocene (Houben et al., 2013; Salamy and Zachos, 1999). An abrupt regional increase in siliceous sedimentation at Southern Ocean sites across the EOT glaciation of Antarctica indicates the initiation of seasonal blooms of phytoplankton in circum-Antarctic seas around this time, analogous to modern ecosystems (Houben et al., 2013). The proposed scenario involves an abrupt shift to high seasonal primary productivity associated with the development of seasonal sea ice. It provides the most parsimonious explanation for the abundant appearance of protoperidiniacean dinocysts at EOIS times (Houben et al., 2013). This is in agreement with numerical climate models simulations indicating that sea-ice formation along Antarctic margins may have followed full-scale Antarctic glaciation (DeConto et al., 2007). However, sea ice–related dinocyst species, *Selenopemphix antarctica*, occurs only for the first 1.5 Myr of the early Oligocene, following the onset of full continental glaciation on Antarctica, and after the mid-Miocene Transition (Bijl et al., 2018). For the remainder of the Oligocene and Miocene, less extensive sea ice season is suggested by dinocyst assemblages generally bearing strong similarity to present-day open-ocean, high-nutrient settings north of the sea-ice edge, with episodic dominance of temperate species similar to those found in the present-day subtropical front (Bijl et al., 2018). This agrees with repetitive incursions of north component waters to Site U1356, bathed today by cold Antarctic Bottom Waters (AABW) (Salabarnada et al., 2018), and with temperate surface waters that prevailed over the site notably during interglacial times (Hartman et al., 2018). All evidence points to the existence of a weaker-than present ACC (Bijl et al., 2018, Hartman et al., 2018; Salabarnada et al., 2018). This interpretation is in line with numerical ocean modelling (Herold et al., 2012; Hill et al., 2013) and argues against the formation of a vigorous ACC at 30 Ma as inferred by Scher et al. (2015).

7.4 Summary of climate signals from Antarctic sedimentary archives

7.4.1 Longer-term changes

For tens of millions of years preceding the EOT global climate remained in a greenhouse state, characterised by atmospheric CO_2 levels up to 2000 ppmv

and global average temperature much higher than present day (e.g., Anagnostou et al., 2020; Foster et al., 2017). Under these conditions, the Antarctic continent remained largely ice free, in spite of its polar position (e.g., Francis and Poole, 2002; Klages et al., 2020; Pross et al., 2012). During the early Eocene when mean global temperature was as high as 29°C (Cramwinckel et al., 2018), near-tropical forests could develop over the Antarctic continent (Contreras et al., 2013; Pross et al., 2012;). Organic biomarker paleotemperature reconstructions also reveal extremely warm Southern Ocean SSTs of 28°C (calibration error ±4.0°C) based on TEX_{86}, in the Wilkes Land margin at that time (Bijl et al., 2013). While the temperature estimates remain uncertain, both lines of evidence indicate remarkably warm climate conditions for the highest southern latitudes during peak Cenozoic greenhouse conditions, although the Wilkes Land region was likely the warmest Antarctic sector due to its northern paleolatitude (van Hinsbergen et al., 2015) and oceanographic setting (Bijl et al., 2013).

Mean global temperatures remained high through the early middle Eocene (26°C) and late middle Eocene (23°C) (Cramwinckel et al., 2018). Importantly, Eocene climates were characterised by a reduced equator-to-pole temperature gradient compared to present day (Baatsen et al., 2018, 2020; Bijl et al., 2009; Huber and Caballero, 2011; Greenwood and Wing, 1995). This characteristic of the global climate system has proven difficult to adequately simulate with climate models (e.g., Caballero and Huber, 2013; Cramwinckel et al., 2018; Huber and Caballero, 2011; Klages et al., 2020; Lunt et al., 2012; Spicer et al., 2008), although recent modelling efforts come to closer agreement (Baatsen et al., 2018, 2020).

Significant information on the evolution of climate on the Antarctica continent have been derived from fossil plants and palynomorphs, mineralogy and geochemistry through the analysis of outcrops, marine sedimentary cores and glacial erratics. Paleogene fossil plants are indicative of a high southern latitude flora of variable diversity but dominated by fossils comparable to modern Nothofagus and conifer trees. The fossil plant record suggests that during the late Palaeocene to early Eocene moist, cool temperate rainforests existed in Antarctica, similar to modern low to mid-latitude Valdivian rainforests in southern Chile. These forests were dominated by Nothofagus and conifer trees, with ferns, horsetails and some less-prominent angiosperm groups. TEX_{86} temperature proxies show cooling of around 4°C in the Wilkes Land margin during the middle Eocene. Multiproxy data from Seymour Island provide well-constrained evidence for annual SST of 10°C−17°C during the middle and late Eocene with distinctly higher temperatures recorded between ca. 45 and 41 Ma (Douglas et al., 2014). The difference was originally attributed to zonal heterogeneity (Douglas et al., 2014), but the application of the proper paleomagnetic reference frame in tectonic reconstructions (Van Hinsbergen et al., 2015) implies a much higher latitude for the Antarctic Peninsula relative to East Antarctica at that time.

From the early middle to late Eocene (38–35 Ma), global temperatures dropped to as low as 19°C (Cramwinckel et al., 2018). Evidence for limited glaciation during this time interval comes from different areas around Antarctica. Gulick et al. (2017) found evidence that marine-terminating glaciers existed in the Wilkes Land area at some point during the early to middle Eocene, the precise age of which is poorly constrained. This was based on ice rafted debris found in piston cores and seismostratigraphic interpretations from offshore of the Sabrina Coast in Wilkes Land. There is additional information from airborne radar data of a preserved alpine landscape in the Gamburtsev Mountains, suggesting mountain glaciers existed in central Antarctica prior to the EOT (Bo et al., 2009; Rose et al., 2013). It is possible that ice located in the Gamburtsevs during the Eocene fed glaciers terminating at the Sabrina Coast (Gulick et al., 2017) supported by high precipitation (Baatsen et al., 2018, 2020). Further evidence for partial glaciation prior to the EOT is seen in records from the South Orkney Islands, which show the delivery of distal ice rafted sediments 2.5 Myr prior to this chronohorizon. The sediment provenance signature supports rafting of sediments from glaciers terminating at the coast in the Weddell Sea sector (Carter et al., 2017).

Cooling during the late Eocene is apparent at several sites, including the Weddell Sea based on terrestrial (Carter et al., 2017) and marine (Houben, 2019) records, Prydz Bay (Passchier et al., 2017), Maud Rise SST records (Petersen and Schrag, 2015), and the vegetation records from South Australia and the South Atlantic (Pound and Salzmann, 2017). Evidence of pronounced cooling and ice preceding the EOT have been found in terrestrial records from the Weddell Sea (Carter et al., 2017; Ehrmann and Mackensen, 1992), Maud Rise SST records (Petersen and Schrag, 2015), Seymour Island (Anderson et al., 2011), and vegetation from the most distal site in South Australia and the South Atlantic (Pound and Salzmann, 2017). The results indicate that from about 35.7 million years ago onward, enhanced surface ocean circulation led to sediment winnowing, higher biological productivity and cooling of surface waters around Antarctica (Houben, 2019). Similarly, organic biomarker paleothermometry and dinocyst distribution from different sites located in the southwest Atlantic (DSDP Site 511), Weddell Sea (ODP Site 696) and the south margin of Australia (ODP Sites 1128, 1168 and 1172) indicate a major oceanographic invigoration including the onset of an Antarctic Countercurrent, starting at 35.7 Ma (Houben, 2019). At localities affected by the Antarctic Countercurrent, sea surface productivity increased and simultaneously circum-Antarctic surface waters cooled, which might have preconditioned the Antarctic continent for glaciation. Significant regional differences in terms of absolute temperature values might reflect a large-scale zonal SST gradient between the South Atlantic and the southwest Pacific sectors throughout the middle-late Eocene, which has been interpreted to reflect water mass organisation (Douglas et al., 2014; Houben et al., 2013).

Sedimentary archives from various Antarctic localities, hence, provide a consistent but broad picture of climate evolution that is in line with the Cenozoic climate history derived from various proxies in lower latitude settings. Although there is evidence for glaciation and for marine-terminating glaciers, much uncertainty remains about the nature and geographical extent of ice on Antarctica before the EOT.

7.4.2 The climate of the Eocene-Oligocene transition

While a consistent picture on the long-term environmental and climatic evolution during the middle-late Eocene and the Oligocene emerges from a wealth of data at different localities on the Antarctic margin, detailed insights into the timing and paleoenvironmental implications of ice growth close to the locus of ice formation on Antarctica are sparse. A comprehensive summary of temperature proxy records across the EOT in Antarctic and peri-Antarctic settings has been recently compiled by Kennedy-Asser et al. (2020) including 14 sites (10 marine and four terrestrial) ranging in paleolatitude from 53 to 77°S (Fig. 7.10). Comparison of late Eocene and early Oligocene temperatures provide a coherent picture of climate deterioration over the Antarctic margin with a mean temperature drop of around 3.4°C (Kennedy-Asser et al., 2020) (Fig. 7.11).

However, only a few Antarctic sites provide a continuous record across the EOT, which is crucial to determine the tempo and mode of the evolution of the nascent ice sheet in comparison with data from far-field proxies. These include the CRP-3 (Florindo et al., 2005; Galeotti et al., 2012; Passchier et al., 2013) and, possibly, CIROS-1 (Roberts et al., 2003) drillholes in the Ross Sea, ODP Site 696 in the Weddell Sea (Carter et al., 2017; Ehrmann and Mackensen, 1992) and ODP Site 739 in the Prydz Bay (O'Brien et al., 2001; Passchier et al., 2013, 2017). In addition, sediments recovered from the eastern Wilkes Land margin at Site U1360 attest to ice sheet advance to the coast/continental shelf by the earliest Oligocene (33.6 Ma; Escutia and Brinkhuis, 2014; Escutia et al., 2011). All these records provide evidence for a major glacial expansion across the EOT. However, there is no unequivocal evidence for a fully developed ice sheet at all sites.

At Prydz Bay three ODP drill holes were drilled at Sites 739, 742 and 1166 (O'Brien et al., 2001). The position of the EOT has been constrained by dinoflagellate cyst biostratigraphy in Hole 739C (Houben et al., 2013), which, using seismostratigraphy, allowed the age model for the three sites to be refined (Passchier et al., 2017) with a strong age control. Analysis of the Chemical Index of Alteration and the S-index (Sheldon et al., 2002) allows reconstruction of near-field Antarctic continental ice growth, temperature and weathering changes during the EOT on the East Antarctic margin. These geochemical data suggest the presence of ephemeral

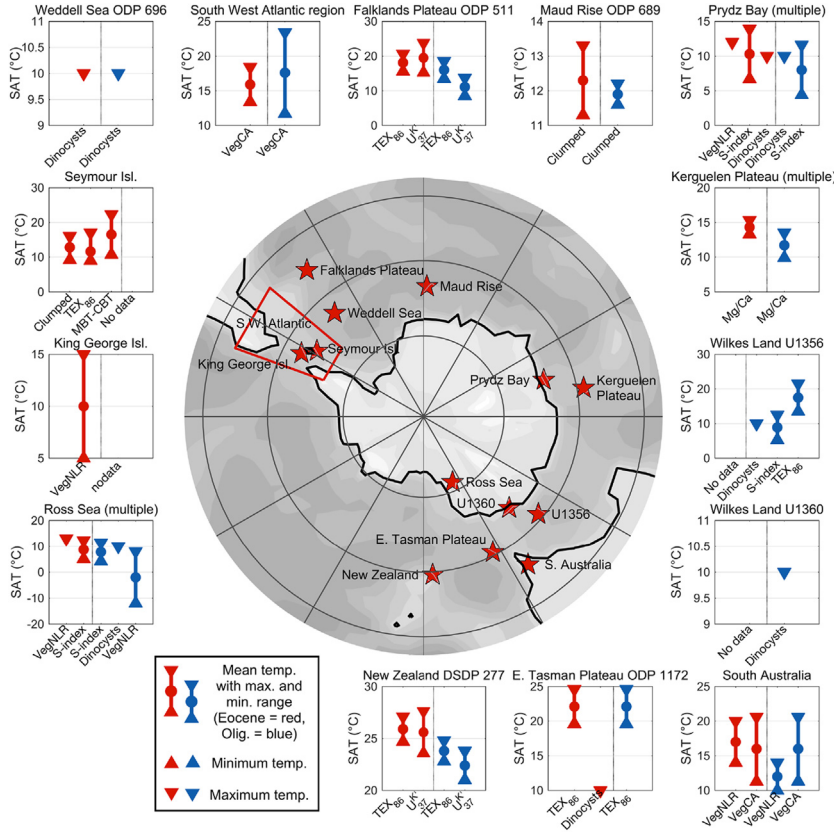

FIGURE 7.10 Mean annual temperature (°C) from proxy records for all sites during the late Eocene and early Oligocene. The mean values (circles) are shown with maximum and minimum values (error bars), while ordinal limits are shown by upward-pointing (greater than) or downward-pointing (less than) triangles. Late Eocene records are in red and early Oligocene records in blue. *From Kennedy-Asser et al. (2020).*

mountain glaciers on East Antarctica during the late Eocene between 35.9 and 34.4 Ma. High latitude warming events are recognised at ~35.8 and 34.8 Ma. A stepwise climate cooling of the Antarctic hinterland occurred from 34.4 Ma as the ice sheet advanced towards the edges of the continent slightly before the EOB. A temperature decline of >3°C is captured by S-index data between 34.4 Ma and the Oi-1 when, finally, the ice sheet extended to the outer shelf.

A different history comes from other sites where the EOT did not lead to fully glaciated conditions. Seismic reflection profiles show a relatively limited extent of glacial deposits in the southern Weddell Sea, which is indicative of a WAIS less expanded than present day (Huang et al., 2014).

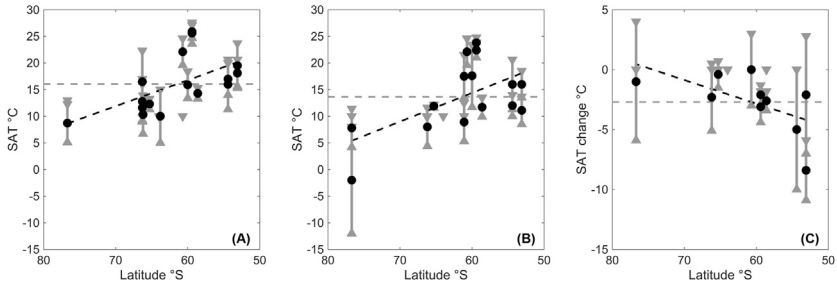

FIGURE 7.11 Latitudinal profiles of (A) late Eocene absolute temperature, (B) early Oligocene absolute temperature and (C) EOT temperature change from proxy records. The mean values are plotted in grey dotted lines and latitudinal gradients (calculated using ordinary least squares) in black dotted lines. Circles show mean values, uncertainty ranges and maximum/minimum limits are shown by the bars and triangles. *Adapted from Kennedy-Asser et al. (2020).*

Fully glaciated conditions were reached only during the Miocene in this area, according to Huang et al. (2014). In line with this observation, relatively diverse vegetation biomes persisted around most of the coastal regions of the continent well in into the early Oligocene (Francis et al., 2008). Yet, significant ice must have been present across Antarctica in the late Eocene to enable it to calve icebergs along the coastlines of the southern Weddell Sea by ca. 36.5 Ma or slightly earlier (Scher et al., 2014), as also revealed by the occurrence of iceberg-rafted sediment grains with both East and West Antarctic provenance at Weddell Sea ODP Site 696 (Barker et al., 1988; Carter et al., 2017).

The orbitally-resolved record of the shallow-water glaciomarine sedimentary succession recovered with the CRP-3 drillhole offers a detailed history of glaciation in the Ross Sea (Galeotti et al., 2012, 2016). The well-dated CRP-3 drill core suggests the development of a stable continental-scale ice sheet calving at the coastline only at 32.8 Ma (Galeotti et al., 2016). There is evidence for orbital pacing of glacial advance and retreat cycles between 34 and 31 Ma, indicating that the nascent Antarctic ice responded to local insolation forcing. The stabilisation of a continental scale ice sheet at 32.8 Ma appears to have been related to the crossing of a CO_2 threshold, although the precise CO_2 level triggering ice expansion into the marine realm remains uncertain (Anagnostou et al., 2016; Gasson et al., 2014).

In the eastern sector of the Wilkes Land margin, the EOT was not fully recovered. Instead at Site U1356, a ~13 m.y. hiatus separates middle Eocene from earliest Oligocene (33.6 Ma) sediments (Escutia et al., 2011; Tauxe et al., 2012). Coeval early Oligocene sediments were also recovered from continental shelf Site U1360. Both sites provide evidence for the existence of an ice sheet advanced to the continental shelf depositing ice-proximal sediments (diamictons) at Site U1360 and dropstones resulting from calved icebergs at distal Site U1356 (Escutia et al., 2011).

Despite the development of a large AIS at the EOT, the presence of tundra paleo-biome localities on Antarctica demonstrates the survival of vegetation in the early Oligocene on the continent (Francis, 1991; Francis and Poole, 2002; Francis et al., 2004, 2008; Poole et al., 2005; Prebble et al., 2006; Strother et al., 2017). Interpretations based on fossil plants are supported by the analysis of n-alkane from various localities on the Antarctic margin, which shows a shift from n-C29 to n-C27 dominated chain length n-alkane between the late Eocene and the Oligocene (Duncan et al., 2019). Such a change is inferred to result from both a shift in plant community, as well as a response to significant climate cooling.

The evidence for the presence of vegetation in the early Oligocene is at odds with geochemical proxy records from marine sedimentary archives suggesting that the EOT ice sheet had a volume of 60%−130% of the modern day, depending on the oxygen isotopic composition of the ice sheet (Bohaty et al., 2012). On the one hand, sub-aerial continental areas were larger than present day (Paxman et al., 2019; Wilson et al., 2012), thus leaving more land available to sustain vegetation. On the other hand, however, the warm Southern Ocean (Hartman et al., 2018; Houben, 2019) provided a local, isotopically heavier than previously assumed, source of precipitation entailing a larger ice sheet to explain the geochemical record. Fossil records indicating the survival of vegetation in the early Oligocene and geochemical proxy records from marine sedimentary successions remain, therefore, difficult to reconcile.

7.5 The global context of Earth and climate system changes across the EOT

The E-O transition marks a momentous shift in the state of the Earth system when a long-term decline in global temperatures and atmospheric CO_2 concentration that began in the early Eocene at ~50 Ma (Anagnostou et al., 2020) culminated in the rapid expansion of a permanent, albeit dynamic, ice sheet over the Antarctic continent at ~34 Ma (DeConto and Pollard, 2003; Katz et al., 2008; Lear et al., 2008; Zachos et al., 2001). Proposed causes for this fundamental change in Earth's climate state include changes in ocean circulation (and associated ocean heat transport) due to the opening of Southern Ocean gateways (Kennett, 1977), a decrease in atmospheric CO_2 (DeConto and Pollard, 2003) and a minimum in solar insolation (Coxall et al., 2005). Also, there is evidence for a long-term climate transition that lasted up to several millions of years before the inception of an AIS (e.g., Bohaty et al., 2012; Coxall and Pearson, 2007; Coxall et al., 2005, 2018; Scher et al., 2011). Associated changes in the global ecosystem were influenced by ocean circulation and overturning (e.g., Coxall et al., 2018; Katz et al., 2011), ocean biogeochemistry (e.g., Lear et al., 2008; Pälike et al., 2012), global temperatures (e.g., Liu et al., 2009), marine biology

(e.g., Houben et al., 2013; Villa et al., 2013) and terrestrial fauna (e.g., Costa et al., 2011; Kraatz and Geisler, 2010; Prothero, 1994). Here, we summarise existing model experiments that test the mechanisms proposed to have been driving the EOT.

7.5.1 Climate modelling

The Eocene-Oligocene transition has been the target of climate and ice sheet modelling studies for over two decades. An array of computer models have been used, including ocean-only models (Sauermilch et al., 2021), coupled atmosphere-ocean models (Baatsen et al., 2018, 2020; Goldner et al., 2014; Hutchinson et al., 2019; Kennedy-Asser et al., 2015; Sijp et al., 2011) and coupled climate−ice sheet models (DeConto and Pollard, 2003; Gasson et al., 2014; Ladant et al., 2014), with the common goal of finding a mechanistic explanation for the global cooling that culminated in Antarctica's transition to an ice-covered continent.

The onset of Antarctic glaciation has long been linked with the opening of ocean gateways following the tectonic separation of Antarctica from Australia (the Tasman Gateway) and South America (the Drake Passage) (Kennett, 1977; Livermore et al., 2007; Scher and Martin, 2006; Shackleton and Kennett, 1976). It was thought that the opening and subsequent deepening of these gateways represented the final barrier of the development of strong circumpolar ocean flow, the ACC. It is hypothesised the developing ACC led to the thermal isolation of Antarctica from the lower latitudes, cooling the southern high latitude climate and allowing for the formation of the AIS. Testing this hypothesis has focused on several aspects, e.g., dating of gateway opening and deepening, also by reconstructing the evolution of the oceanic frontal systems (Bijl et al., 2018, Evangelinos et al., 2020; Salabarnada et al., 2018; Sangiorgi et al., 2018), and correlating these to ice sheet inception, and using climate and ice sheet models to determine how significant the opening of these gateways was to the climate of Antarctica.

Meanwhile, ice sheet models have been used to test the alternative explanation for the formation of the AIS, that glaciation was caused by a drop in atmospheric CO_2 across the EOT. A key advantage of modelling is that it allows the individual role of these different cooling and glaciation mechanisms to be examined.

Some of the earliest modelling studies produced conflicting results as to the significance of ocean gateway opening. Ocean modelling showed several degrees of surface ocean cooling around Antarctica with the opening of the Drake and Tasman gateways following a reduction in heat convergence to the Southern Ocean, supporting the thermal isolation hypothesis (Nong et al., 2000; Toggweiler and Bjornsson, 2000). This contrasted with a coupled ocean−atmosphere study showing a much smaller effect on sea surface temperatures around Antarctica with the opening

of the Tasman Gateway (Huber et al., 2004). More recent modelling work with high-resolution, eddy-permitting ocean simulations and detailed paleobathymetry demonstrate a dramatic surface water cooling along the Antarctic coast (>4°C) by changing the gateways depth from 300 to 600 m (Sauermilch et al., 2021). In contrast, other recent modelling work has shown that the formation of the AIS had a large effect on ocean circulation, suggesting that some of the observed changes in circulation may have been *feedbacks* from glaciation, rather than a *forcing* from the opening of gateways (Goldner et al., 2014; Kennedy-Asser et al., 2015). Although the relative importance of atmospheric CO_2 vs ocean gateways as the primary control on the climate changes across the EOT continues to be debated, it is clear that both had an impact on regional climate and oceanography.

As the direct impact of Southern Ocean gateways on Antarctic climate continues to be debated, focus has shifted to a wider view of Earth system changes around the EOT. The interconnection between ocean basins and processes has led some studies to assess the impact of low latitude and Northern Hemisphere gateways on Southern Ocean and Antarctic climate (Yang et al., 2014). Changes in these distant gateways have been shown to potentially cause Southern Ocean cooling by enhancing North Atlantic overturning at the expense of Southern Ocean overturning (Yang et al., 2014). However, an alternative theory is that overturning shifted from the North Pacific to the North Atlantic due to salt-advection feedbacks, while Southern Ocean overturning continued across the EOT (Hutchinson et al., 2019; McKinley et al., 2019). Other studies have assessed how ocean gateway changes can have impacts on ocean overturning and carbon uptake (Elsworth et al., 2017; Fyke et al., 2015; Mikolajewicz et al., 1993). Although these investigations are somewhat idealised, they emphasise the importance of ocean gateways as potential long-term contributors to the changes associated with the EOT, even if the direct climatic effect associated with gateway changes is limited. In a recent synthesis of EOT modelling, the reduction in atmospheric CO_2, rather than the opening of ocean gateways or formation of the AIS, showed a better match to global proxy reconstructions from before and after the EOT (Hutchinson et al., 2021).

Notable challenges remain in modelling the high latitude climate before, after and across the EOT. Not least this includes issues regarding the higher absolute polar temperatures that are recorded in the proxy observations compared to many model simulations at reasonable CO_2 levels. Some of the most recent modelling studies appear to have made progress in reducing this mismatch, citing improved cloud and water vapour feedbacks associated with higher resolution (Baatsen et al., 2018, 2020) or enhanced climate sensitivity to CO_2 (Hutchinson et al., 2018). A significant component of this warming is also due to changes in land-surface properties, independent of CO_2 forcing. Lunt et al. (2020) found that when moving from pre-industrial to

Eocene boundary conditions in a multi-model ensemble, global mean temperatures increased by 3°C−5°C, due to changes in palaeogeography, vegetation, aerosols and the removal of ice sheets. These factors are all 'prescribed' in Eocene climate models, whereas in reality they may act as feedbacks to a perturbation such as the Antarctic glaciation.

Another challenge is the need for models simulating oceanographic conditions in high, eddy-permitting resolutions (<0.25°). Most paleo simulations run in low resolution (1−3.75°) using coarse paleobathymetries without prominent seafloor roughness and detailed geometric features (Baatsen et al., 2018; Huber et al., 2004) or modified present-day bathymetry grids (Hill et al., 2013), as boundary conditions. Recently, numerous studies in the field of modern physical oceanography have shown that small-scale features in ocean currents and seafloor topography strongly influence large-scale ocean circulation patterns. Mesoscale eddies (<100 km) are key components for ocean circulation and, in large parts of the ocean, eddies are responsible for the majority of the heat transport (Griffies et al., 2015; Jayne and Marotzke, 2002; Morrison and Hogg, 2012; Newsom et al., 2016; Viebahn et al., 2016), and small-scale seafloor features with slope gradients in the order of 10^{-4} to 10^{-5} (>0.05°) significantly influence subsurface velocities and vertical structure of ocean currents (LaCasce, 2017; LaCasce et al., 2019). Using low-resolution ocean model configurations with simplified bathymetries to reconstruct reorganisations of oceanographic conditions during key climate changes, such as the EOT, carries the potential to severely underestimate ocean heat transport processes, as well as the influence of tectonic processes, on changing ocean circulation.

This has been shown in a recent study using high-resolution (0.25°) ocean model configurations with detailed paleobathymetry (Sauermilch et al., 2021). This model demonstrates that the Southern Ocean's tectonic processes across the EOT (including gateway deepening and paleolatitudinal shifts) play a crucial role in reorganising the ocean circulation patterns and temperature distribution around Antarctica (Hochmuth et al., 2020; Xing et al., 2020; Sauermilch et al., 2021). Changing the gateway depths from only 300 to 600 m causes the Pacific and Indo-Atlantic subpolar gyres to weaken and Antarctic surface waters to cool dramatically by >4°C. These results are consistent with existing paleo-sea surface temperatures from proxy records, as well as plankton biogeographic patterns and Neodymium records constraining surface and bottom currents, respectively (Sauermilch et al., 2021).

In addition to climate modelling studies, ice sheet models coupled in various ways to climate models have also tried to determine what caused the rapid onset of Antarctic glaciation across the EOT. The first Antarctic ice sheet study to systematically test the two leading hypotheses of ocean gateway opening vs CO_2 drawdown was carried out by DeConto and Pollard (2003). They used a slab ocean model to mimic the effect of the thermal isolation of Antarctica and compared this to the impact of declining

atmospheric CO_2 and changes in Earth's orbit and obliquity. Their results showed a strong sensitivity to CO_2 drawdown, with a critical threshold of 780 ppm identified for ice sheet formation. This value was in remarkable agreement to proxy reconstructions of atmospheric CO_2 concentrations published a few years later (Pagani et al., 2011; Pearson et al., 2009). Although CO_2 was the predominant control on ice sheet volume, reduced ocean heat transport had a smaller impact, increasing the CO_2 threshold by 140 ppm (DeConto and Pollard, 2003). A data-driven (CO_2 and summer insolation) ice sheet model was able to simulate the ice evolution through the EOT and to reproduce the timing and the magnitude of the two steps evident in oxygen isotope records (Ladant et al., 2014). The latter study suggests a substantial impact of the combination of ice feedbacks (height-mass balance and albedo) and insolation, which gives a large-scale glaciation threshold of about 900 ppm more than 100−150 ppm higher than previously thought by DeConto and Pollard (2003) (Fig. 7.12).

Using a range of different GCMs Gasson et al. (2014) showed a larger spread in the glacial CO_2 threshold between ~560 and 920 ppm, although still clustered around the earlier estimate of DeConto and Pollard (2003). One model (HadCM3L) did not produce any glaciation, even with a much lower concentration of atmospheric CO_2 (280 ppm). Part of the cause of the large spread in results was model-dependent. In particular, the topography over the Antarctic continent differed significantly among the models used (Gasson et al., 2014). The results of a recent model inter-comparison project in which GCMs are setup in an identical way (Lunt et al., 2020) will help shed new light on the nature of the model dependency of glaciation threshold. Other important aspects that are not adequately incorporated in ice sheet models are ice−ocean interactions and GIA effects, incorporation of which will further refine simulations of EOT glaciation in the future (Fig. 7.13).

7.5.2 Relative sea-level change around Antarctica

The onset of the first continent-size AIS across the EOT was accompanied by a regression that left a clear mark in ocean-sediment cores and geologic sections in the Northern Hemisphere (Houben et al., 2012; Kominz and Pekar, 2001; Miller et al., 2008).

These far-field sites haves recorded a 60 ± 20 m sea-level drop that, according to the concept of glacioeustasy, and hence under the assumption that the Earth is rigid and non-gravitating, is consistent with a larger Antarctic continent, thus capable of hosting a large ice sheet (Wilson et al., 2012).

However, near-field sections and cores from East Antarctica, such as Wilkes Land (IODP 318, Escutia et al., 2011), Prydz Bay (ODP, Barron et al., 1991; O'Brien et al., 2001) and Cape Roberts (CRP-3, Fielding et al., 2001; Galeotti et al., 2012), show significant local and regional deviations of

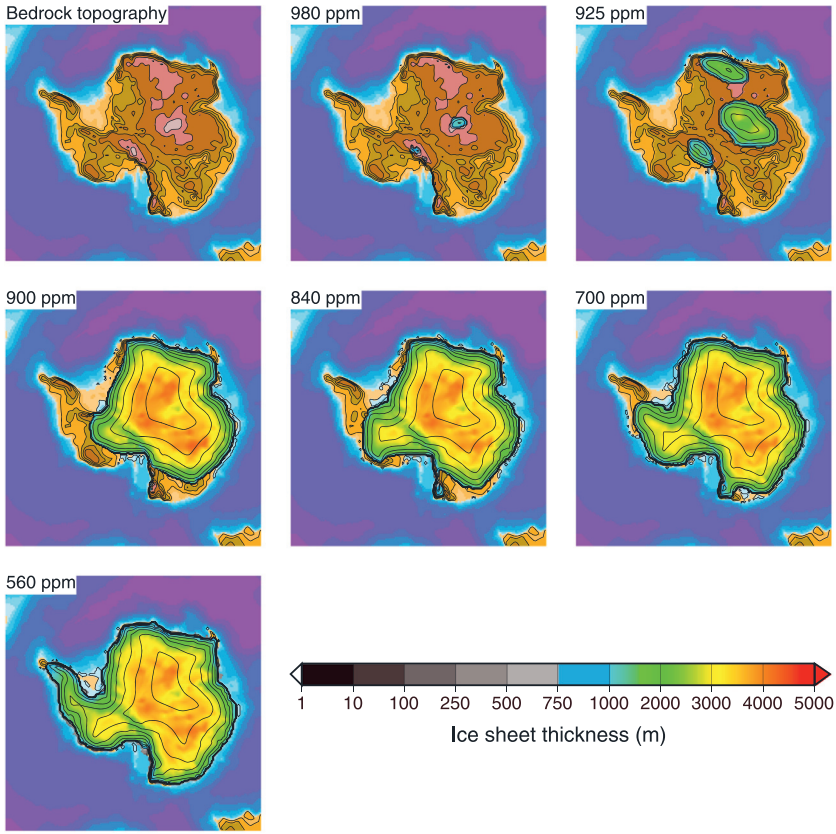

FIGURE 7.12 Numerical simulation of the maximum volume of ice sheet attained with different atmospheric CO_2 concentrations based on a data-driven (CO_2 and summer insolation) ice sheet model. The modelled CO_2 threshold for the onset of a large-scale glaciation is approximately 900−925 ppm. Fully glaciated conditions are reached with atmospheric CO_2 level of approximately 560 ppm. *From Ladant et al. (2014).*

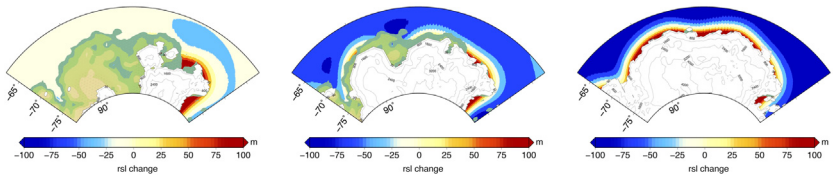

FIGURE 7.13 Seven hundred kyr-long EAIS growth and GIA-driven RSL changes at three model run times, and relative to the pre-glacial state. The ice-sheet extent is shown in white. Left: model run time is 1.5 Myr (since the beginning of the simulation). Centre: model run time is 1.55 Myr, which correlates to the end of the first $\delta^{18}O$ step. Right: model run time is 2.2 Myr.

sea-level change from the Northern Hemisphere trend (Galeotti et al., 2016; Stocchi et al., 2013). Furthermore, the inferred ice-proximal sea-level variations across the EOT vary in space and time, mostly as a function of the distance from the ice sheet margin.

The occurrence of a hiatus in the sediment cores and stratigraphic sections from the offshore sites at Wilkes Land (IODP 318, Escutia et al., 2011) implies that a sea-level drop, which is consistent with the eustatic trend from the NH caused the erosion of late Eocene material as the ice sheet was growing. This is particularly clear because early Oligocene sediments contain reworked late Eocene microfossils (Bijl et al., 2018; Houben et al., 2013), demonstrating profound erosion on the Wilkes Land continental margin, possibly as a consequence of tectonic deformation from the inception of Antarctic glaciation.

At the same time, the occurrence of fining upward Oligocene sediments above the hiatus shows that accommodation space was created on the shelf (Stocchi et al., 2013), which can only be explained with a local sea-level rise. This is obviously at odds with the 60 ± 20 m glacioeustatic sea-level drop as inferred from the Northern Hemisphere geological records.

The change in local sea-level trend in the offshore sites and the continuous increase of bathymetry along the inner margins cannot be explained under the glacioeustatic approximation. By solving the SLE, Stocchi et al. (2013) have shown that when the AIS grows during the EOT, the newly formed excess of Antarctic ice mass causes the solid Earth's surface to subside in order to reestablish an isostatic equilibrium. Because of basin subsidence, the coastal areas experience a progressive relative sea-level rise throughout the EOT.

However, as the ice sheet was growing, the gravitational pull exerted by the ice mass on the surrounding ocean water caused the mean sea surface, which is an equipotential surface of gravity, to rise towards the ice margins. This process, known as self-gravitation, further exacerbated the regional RSL change pattern. It increased the RSL drop over the uplifting forebulges (thus decreasing the column of water) and increased the RSL rise along the coasts, thus facilitating the formation of accommodation space.

The sedimentary cycles observed in the CRP-3 section (Cape Roberts, Ross Sea) are the result of periodic fluctuations in both grounding-line proximity and RSL change (Fielding et al., 2001). The interpretation of the sedimentological evidence implies that glacial maxima and minima locally coincided with times of minimum and maximum RSL, respectively (Fielding et al., 2001). This is in line with the glacioeustatic approximation. However, given the ice marginal position of the CRP-3 site, any proximal ice-thickness variation would have resulted in local RSL change with the opposite sign of eustatic trends and of larger amplitude. Galeotti et al. (2016) suggest that the GIA-induced RSL rise caused by the expansion and grounding of the ice sheet at the CRP-3 site had to be counter-balanced by a strong RSL drop in

response to the uplifting forebulge driven by a synchronous thickening of the EAIS. Therefore, the appearance of marine-grounded ice near the CRP-3 site was facilitated by flexural crustal uplift as the EAIS expanded, resulting in a RSL fall (>40 m) in phase with the hypothetical eustatic trend. Accordingly, Galeotti et al. (2016) postpone the timing of maximum, continental-scale ice growth to 32.8 Ma, when CO_2 levels dropped below 600 ppm.

Important outcomes from the numerical modelling of the EOT GIA processes can be summarised as follows:

1. The large RSL rise in the proximity of the Antarctic ice-sheet margins might provide a strong dynamical feedback on ice-sheet stability (Gomez et al., 2010). Accordingly, the near-field processes such as local sea-level change influence the equilibrium state obtained by an ice sheet grounding line. This implies that ice sheets models should be fully coupled to Earth models that capture GIA. It has been shown that self-gravitation operates such as a self-regulating mechanism. As shown by Gomez et al. (2010) and De Boer et al. (2014, 2017), self-gravitation and subsidence cause major local RSL rise at the ice margin, which prevents from further growth over the continental shelf, thus limiting the maximum size that an ice sheet can grow. Obviously, this also works the other way around. When and ice sheet melts, crustal uplift and sea level drop might limit its retreat and actually favour an expansion.
2. The infill of sediments is expected to further alter the local RSL change along the Antarctic margins and should therefore be included in a gravitationally self-consistent manner within the GIA models (Boulton, 1990; Ohneiser et al., 2015; Stocchi et al., 2013; Whitehouse et al., 2019).
3. The uneven local RSL changes might have impacted Southern Ocean surface and deep oceanography by affecting the bathymetry, as shown by Rugenstein et al. (2014). The GIA-induced regional deformations of the sea bottom, although of the order of 50 m, are large enough to affect pressure and density variations, which drive the ocean flow around Antarctica. Throughout the Southern Ocean, frontal patterns are shifted several degrees, velocity changes are regionally more than 100%, and the zonal transport decreases in mean and variability. The model analysis suggests that GIA-induced ocean flow variations alone could impact local nutrient variability, erosion and sedimentation rates, as well as ocean heat transport.

7.6 Summary

The Eocene-Oligocene climatic transition marks the crossing of a threshold in a long-term cooling trend that began following the early Eocene Climatic Optimum ca. 51 Ma. For about 17 Myr global temperatures cooled gradually, although with some more abrupt changes, in concert with a

generalised decrease of atmospheric CO_2 levels. A range of data sources from Antarctic drillholes and outcrops outlines a picture of the response to this long-term change and provides crucial information on the environmental conditions that allowed the onset of Antarctica's glaciation as well as its aftermath. The integration of these records with lower latitude data and paleoclimate numerical climate and ice sheet modelling is crucial to test existing hypotheses explaining the transition from a greenhouse to an icehouse climate state.

7.6.1 Early–middle Eocene polar warmth

The early Eocene climate record is associated with high atmospheric CO_2 concentrations and global temperatures much warmer than present day. Evidence from fossil plants, palynology and geochemistry indicates that the early Eocene climate was characterised by warm and wet climates at high latitudes, with the development of tropical forests on the Antarctic margin and temperate forest conditions at high altitudes. The oldest record of some glacial activity, i.e. valley-type tillites, comes from the middle Eocene of King George Island, indicating the presence of alpine glaciers. While the sporadic presence of alpine-type glaciers at high elevation cannot be excluded, floras of middle Eocene age from King George and Seymour islands suggest warm to cool temperate climates, generally moist and probably frost-free on coastal settings. Accordingly, marine isotope records suggest that climates were generally warm until the middle Eocene, although the climate trend was towards cooling.

7.6.2 Late Eocene cooling

Following the middle Eocene climatic optimum at $\sim$40 Ma, stable isotope records capture the continuation of the long-term cooling trend that initiated at $\sim$51 Ma. Marine geochemical proxy records, while uncertain, are indicative of atmospheric CO_2 levels decreasing from $\sim$1000 ppm in the late Eocene to $\sim$700–800 ppm across the EOT.

A generalised cooling trend is evident in geochemical, sedimentary and palaeontological Antarctic records. The period of relative tropicality in southern high latitudes that dominated the early Eocene persisted to some extent into the middle Eocene and ended in the late Eocene. A number of geological data sources suggest that during the early late Eocene, climates cooled but perhaps not to the point of allowing significant ice build-up. The late Eocene sediment record in the Ross Sea region (McMurdo Erratics, magnetic and clay mineral record) and in the Prydz Bay area could be indicative of cold climates, but the coastal/open marine shelf and fluvial-deltaic environments in these two areas, respectively, do not show signs of the presence of persistent ice. Further cooling and a major oceanographic

reorganisation with the emplacement of an Antarctic Countercurrent, starting at about 35.7 Ma, is recorded in organic biomarker values. Cooling of surface waters across this time interval is also captured by clumped isotope records.

The late Eocene intensification of the Antarctic Countercurrent and its climatic and environmental feedbacks may have helped set the stage of minor scale, ephemeral Antarctic glaciations prior to the EOT. In the Weddell Sea, there is evidence of iceberg calving from both West and East Antarctica from approximately 36.5 Ma. Evidence for precursor glaciation comes from the Prydz Bay, 0.5 Ma prior to the EOT. A pulse of IRD and a perturbation in the Nd record indicates the presence of a small precursor glaciation at the Kerguelen Plateau. This pattern of transient precursor glaciations leading to major and sudden glacial expansion is in line with the hypothesised role of powerful nonlinear feedbacks in the coupled climate−ice sheet system.

7.6.3 Eocene-Oligocene transition

The widespread occurrence of glaciomarine deposits and/or hiatuses and/or increased physical weathering at a number of sites provide a robust ensemble of evidence for a major glacial expansion over Antarctica across the EOT. Refinement of the biomagnetostratigraphic interpretation (Prydz Bay), astrochronological calibration (Ross Sea) and newly available sedimentary archives from drilling sites (Wilkes Land) allows these Antarctic sedimentary, geochemical and palaeontological records to be correlated with the global record of climate change captured by oxygen isotope values and far-field proxy records in general. The latter indicates a $\sim$500-kyr period characterised by intensified climate instability as the world transitioned from greenhouse to icehouse. The global temperature drop and the build-up of ice across the EOT were followed by a prolonged interval of maximal glacial growth known as the earliest Oligocene Glacial Maximum (EOGM). While near-field and far-field evidence define a picture of major glacial expansion across the EOT, no conclusive agreement on the amount of ice has been reached. A $\sim$70 m sea-level drop together with geochemical evidence suggest that during the EOGM the AIS might have been larger than it is today. While a larger extent of land above sea level could have accommodated a large terrestrial ice sheet, contrasting signals leave the precise size of the EOGM ice sheet in question. While no individual proxy can quantify the amount of ancient Antarctic ice based on near-field sedimentary archives, several lines of independent evidence suggest that glaciation did not reach its maximal extent until after the EOGM. Such data include the persistence of some vegetation, as observed in earliest Oligocene records from marginal settings. Furthermore, the ice sheet did not appear to have reached its maximum seaward extent at some localities.

In summary, the EOT and the associated timing and character of glaciation were much more complex than previously reconstructed from sparse Antarctic evidence and marine oxygen isotope records. A relatively major glacial expansion over East Antarctica did occur across the EOT but it possibly took millions of years for the ice sheet to reach its maximum extent over East Antarctica and parts of West Antarctica. This newly-revised view of Antarctic glacial evolution seems to be more consistent with estimates of ice sheet volume based upon oxygen isotopes (e.g., Bohaty et al., 2012; DeConto et al., 2008; Wilson et al., 2013). Accordingly, the persistence of vegetation at several Antarctic localities provides a clear indication that climate was warmer than present day during the early Oligocene.

Acknowledgements

SG and LL acknowledges funding from the Department of Pure and Applied Sciences. CE acknowledges funding by the Spanish Ministry of Economy, Industry and Competitivity (grants CTM2017-89711-C2-1/2-P), cofunded by the European Union through FEDER funds. IS was supported by the Australian Research Council Discovery Project 180102280. A.T. Kennedy Asser was supported by NERC funding (grant no. NE/L002434/1) Edward Gasson is funded by the Royal Society. EG is funded by the Royal Society. AS thanks the European Research Council for Consolidator Grant #771497 (SPANC).

References

Acosta Hospitaleche, C., 2014. New giant penguin bones from Antarctica: systematic and paleobiological significance. Comptes Rendus Palevol 13 (7), 555–560. Available from: https://doi.org/10.1016/j.crpv.2014.03.008.

Acosta Hospitaleche, C., Reguero, M., 2014. Palaeeudyptes klekowskii, the best-preserved penguin skeleton from the Eocene–Oligocene of Antarctica: taxonomic and evolutionary remarks. Geobios 47 (3), 77–85. Available from: https://doi.org/10.1016/j.geobios.2014.03.003.

Amenábar, C., Montes, M., Nozal, F., Santillana, S., 2020. Dinoflagellate cysts of the La Meseta Formation (middle to late Eocene), Antarctic Peninsula: Implications for biostratigraphy, palaeoceanography and palaeoenvironment. Geological Magazine 157 (3), 351–366. Available from: https://doi.org/10.1017/S0016756819000591.

Anagnostou, E., John, E.H., Babila, T.L., et al., 2020. Proxy evidence for state-dependence of climate sensitivity in the Eocene greenhouse. Nature Communications 11, 4436. Available from: https://doi.org/10.1038/s41467-020-17887-x.

Anagnostou, E., John, E., Edgar, K., et al., 2016. Changing atmospheric CO_2 concentration was the primary driver of early Cenozoic climate. Nature 533, 380–384. Available from: https://doi.org/10.1038/nature17423.

Anderson, J., Warny, S., Askin, R., Wellner, J., Bohaty, S., Kirshner, A., et al., 2011. Progressive Cenozoic cooling and the demise of Antarctica's last refugium. Proceedings of the National Academy of Sciences 108, 11356–11360. Available from: https://doi.org/10.1073/pnas.1014885108.

Askin, R.A., 1992. Late Cretaceous–Early Tertiary Antarctic outcrop evidence for past vegetation and climate. In: Kennett, J.P., Warnke, D.A. (Eds.), The Antarctic Paleoenvironment: A Perspective on Global Change. Antarctic Research Series, vol. 56. American Geophysical Union, Washington, DC, pp. 61–75.

Askin, R.A., 2000. Spores and pollen from the McMurdo sound erratics, Antarctica. In: Stilwell, J.D., Feldmann, R.M. (Eds.), Paleobiology and Paleoenvironments of Eocene Rocks, McMurdo Sound, East Antarctica. Antarctic Research Series, vol. 76. American Geophysical Union, Washington, DC, pp. 161–181.

Askin, R.A., Raine, J.I., 2000. Oligocene and early Miocene terrestrial palynology of the cape roberts drill hole CRP-2/2A, Victoria Land Basin, Antarctica. Terra Antartica 7 (4), 493–501.

Baatsen, M., von der Heydt, A., Huber, M., Kliphuis, M., Bijl, P., Sluijs, A., et al., 2020. The middle-to-late Eocene greenhouse climate, modelled using the CESM 1.0.5. Climate of the Past 16, 2573–2597. Available from: https://doi.org/10.5194/cp-16-2573-2020.

Baatsen, M., van Hinsbergen, D.J.J., von der Heydt, A.S., Dijkstra, H.A., Sluijs, A., Abels, H.A., et al., 2016. Reconstructing geographical boundary conditions for palaeoclimate modelling during the Cenozoic. Climate of the Past 12, 1635–1644. Available from: https://doi.org/10.5194/cp-12-1635-2016.

Baatsen, M.L.J., von der Heydt, A.S., Kliphuis, M., Viebahn, J., Dijkstra, H.A., 2018. Multiple states in the late Eocene ocean circulation. Global and Planetary Change 163 (2018), 18–28. Available from: https://doi.org/10.1016/j.gloplacha.2018.02.009.

Barker, P.F., 2001. Scotia Sea regional tectonic evolution: implications for mantle flow and palaeocirculation. Earth-Science Reviews 55 (1–2), 1–39.

Barker, P.F., Filippelli, G.M., Florindo, F., Martin, E.E., Scher, H.D., 2007. Onset and role of the Antarctic circumpolar current. Deep Sea Research II 54, 2388–2398.

Barker, P.F., Kennett, J.P., O'Connell, S., Berkowitz, S., Bryant, W.P., Burckle, H., et al., 1988. Preliminary-results of ODP Leg-113 of Joides-resolution in the Weddell Sea – history of the Antarctic Glaciation. Comptes Rendus de L'Academie des Sciences Serie II 306, 73–78.

Barrett, P.J. (Ed.), 1989. Antarctic Cenozoic History from the CIROS-1 Drillhole, McMurdo Sound, vol. 245. New Zealand DSIR Bulletin, Wellington, p. 251.

Barrett, P.J., 1996. Antarctic paleoenvironments through Cenozoic time – a review. Terra Antartica 3, 103–119.

Barrett, P.J., Hambrey, M.J., Harwood, D.M., Pyne, A.R., Webb, P.-N., 1989. Synthesis. In: Barrett, P.J. (Ed.), Antarctic Cenozoic History from the CIROS-1 Drillhole, McMurdo Sound, vol. 245. New Zealand DSIR Bulletin, Wellington, pp. 241–251.

Barrett, P.J., Hambrey, M.J., Robinson, P.H., 1991. Cenozoic glacial and tectonic history from CIROS-1, McMurdo Sound. In: Thomson, M.R.A., Crame, A., Thomson, J.W. (Eds.), Geological Evolution of Antarctica. Cambridge University Press, New York, pp. 651–656.

Barron, J., Larsen, B., Shipboard Scientific Party, 1991. In: Proceedings of the Ocean Drilling Program, Scientific Results, Leg 119. Available from: <http://www-odp.tamu.edu/publications/119_SR/119TOC.HTM>.

Beamud, E., Montes, M., Santillana, S., Nozal, F., Marenssi, S., 2015. Magnetostratigraphic dating of Paleogene sediments in the Seymour Island (Antarctic Peninsula): a preliminary chronostratigraphy. American Geophysical Union, Fall Meeting, Abstract GP51B-1331.

Bijl, P., Schouten, S., Sluijs, A., et al., 2009. Early Palaeogene temperature evolution of the southwest Pacific Ocean. Nature 461, 776–779. Available from: https://doi.org/10.1038/nature08399.

Bijl, P.K., Bendle, J.A., Bohaty, S.M., Pross, J., Schouten, S., Tauxe, L., et al., 2013. Eocene cooling linked to early flow across the Tasmanian Gateway. Proceedings of the National Academy of Sciences 110 (24), 9645–9650.

Bijl, P.K., Houben, A.J.P., Hartman, J.D., Pross, J., Salabarnada, A., Escutia, C., et al., 2018. Paleoceanography and ice sheet variability offshore Wilkes Land, Antarctica – part 2: insights from Oligocene–Miocene dinoflagellate cyst assemblages. Climate of the Past 14, 1015–1033. Available from: https://doi.org/10.5194/cp-14-1015-2018.

Bindoff, N.L., Rosenberg, M.A., Warner, M.J., 2000. On the circulation and water masses over the Antarctic continental slope and rise between 80 and 150°E. Deep Sea Research Part II: Topical Studies in Oceanography 47 (12–13), 2299–2326. Available from: https://doi.org/10.1016/S0967-0645(00)00038-2.

Birkenmajer, K., 1980a. A revised lithostratigraphic standard for the tertiary of King George Island, South Shetland Islands (West Antarctica). Bulletin of the Polish Academy of Sciences, Earth Sciences 27 (1–2), 49–57.

Birkenmajer, K., 1980b. Tertiary volcanic–sedimentary succession at Admiralty Bay, King George Island (South Shetland Islands, Antarctica). Studia Geologica Polonica 64, 7–65.

Birkenmajer, K., 1981. Lithostratigraphy of the Point Hennequin Group (Miocene volcanics and sediments) at King George Island (South Shetland Islands, Antarctica). Studia Geologica Polonica 74, 175–197.

Birkenmajer, K., 1989. A guide to tertiary geochronology of King George Island, West Antarctica. Polish Polar Research 10, 555–579.

Birkenmajer, K., 1990. Geochronology and climatostratigraphy of tertiary glacial and interglacial successions on King George Island, South Shetland Islands (West Antarctica). Zentralblatt für Geologie und Paläontologie 1, 141–151.

Birkenmajer, K., 1997. Tertiary glacial/interglacial palaeoenvironments and sea-level changes, King George Island, West Antarctica. An overview. Bulletin of the Polish Academy of Sciences, Earth Sciences 44, 157–181.

Birkenmajer, K., Delitala, M.C., Narebski, W., Nicoletti, M., Petrucciani, C., 1986. Geochronology of tertiary island-arc volcanics and glacigenic deposits, King George Island, South Shetland Islands (West Antarctica). Bulletin of the Polish Academy of Sciences, Earth Sciences 34 (3), 257–273.

Birkenmajer, K., Gazdzicki, A., Krajewski, K.P., Przybycin, A., Solecki, A., Tatur, A., et al., 2005. First Cenozoic glaciers in West Antarctica. Polish Polar Research 26, 3–12.

Birkenmajer, K., Zastawniak, E., 1989a. Late cretaceous–early tertiary floras of King George Island, West Antarctica: their stratigraphic distribution and palaeoclimatic significance, origins and evolution of the Antarctic biota. Geological Society of London Special Publication 147, 227–240.

Birkenmajer, K., Zastawniak, E., 1989b. Late cretaceous–early Neogene vegetation history of the Antarctic Peninsula sector, Gondwana breakup and tertiary glaciations. Bulletin of the Polish Academy of Sciences, Earth Sciences 37, 63–88.

Bo, S., Siegert, M., Mudd, S., Sugden, D., Fujita, S., Xiangbin, C., et al., 2009. The Gamburtsev mountains and the origin and early evolution of the Antarctic Ice Sheet, Nature 459, 690–693. Available from: https://doi.org/10.1038/nature08024.

Bohaty, S.M., Delaney, M.L., Zachos, J.C., 2012. Foraminiferal Mg/Ca and Mn/Ca ratios across the Eocene–Oligocene transition. Earth and Planetary Science Letters 317–318, 251.

Boulton, G.S., 1990. Processes and sediments. In: Dowdeswell, J.A., Scourse, J.D. (Eds.), Glaciomarine Environments, vol. 53. Geological Society of London, Special Publications, pp. 15–52.

Brea, M., 1996. Analisis de los anillos de crecimiento de leños fosiles de coniferas de la Formacion La Meseta, Isla Seymour, Antartida. Congreso Paleogeno de America del Sur. Resumenes, Santa Rosa, p. 28.

Brea, M., 1998. Analisis de los Anillos de Crecimiento en Leños Fosiles de Coníferas de la Formacion La Meseta, Isla Seymour (Marambio), Antartida. In: Casadio, S. (Ed.), Paleogeno de America del Sur y de la Peninsula Antartica. Asociacion Paleontologica Argentina, Buenos Aires, pp. 163–175. Publicacion Especial.

Brinkhuis, H., Munsterman, D.K., Sengers, S., Sluijs, A., Warnaar, J., Williams, G.L., 2003. Late Eocene–quaternary dinoflagellate cysts from ODP site 1168, off Western Tasmania. In: Exon, N.F., Kennett, J.P., Malone, M.J. (Eds.), Proceedings of the Ocean Drilling Program, Scientific Results, 189. Available from: <http://www-odp.tamu.edu/publications/189_SR/105/105.htm>.

Caballero, R., Huber, M., 2013. State-dependent climate sensitivity in past warm climates and its implications for future climate projections. PNAS 110 (35), 14162–14167.

Cande, S.C., Mutter, J.C., 1982. A revised identification of the oldest sea-floor spreading anomalies between Australia and Antarctica. Earth and Planetary Science Letters 58 (2), 151–160.

Cande, S.C., Stock, J.M., 2004. Cenozoic reconstructions of the australia-new zealand-south pacific sector of Antarctica. Geophysical Monograph Series 151, 5–17. Available from: https://doi.org/10.1029/151GM02.

Carter, A., Riley, T.R., Hillenbrand, C.-D., Rittner, M., 2017. Widespread Antarctic glaciation during the Late Eocene. Earth and Planetary Science Letters 458, 49–57. Available from: https://doi.org/10.1016/j.epsl.2016.10.045.

Case, J.A., 1988. Paleogene floras from Seymour Island, Antarctic Peninsula. Memoir of the Geological Society of America 169 (1), 523–539. Available from: https://doi.org/10.1130/MEM169-p523.

Colleoni, F., De Santis, L., Montoli, E., Olivo, E., Sorlien, C.C., Bart, P.J., et al., 2018. Past continental shelf evolution increased Antarctic ice sheet sensitivity to climatic conditions. Scientific Reports 8 (1), 11323. Available from: https://doi.org/10.1038/s41598-018-29718-7.

Contreras, L., Pross, J., Bijl, P.K., Koutsodendris, A., Raine, J.I., van de Schootbrugge, B., et al., 2013. Early to Middle Eocene vegetation dynamics at the Wilkes Land Margin (Antarctica). Review of Palaeobotany and Palynology 197, 119–142. Available from: https://doi.org/10.1016/j.revpalbo.2013.05.009.

Cooper, A.K., O'Brien, P.E., 2004. Leg 188 synthesis: transitions in the glacial history of the Prydz Bay region, East Antarctica, from ODP drilling. In: Cooper, A.K., O'Brien, P.E., Richter, C. (Eds.), Proceedings of the Ocean Drilling Program, Scientific Results, 188. Available from: <http://www-odp.tamu.edu.publications/188_SR/synth/synth.htm>.

Cooper, A.K., O'Brien, P.E., Shipboard Scientific Party, 2004. Prydz Bay – Co-operation Sea, Antarctica: glacial history and paleoceanography sites 1165–1167. In: Proceedings of the Ocean Drilling Program, Scientific Results, p. 188. Available from: <http://www-odp.tamu.edu.publications/188_SR/188TOC.HTM>.

Cooper, A.K., Stagg, H., Geist, E.L., 1991. Seismic stratigraphy and structure of Prydz Bay, Antarctica: implications for Leg 119 drilling. In: Proceedings of the Ocean Drilling Program, Scientific Results, 119. Available from: <http://www-odp.tamu.edu/publications/119_SR/119TOC.HTM>.

Costa, E., Garcés, M., Sáez, A., Cabrera, L., López-Blanco, M., 2011. The age of the "Grande Coupure" mammal turnover: new constraints from the Eocene–Oligocene record of the Eastern Ebro Basin (NE Spain). Palaeogeography, Palaeoclimatology, Palaeoecology 301, 97–107.

Coxall, H.K., Huck, C.E., Huber, M., et al., 2018. Export of nutrient rich northern component water preceded early Oligocene Antarctic glaciation. Nature Geoscience 11, 190–196. Available from: https://doi.org/10.1038/s41561-018-0069-9.

Coxall, H.K., Pearson, P.N., 2007. The Eocene-Oligocene transition. Deep Time Perspectives on Climate Change: Marrying the Signal from Computer Models and Biological Proxies. pp. 351–387.

Coxall, H.K., Wilson, P.A., 2011. Early Oligocene glaciation and productivity in the eastern equatorial Pacific: insights into global carbon cycling. Paleoceanography 26, PA2221.

Coxall, H.K., Wilson, P.A., Palike, H., Lear, C.H., Backman, J., 2005. Rapid stepwise onset of Antarctic glaciation and deeper calcite compensation in the Pacific Ocean. Nature 433, 53–57.

Crame, J.A., Beu, A.G., Ineson, J.R., Francis, J.E., Whittle, R.J., Bowman, V.C., 2014. The early origin of the Antarctic Marine Fauna and its evolutionary implications. PLoS One 9 (12), e114743. Available from: https://doi.org/10.1371/journal.pone.0114743.

Cramwinckel, M.J., Huber, M., Kocken, I.J., et al., 2018. Synchronous tropical and polar temperature evolution in the Eocene. Nature 559, 382–386. Available from: https://doi.org/10.1038/s41586-018-0272-2.

CRP Science Team, 2000. Studies from the Cape Roberts Project, Ross Sea, Antarctica. Initial Report on CRP-3. Terra Antartica 7, 1–209. With Supplement, 305 pp.

Dalziel, I., 2006. On the extent of the active West Antarctic Rift System. Terra Antartica Reports 12, 193–202.

Davis, S.N., Torres, C.R., Musser, G.M., Proffitt, J.V., Crouch, N.M.A., Lundelius, E.L., et al., 2020. New mammalian and avian records from the late Eocene la Meseta and Submeseta formations of Seymour Island, Antarctica. PeerJ 2020 (1), 8268. Available from: https://doi.org/10.7717/peerj.8268.

De Boer, B., Stocchi, P., van de Wal, R.W.S., 2014. A fully coupled 3-D ice- sheet – sea-level model: algorithm and applications. Geoscience Model Development Discussions 7, 2141–2156. Available from: https://doi.org/10.5194/gmd-7-2141-2014.

DeConto, R.M., Pollard, D., 2003. Rapid Cenozoic glaciation of Antarctica induced by declining atmospheric CO_2. Nature 421, 245–249.

DeConto, R.M., Pollard, D., Harwood, D., 2007. Sea ice feedback and Cenozoic evolution of Antarctic climate and ice sheets. Paleoceanography 22, PA3214. Available from: https://doi.org/10.1029/2000PA000567.

DeConto, R.M., Pollard, D., Wilson, P.A., Pälike, H., Lear, C.H., Pagani, M., 2008. Thresholds for Cenozoic bipolar glaciation. Nature 455 (7213), 652–656. Available from: https://doi.org/10.1038/nature07337.

Devereux, I., 1967. Oxygen isotope paleotemperature measurements on New Zealand tertiary fossils. New Zealand Journal of Science 10, 988–1011.

Diester-Haass, L., Zahn, R., 1996. Eocene–Oligocene transition in the Southern Ocean: history of water mass circulation and biological productivity. Geology 24, 163–166.

Diester-Haass, L., Zahn, R., 2001. Paleoproductivity increase at the Eocene–Oligocene climatic transition: ODP/DSDP sites 763 and 592. Palaeogeography, Palaeoclimatology, Palaeoecology 172, 153–170.

Dingle, R., Lavelle, M., 1998. Late Cretaceous–Cenozoic climatic variations of the Northern Antarctic Peninsula: new geochemical evidence and review. Palaeogeography, Palaeoclimatology, Palaeoecology 141 (3), 215–232.

Doktor, M., Gazdzicki, A.J., Jermanska, A., Porebski, S., Zastawaniak, E., 1996. A plant–fish assemblage from the Eocene La Meseta Formation of Seymour Island (Antarctic Peninsula) and its environmental implications. Acta Palaeontologica Polonica 55, 127–146.

Doktor, M., Gazdzicki, A., Marenssi, S., Porebski, S., Santillana, S., Vrba, A., 1988. Argentine–Polish geological investigations on Seymour (Marambio) Island, Antarctica. Polish Polar Research 9, 521–541.

Douglas, P.M.J., Affek, H.P., Ivany, L.C., et al., 2014. Pronounced zonal heterogeneity in Eocene southern high-latitude sea surface temperatures. PNAS 111 (18), 6582–6587.

Dunbar, G.B., Naish, T.R., Barrett, P.J., Fielding, C.R., Powell, R.D., 2008. Constraining the amplitude of late Oligocene bathymetric changes in Western Ross Sea during orbitally-induced oscillations in the East Antarctic Ice Sheet: (1) Implications for glacimarine sequence stratigraphic models, Palaeogeography, Palaeoclimatology, Palaeoecology, 260 (1–2), 50–65. Available from: https://doi.org/10.1016/j.palaeo.2007.08.018.

Duncan, B., McKay, R., Bendle, J., Naish, T., Inglis, G.N., Moossen, H., et al., 2019. Lipid biomarker distributions in Oligocene and Miocene sediments from the Ross Sea region, Antarctica: implications for use of biomarker proxies in glacially-influenced settings. Palaeogeography, Palaeoclimatology, Palaeoecology 516, 71–89. Available from: https://doi.org/10.1016/j.palaeo.2018.11.028.

Dutton, A., Lohmann, K., Zinsmeister, W.J., 2002. Stable isotope and minor element proxies for Eocene climate of Seymour Island, Antarctica. Paleoceanography 17 (2), 1016. Available from: https://doi.org/10.1029/2000PA000593.

Eagles, G., Livermore, R., Morris, P., 2006. Small basins in the Scotia Sea; the Eocene drake passage gateway. Earth and Planetary Science Letters 242 (3–4), 343–353.

Ehrmann, W., 1997. Smectite concentrations and crystallinities: Indications for Eocene age of glaciomarine sediments in the CIROS-1 Drill Hole, McMurdo Sound, Antarctic. In: Ricci, E.A. (Ed.), The Antarctic Region, Geological Evolution and Processes. Museo Nazionale dell'Antartide, Siena, pp. 771–780.

Ehrmann, W.U., Mackensen, A., 1992. Sedimentological evidence for the formation of an East Antarctic Ice Sheet in Eocene/Oligocene time. Palaeogeography, Palaeoclimatology, Palaeoecology 93, 85–112.

Eittreim, S.L., Cooper, A.K., Wannesson, J., 1995. Seismic stratigraphic evidence of ice-sheet advances on the Wilkes Land margin of Antarctica. Sedimentary Geology 96 (1–2), 131–156.

Elliot, D.H., Trautman, T.A., 1982. Lower tertiary strata on Seymour Island, Antarctic Peninsula. In: Craddock, C. (Ed.), Antarctic Geoscience. University of Wisconsin Press, Madison, pp. 287–298.

Elsworth, G., Galbraith, E., Halverson, G., Yang, S., 2017. Enhanced weathering and CO2 drawdown caused by latest Eocene 1445 strengthening of the Atlantic meridional overturning circulation. Nature Geoscience 10 (3), 213–216. Available from: https://doi.org/10.1038/ngeo2888.

Escutia, C., Brinkhuis, H., 2014. From greenhouse to icehouse at the Wilkes Land Antarctic Margin: IODP Expedition 318 synthesis of results. Developments in Marine Geology 7, 295–328.

Escutia, C., Brinkhuis, H., Klaus, A., the Expedition 318 Scientists, 2011. Proceedings of Integrated Ocean Drilling Program 318 (Integrated Ocean Drilling Program Management International).

Evangelinos, D., Escutia, C., Etourneau, J., Hoem, F., Bijl, P., Boterblom, W., et al., 2020. Late Oligocene-Miocene proto-Antarctic circumpolar current dynamics off the Wilkes Land margin, East Antarctica. Global and Planetary Change 191, 103221. Available from: https://doi.org/10.1016/j.gloplacha.2020.103221.

Evans, D., Wade, B.S., Henehan, M., Erez, J., Müller, W., 2016. Revisiting carbonate chemistry controls on planktic foraminifera Mg/Ca: implications for sea surface temperature and hydrology shifts over the Paleocene–Eocene Thermal Maximum and 1455 Eocene–Oligocene transition. Climate of the Past 12 (4), 819–835. Available from: https://doi.org/10.5194/cp-12-819-2016.

Farrell, W.E., Clark, J.A., 1976. On postglacial sea level. Geophysical Journal International 46 (3), 647–667. Available from: https://doi.org/10.1111/j.1365-246X.1976.tb01252.x.

Fielding, C., Naish, T.R., Woolfe, K.J., 2001. Facies architecture of the CRP-3 drillhole, Victoria Land Basin, Antarctica. Terra Antarctica 8 (3), 217–224.

Fielding, C.R., Whittaker, J., Henrys, S.A., Wilson, T.J., Naish, T.R., 2008. Seismic facies and stratigraphy of the Cenozoic succession in McMurdo Sound, Antarctica: Implications for tectonic, climatic and glacial history. Palaeogeography, Palaeoclimatology, Palaeoecology 260 (1–2), 8–29.

Fielding, C.R., Woolfe, K.J., Purdon, R.G., Lavelle, M.A., Howe, J.A., 1997. Sedimentological and stratigraphical re-evaluation of the CIROS-1 Core, McMurdo Sound, Antarctica. Terra Antartica 4, 149–160.

Fioroni, C., Villa, G., Persico, D., Wise, S.W., Pea, L., 2012. Revised middle Eocene-upper Oligocene calcareous nannofossil biozonation for the Southern Ocean. Revue de Micropaléontologie 55, 53–70. Available from: https://doi.org/10.1016/j.revmic.2012.03.001.

Florindo, F., Wilson, G.S., Roberts, A.P., Sagnotti, L., Verosub, K.L., 2005. Magnetostratigraphic chronology of a late Eocene to early Miocene glacimarine succession from the Victoria Land Basin, Ross Sea, Antarctica. Global and Planetary Change 45, 207–236.

Foster, G.L., Royer, D.L., Lunt, D.J., 2017. Future climate forcing potentially without precedent in the last 420 million years. Nature Communications 8, 14845. Available from: https://doi.org/10.1038/ncomms14845.

Francis, J.E., 1991. Palaeoclimatic significance of Cretaceous–Early Tertiary fossil forests of the Antarctic Peninsula. In: Thomson, M.R.A., Crame, A., Thomson, J.W. (Eds.), Geological Evolution of Antarctica. Cambridge University Press, New York, pp. 623–627.

Francis, J.E., 1999. Evidence from fossil plants for Antarctic palaeoclimates over the past 100 million years. In: Barrett, P.J., Orombelli, G. (Eds.), Geological Records of Global and Planetary Changes. Terra Antartica Report 3, Siena, pp. 43–52.

Francis, J.E., 2000. Fossil wood from Eocene high latitude forests, McMurdo Sound, Antarctica. In: Stilwell, J.D., Feldmann, R.M. (Eds.), Paleobiology and Palaeoenvironments of Eocene Rocks, McMurdo Sound, East Antarctica. Antarctic Research Series, vol. 76. American Geophysical Union, Washington, DC, pp. 253–260.

Francis, J.E., Ashworth, A., Cantrill, D.J., Crame, J.A., Howe, J., Stephens, R., et al., 2008. 100 Million Years of Antarctic Climate Evolution: Evidence from Fossil Plants. United States Geological Survey and The National Academies; USGS OFR-2007.

Francis, J.E., Marenssi, S., Levy, R., Hambrey, M., Thorn, V.C., Mohr, B., et al., 2009. Chapter 8: From greenhouse to icehouse – the Eocene/Oligocene in Antarctica. In: Florindo, F., Siegert, M.J. (Eds.), Developments in Earth and Environmental Sciences. Antarctic Climate Evolution, vol. 8. Elsevier, pp. 309–368.

Francis, J.E., Poole, I., 2002. Cretaceous and early tertiary climates of Antarctica: evidence from fossil wood. Palaeogeography, Palaeoclimatology, Palaeoecology 182 (1–2), 47–64.

Francis, J.E., Tosolini, A.-M., Cantrill, D., 2004. Biodiversity and climate change in Antarctic Palaeogene floras. In: VII International Organisation of Palaeobotany Conference, Bariloche, Argentina, pp. 33–34, Abstract Volume.

Fyke, J.G., D'Orgeville, M., Weaver, A.J., 2015. Drake passage and Central American Seaway controls on the distribution of the oceanic carbon reservoir. Global and Planetary Change 128 (0), 72–82. Available from: https://doi.org/10.1016/j.gloplacha.2015.02.011.

Galeotti, S., DeConto, R., Naish, T., Stocchi, P., Florindo, F., Pagani, M., et al., 2016. Antarctic Ice Sheet variability across the Eocene-Oligocene boundary climate transition. Science (New York, N.Y.) 352 (6281), 76–80. Available from: https://doi.org/10.1126/science.aab0669.

Galeotti, S., Lanci, L., Florindo, F., Naish, T.R., Sagnotti, L., Sandroni, S., et al., 2012. Cyclochronology of the Eocene–Oligocene transition from a glacimarine succession off the Victoria Land coast, Cape Roberts Project, Antarctica. Palaeogeography, Palaeoclimatology, Palaeoecology 335–336, 84–94. Available from: https://doi.org/10.1016/j.palaeo.2011.08.011.

Gandolfo, M.A., Hoc, P., Santillana, S., Marenssi, S.A., 1998a. Una Flor Fosil Morfologicamente Afın a las Grossulariaceae (Orden Rosales) de la Formacion La Meseata (Eoceno medio), Isla Marambio, Antartida. In: Casadio, S. (Ed.), Paleógeno de America del Sur y de la Peninsula Antartica. Asociacion Paleontologica Argentina, Buenos Aires, pp. 147–153. Publicación Especial.

Gandolfo, M.A., Marenssi, S.A., Santillana, S.N., 1998b. Flora y Paleoclima de la Formacion La Meseta (Eoceno medio), Isla Marambio (Seymour), Antartida. In: Casadio, S. (Ed.), Paleogeno de America del Sur y de la Peninsula Antartica. Asociacion Paleontologica Argentina, Buenos Aires, pp. 155–162. Publicacion Especial.

Gandolfo, M.A., Marenssi, S.A., Santillana, S.N., 1998c. Flora y Paleoclima de la Formacion La Meseta (Eoceno-Oligoceno Inferior?) Isla Marambio (Seymour), Antartida. In: I Congreso del Paleogeno de America del Sur, La Pampa, Argentina, Actas, pp. 31–32.

Gasson, E.G.W., Keisling, B.A., 2020. The antarctic ice sheet: a paleoclimate modeling perspective. Oceanography 33 (2), 91–100. Available from: https://doi.org/10.5670/oceanog.2020.208.

Gasson, E., Lunt, D.J., Deconto, R., Goldner, A., Heinemann, M., Huber, M., et al., 2014. Uncertainties in the modelled CO_2 threshold for Antarctic glaciation. Climate of the Past 10 (2). Available from: https://doi.org/10.5194/cp-10-451-2014.

Gelfo, J.N., Goin, F.J., Bauzá, N., Reguero, M., 2019. The fossil record of Antarctic land mammals: commented review and hypotheses for future research. Advances in Polar Science 30, 274–292.

Goldner, A., Herold, N., Huber, M., 2014. Antarctic glaciation caused ocean circulation changes at the Eocene-Oligocene transition. Nature 511 (7511), 574–577. Available from: https://doi.org/10.1038/nature13597.

Goldner, A., Huber, M., Caballero, R., 2013. Does antarctic glaciation cool the world? Climate of the Past 9 (1), 173–189. Available from: https://doi.org/10.5194/cp-9-173-2013.

Gomez, N., et al., 2010. A new projection of sea level change in response to collapse of marine sectors of the Antarctic Ice-Sheet. Geophysical Journal International 180, 623–634.

Gothan, W., 1908. Die Fossilen Holzer von der Seymour und Snow Hill Insel. In: Nordenskjold, O. (Ed.), Wissenschaftliche Erbegnesse Schwedischen Sudpolar Expedition 1901–1903. pp. 1–33. Stockholm.

Greenwood, D.R., Wing, S.L., 1995. Eocene continental climates and latitudinal temperature gradients. Geology 23 (11), 1044–1048. Available from: https://doi.org/10.1130/0091-7613.

Griffies, S.M., Winton, M., Anderson, W.G., Benson, R., Delworth, T.L., Dufour, C.O., et al., 2015. Impacts on ocean heat from transient mesoscale eddies in a hierarchy of climate models. Journal of Climate 28 (3), 952–977. Available from: https://doi.org/10.1175/JCLI-D-14-00353.1.

Gulick, S.P.S., Shevenell, A.E., Montelli, A., Fernandez, R., Smith, C., Warny, S., et al., 2017. Initiation and long-term instability of the East Antarctic Ice Sheet. Nature 552 (7684), 225–229. Available from: https://doi.org/10.1038/nature25026.

Hambrey, M.J., Barrett, P.J., 1993. Cenozoic sedimentary and climatic record, Ross Sea region, Antarctica. In: Kennett, J.P., Warnke, D.A. (Eds.), The Antarctic Paleoenvironment: A Perspective on Global Change, Part 2. Antarctic Research Series, vol. 60. American Geophysical Union, Washington, DC, pp. 91–124.

Hambrey, M.J., Barrett, P.J., Ehrmann, E.H., Larsen, B., 1992. Cenozoic sedimentary processes on the Antarctic continental shelf: The record from deep drilling. Zeitschrift für Geomorphologie 86 (Suppl), 73–99.

Hambrey, M.J., Barrett, P.J., Powell, R.D., 2002. Late Oligocene and early Miocene glacimarine sedimentation in the SW Ross Sea, Antarctica: the record from offshore drilling. In: O'Cofaigh, C., Dowdeswell, J.A. (Eds.), Glacier-Influence Sedimentation on High-Latitude Continental Margins, 203. Geological Society of London Special Publication, pp. 105–128.

Hambrey, M.J., Barrett, P.J., Robinson, P.H., 1989. Stratigraphy. In: Barrett, P.J. (Ed.), Antarctic Cenozoic History from the CIROS-1 Drillhole, McMurdo Sound, 245. New Zealand DSIR Bulletin, Wellington, pp. 23–48.

Hambrey, M.J., Ehrmann, E.H.R., Larsen, B., 1991. The Cenozoic glacial record of the Prydz Bay continental shelf, East Antarctica. In: Barron, J., Larsen, B., Shipboard Scientific Party (Eds.), Proceedings of the Ocean Drilling Program, Scientific Results, p. 119. Available from: <http://www-odp.tamu.edu/publications/119_SR/119TOC.HTM>.

Haomin, L., 1994. Early tertiary fossil hill flora from Fildes Peninsula of King George Island, Antarctica. In: Yanbin, S. (Ed.), Stratigraphy and Palaeontology of Fildes Peninsula, King George Island, Antarctica, State Antarctic Committee. Science Press, Beijing, pp. 165–171. Monograph 3.

Hartman, J.D., Sangiorgi, F., Salabarnada, A., Peterse, F., Houben, A.J.P., Schouten, S., et al., 2018. Paleoceanography and ice sheet variability offshore Wilkes Land, Antarctica-Part 3: Insights from Oligocene-Miocene TEX86-based sea surface temperature reconstructions. Climate of the Past 14 (9), 1275–1297. Available from: https://doi.org/10.5194/cp-14-1275-2018.

Haywood, A.M., Smellie, J.L., Ashworth, A.C., Cantrill, D.J., Florindo, F., Hambrey, M.J., et al., 2008. Middle Miocene to Pliocene history of Antarctica and the Southern Ocean 405. In: Florindo, F., Siegert, M. (Eds.), Antarctic Climate Evolution, vol. 8. Elsevier, Amsterdam, pp. 401–463.

Henrys, S.A., Wilson, T., Whittaker, J.M., Fielding, C., Hall, J., Naish, T., 2007. Tectonic history of mid-Miocene to present southern Victoria Land Basin, inferred from seismic stratigraphy in McMurdo Sound, Antarctica. In: Cooper, A.K., Raymond, C.R., et al. (Eds.), Antarctica: A Keystone in a Changing World – Online Proceedings of the 10th International Symposium on Antarctic Earth Sciences, United States Geological Survey Open-File Report 2007-1047, Short Research Paper 049. 4 pp. Available from: https://doi.org/10.3133/of2007-1047.srp049.

Herold, N., Huber, M., Müller, R.D., Seton, M., 2012. Modeling the Miocene climatic optimum: ocean circulation. Paleoceanography 27 (1), PA1209. Available from: https://doi.org/10.1029/2010PA002041.

Hiemstra, J.F., 1999. Microscopic evidence of grounded ice in the sediments of the CIROS-1 Core, McMurdo Sound, Antarctica. Terra Antartica 6, 365–376.

Hill, D.J., Haywood, A.M., Valdes, P.J., Francis, J.E., Lunt, D.J., Wade, B.S., 2013. Paleogeographic controls on the onset of the Antarctic circumpolar current. Geophysical Research Letters 40 (19), 5199–5204.

Hill, R.S., 1989. Palaeontology-fossil leaf. In: Barrett, P.J. (Ed.), Antarctic Cenozoic History from the CIROS-1 Drillhole, McMurdo Sound, 245. New Zealand DSIR Bulletin, Wellington, pp. 143–144.

Hill, P.J., Exon, N.F., 2004. Tectonics and basin development of the offshore Tasmanian area incorporating results from deep ocean drilling. Geophysical Monograph Series 151, 19–42. Available from: https://doi.org/10.1029/151GM03.

Hochmuth, K., et al., 2020. The evolving paleobathymetry of the Circum-Antarctic Southern Ocean since 34 Ma: a key to understanding past cryosphere-ocean developments. Geochemistry, Geophysics, Geosystems 21 (8), e2020GC009122.

Houben, A.J.P., et al., 2012. The Eocene–Oligocene transition: changes in sea level, temperature or both? Palaeogeography, Palaeoclimatology, Palaeoecology 335–336, 75–83.

Houben, A.J.P., 2019. Late Eocene Southern Ocean cooling and invigoration of circulation preconditioned Antarctica for full-scale glaciation. Geochemistry, Geophysics, Geosystems 20 (5), 2214–2234.

Houben, A.J.P., Bijl, P.K., Guerstein, G.R., Sluijs, A., Brinkhuis, H., 2011. Malvinia escutiana, a new biostratigraphically important Oligocene dinoflagellate cyst from the Southern Ocean. Review of Palaeobotany and Palynology 165 (3–4), 175–182. Available from: https://doi.org/10.1016/j.revpalbo.2011.03.002.

Houben, A.J.P., Bijl, P.K., Pross, J., Bohaty, S.M., Stckley, C.E., Passchier, S., et al., 2013. Reorganization of Southern ocean plankton ecosystem at the onset of Antarctic glaciation. Science (New York, N.Y.) 340 (6130), 341–344.

Huang, X., Gohl, K., Jokat, W., 2014. Variability in Cenozoic sedimentation and paleo-water depths of the Weddell Sea basin related to pre-glacial and glacial conditions of Antarctica. Global and Planetary Change 118, 25–41. Available from: https://doi.org/10.1016/j.gloplacha.2014.03.010.

Huber, M., Caballero, R., 2011. The early Eocene equable climate problem revisited. Climate of the Past 7, 603–633. Available from: https://doi.org/10.5194/cp-7-603-2011.

Huber, M., Nof, D., 2006. The ocean circulation in the southern hemisphere and its climatic impacts in the Eocene. Palaeogeography, Palaeoclimatology, Palaeoecology 231, 9–28.

Huber, M., Brinkhuis, H., Stickley, C.E., Döös, K., Sluijs, A., Warnaar, J., et al., 2004. Eocene circulation of the Southern Ocean: Was Antarctica kept warm by subtropical waters? Paleoceanography 19 (4), PA4026. Available from: https://doi.org/10.1029/2004PA001014.

Hunt, R., 2001. Biodiversity and Palaeoecology of Tertiary Fossil Floras in Antarctica. Ph.D. Thesis, University of Leeds, Leeds, United Kingdom.

Hunt, R.J., Poole, I., 2003. Paleogene West Antarctic climate and vegetation history in light of new data from King George Island. In: Wing, S.L., Gingerich, P.D., Schmitz, B., Thomas, E. (Eds.), Causes and Consequences of Globally Warm Climates in the Early Paleogene, vol. 369. Geological Society of America, Boulder, CO, pp. 395–412.

Hutchinson, D.K., Coxall, H.K., Lunt, D.J., Steinthorsdottir, M., de Boer, A.M., Baatsen, M., et al., 2021. The Eocene-Oligocene transition: a review of marine and terrestrial proxy data, models and model-data comparisons. Climate of the Past 17 (1), 269–315. Available from: https://doi.org/10.5194/cp-17-269-2021.

Hutchinson, D.K., Coxall, H.K., O'Regan, M., Nilsson, J., Caballero, R., de Boer, A.M., 2019. Arctic closure as a trigger for Atlantic overturning at the Eocene-Oligocene Transition. Nature Communications 10 (1). Available from: https://doi.org/10.1038/s41467-019-11828-z.

Hutchinson, D.K., de Boer, A.M., Coxall, H.K., Caballero, R., Nilsson, J., Baatsen, M.J.L., 2018. Climate sensitivity and meridional overturning circulation in the late Eocene using GFDL CM2.1. Climate of the Past 14, 789–810. Available from: https://doi.org/10.5194/cp-14-789-2018.

Ivany, L.C., Lohmann, K.C., Hasiuk, F., Blake, D.B., Glass, A., Aronson, R.B., et al., 2008. Eocene climate record of a high southern latitude continental shelf: Seymour Island, Antarctica. Bulletin of the Geological Society of America 120 (5–6), 659–678. Available from: https://doi.org/10.1130/B26269.1.

Jadwiszczak, P., Mörs, T., 2019. First partial skeleton of Delphinornis larseni Wiman, 1905, a slender-footed penguin from the Eocene of Antarctic Peninsula. Paleontologia Electronica 22, 1–31. Available from: https://doi.org/10.26879/933.

Jayne, S.R., Marotzke, J., 2002. The oceanic eddy heat transport. Journal of Physical Oceanography 32 (12), 3328–3345.

Jones, C.M., 2000. The first record of a fossil bird from East Antarctic. In: Stilwell, J.D., Feldmann, R.M. (Eds.), Paleobiology and Palaeoenvironments of Eocene Rocks, McMurdo Sound, East Antarctica. Antarctic Research Series, vol. 76. American Geophysical Union, Washington, DC, pp. 359–364.

Judd, E.J., Ivany, L.C., DeConto, R.M., Halberstadt, A.R.W., Miklus, N.M., Junium, C.K., et al., 2019. Seasonally resolved proxy data from the Antarctic Peninsula support a heterogeneous middle Eocene Southern Ocean. Paleoceanography and Paleoclimatology 34 (5), 787–799. Available from: https://doi.org/10.1029/2019PA003581.

Katz, M.E., Cramer, B.S., Toggweiler, J.R., Esmay, G., Liu, C., Miller, K.G., Rosenthal, Y., Wade, B.S., Wright, J.W., 2011. Impact of Antarctic Circumpolar Current Development on Late Paleogene Ocean Structure. Science 332, 1076–1079. Available from: https://doi.org/10.1126/science.1202122.

Katz, M.E., Miller, K.G., Wright, J.D., Wade, B.S., Browning, J.V., Cramer, B.S., et al., 2008. Stepwise transition from the Eocene greenhouse to the Oligocene icehouse. Nature Geoscience 1, 329. Available from: https://doi.org/10.1038/ngeo179 [online].

Keigwin Jr., L.D., 1980. Palaeoceanographic change in the pacific at the Eocene-Oligocene boundary. Nature 287 (5784), 722–725. Available from: https://doi.org/10.1038/287722a0.

Keigwin, L.D., Corliss, B.H., 1986. Stable isotopes in late middle Eocene to Oligocene foraminifera. Geological Society of America Bulletin 97 (3), 335–345. Available from: https://doi.org/10.1130/0016-7606(1986)97(335:SIILME)2.0.CO;2.

Kennedy-Asser, A.T., Farnsworth, A., Lunt, D.J., Lear, C.H., Markwick, P.J., 2015. Atmospheric and oceanic impacts of Antarctic glaciation across the Eocene-Oligocene transition. Philosophical Transactions of the Royal Society A: Mathematical, Physical and Engineering Sciences 373 (2054). Available from: https://doi.org/10.1098/rsta.2014.0419.

Kennedy-Asser, A.T., Lunt, D.J., Valdes, P.J., Ladant, J.-B., Frieling, J., Lauretano, V., 2020. Changes in the high-latitude Southern Hemisphere through the Eocene-Oligocene transition: a model-data comparison. Climate of the Past 16 (2), 555–573. Available from: https://doi.org/10.5194/cp-16-555-2020.

Kennett, J.P., 1977. Cenozoic evolution of Antarctic glaciation, the circum-Antarctic oceans and their impact on global paleoceanography. Journal of Geophysical Research 82, 3843–3859.

Kennett, J.P., Shackleton, N.J., 1976. Oxygen isotopic evidence for the development of the psychryosphere 38 my ago. Nature 260, 513–515.

Klages, J.P., Salzmann, U., Bickert, T., et al., 2020. Temperate rainforests near the South Pole during peak Cretaceous warmth. Nature 580, 81–86. Available from: https://doi.org/10.1038/s41586-020-2148-5.

Kominz, M.A., Pekar, S.F., 2001. Oligocene eustasy from two-dimensional sequence stratigraphic backstripping. GSA Bulletin 113, 291–304.

Kraatz, B.P., Geisler, J.H., 2010. Eocene–Oligocene transition in Central Asia and its effects on mammalian evolution. Geology 38, 111–114. Available from: https://doi.org/10.1130/G30619.1.

LaCasce, J.H., 2017. The prevalence of oceanic surface modes. Geophysical Research Letters 44 (21), 11–097.

LaCasce, J.H., Escartin, J., Chassignet, E.P., Xu, X., 2019. Jet instability over smooth, corrugated, and realistic bathymetry. Journal of Physical Oceanography 49 (2), 585–605.

Ladant, J.B., Donnadieu, Y., Lefebvre, V., Dumas, C., 2014. The respective role of atmospheric carbon dioxide and orbital parameters on ice sheet evolution at the Eocene-Oligocene transition. Paleoceanography 29 (8), 810–823. Available from: https://doi.org/10.1002/2013PA002593.

Lagabrielle, Yves, et al., 2009. The tectonic history of Drake Passage and its possible impacts on global climate. Earth and Planetary Science Letters 279 (3–4), 197–211.

Langton, S.J., Rabideaux, N.M., Borrelli, C., Katz, M.E., 2016. Southeastern Atlantic deep-water evolution during the late-middle Eocene to earliest Oligocene (ocean drilling program site 1263 and deep sea drilling project site 366). Geosphere 12 (3), 1032–1047. Available from: https://doi.org/10.1130/GES01268.1.

Lear, C.H., Bailey, T.R., Pearson, P.N., Coxall, H.K., Rosenthal, Y., 2008. Cooling and ice growth across the Eocene-Oligocene transition. Geology 36 (3), 251. Available from: https://doi.org/10.1130/G24584A.1.

Levy, R.H., Harwood, D.M., 2000a. Sedimentary lithofacies of the McMurdo sound erratics. In: Stilwell, J.D., Feldmann, R.M. (Eds.), Paleobiology and Paleoenvironments of Eocene Rocks, McMurdo Sound, East Antarctica. Antarctic Research Series, vol. 76. American Geophysical Union, Washington, DC, pp. 39–61.

Levy, R.H., Harwood, D.M., 2000b. Tertiary marine palynomorphs from the McMurdo sound erratics, Antarctica. In: Stilwell, J.D., Feldmann, R.M. (Eds.), Paleobiology and Paleoenvironments of Eocene Rocks, McMurdo Sound, East Antarctica. Antarctic Research Series, vol. 76. American Geophysical Union, Washington, DC, pp. 183–242.

Lewis, A.R., Marchant, D.R., Ashworth, A.C., Hedenäs, L., Hemming, S.R., Johnson, J.V., et al., 2008. Mid-Miocene cooling and the extinction of tundra in continental Antarctica. Proceedings of the National Academy of Sciences 105, 10676–10680.

Li, H.M., 1992. Early Tertiary palaeoclimate of King George Island, Antarctica – evidence from the fossil hill flora. In: Yoshida, Y., Kaminuma, K., Shiraishi, K. (Eds.), Recent Progress in Antarctic Earth Science. Terra Scientific Publishing Company, Tokyo, pp. 371–375.

Liu, Z., Pagani, M., Zinniker, D., DeConto, R., Huber, M., Brinkhuis, H., et al., 2009. Global cooling during the eocene-oligocene climate transition. Science (New York, N.Y.) 323 (5918), 1187–1190. Available from: https://doi.org/10.1126/science.1166368.

Livermore, R., Hillenbrand, C.D., Meredith, M., Eagles, G., 2007. Drake Passage and Cenozoic climate: an open and shut case? Geochemistry, Geophysics, Geosystems 8 (1). Available from: https://doi.org/10.1029/2005GC001224.

Long, D.H., Stilwell, J.D., 2000. Fish remains from the Eocene of Mount Discovery, East Antarctic. In: Stilwell, J.D., Feldmann, R.M. (Eds.), Paleobiology and Palaeoenvironments of Eocene Rocks, McMurdo Sound, East Antarctica. Antarctic Research Series, vol. 76. American Geophysical Union, Washington, DC, pp. 349–354.

López-Quirós, A., Escutia, C., Sánchez-Navas, A., Nieto, F., García-Casco, A., Martín-Algarra, A., et al., 2019. Glaucony authigenesis, maturity and alteration in the Weddell Sea: An indicator of paleoenvironmental conditions before the onset of Antarctic glaciation. Scientific Reports 9 (1), 13580. Available from: https://doi.org/10.1038/s41598-019-50107-1.

Lunt, D.J., Bragg, F., Chan, W.-L., Hutchinson, D.K., Ladant, J.-B., Niezgodzki, I., et al., 2020. DeepMIP: YEAR Model intercomparison of early Eocene climatic optimum (EECO) large-scale climate features and comparison with proxy data. Climate of the Past Discussions. Available from: https://doi.org/10.5194/cp-2019-149.

Lunt, D.J., Dunkley Jones, T., Heinemann, M., Huber, M., LeGrande, A., Winguth, A., et al., 2012. A model− data comparison for a multi-model ensemble of early Eocene atmosphere−ocean simulations: EoMIP. Climate of the Past 8, 1717−1736. Available from: https://doi.org/10.5194/cp-8-1717-2012.

Marenssi, S.A., 2006. Eustatically controlled sedimentation recorded by Eocene strata of the James Ross Basin, Antarctica. Geological Society, London, Special Publications 258, 125−133. Available from: https://doi.org/10.1144/GSL.SP.2006.258.01.09.

Marenssi, S.A., Santillana, S., Rinaldi, C.A., 1998. Stratigraphy of the La Meseta Formation (Eocene), Marambio (Seymour) Island, Antarctica. In: Casadıio, S. (Ed.), Paleogeno de America del Sur y de la Penınsula Antartica, Publicacion Especial 5. Asociacion Paleontologica Argentina, Buenos Aires, pp. 137−146.

Matthews, R.K., Poore, R.Z., 1980. Tertiary delta^{18}O record and glacio-eustatic sea-level fluctuations. Geology 8 (10), 501−504. Available from: https://doi.org/10.1130/0091-7613(1980)8(501:TORAGS)2.0.CO.

McKay, R.M., et al., 2021. Cenozoic History of Antarctic Glaciation and Climate from onshore and offshore studies. In: Florindo, F., et al. (Eds.), Antarctic Climate Evolution, second edition, Elsevier.

McKinley, C.C., Thomas, D.J., Le Vay, L.J., Rolewicz, Z., 2019. Nd isotopic structure of the Pacific Ocean 40−10 Ma, and evidence for the reorganization of deep North Pacific Ocean circulation between 36 and 25 Ma. Earth and Planetary Science Letters 521, 139−149. Available from: https://doi.org/10.1016/j.epsl.2019.06.009.

Mikolajewicz, U., Maier-Reimer, E., Crowley, T.J., Kim, K.-Y., 1993. Effect of Drake and Panamanian gateways on the circulation of an ocean model. Paleoceanography 8 (4), 409−426.

Mildenhall, D.C., 1989. Terrestrial palynology. In: Barrett, P.J. (Ed.), Antarctic Cenozoic History from the CIROS-1 Drillhole, McMurdo Sound, vol. 245. New Zealand DSIR Bulletin, Wellington, pp. 119−127.

Miller, K.G., Browning, J.V., Aubry, M.-P., Wade, B.S., Katz, M.E., Kulpecz, A.A., et al., 2008. Eocene-Oligocene global climate and sea-level changes: St. Stephens Quarry, Alabama. Bulletin of the Geological Society of America 120 (1−2), 34−53. Available from: https://doi.org/10.1130/B26105.1.

Miller, K.G., Curry, W.B., 1982. Eocene to Oligocene benthic foraminiferal isotopic record in the Bay of Biscay. Nature 296 (5855), 347−350. Available from: https://doi.org/10.1038/296347a0.

Miller, K.G., Fairbanks, R.G., Mountain, G.S., 1987. Tertiary oxygen isotope synthesis, sea level history, and continental margin erosion. Paleoceanography 2 (1), 1−19. Available from: https://doi.org/10.1029/PA002i001p00001.

Miller, K.G., Wright, J.D., Fairbanks, R.G., 1991. Unlocking the ice house: Oligocene-Miocene oxygen isotopes, eustasy, and margin erosion. Journal of Geophysical Research 96 (B4), 6829−6848. Available from: https://doi.org/10.1029/90JB02015.

Mohr, B.A.R., 1990. Eocene and Oligocene sporomorphs and dinoflagellate cysts from Leg 113 Drill Sites, Weddell Sea, Antarctica. In: Stewart, N.J. (Ed.). Proceedings of the Ocean Drilling Program, Scientific Results, vol. 113, pp. 595−612.

Morrison, A.K., Hogg, A.M., 2012. On the relationship between Southern Ocean overturning and ACC transport. Journal of Physical Oceanography 43, 140−148. Available from: https://doi.org/10.1175/JPO-D-12-057.1.

Murphy, M.G., Kennett, J.P., 1986. Development of latitudinal thermal gradients during the Oligocene: oxygen-isotope evidence from the southwest Pacific. Initial reports DSDP, Leg 90, Noumea, New Caledonia to Wellington, New Zealand. Part 2, pp. 1347−1360.

Naish, T.R., Woolfe, K.J., Barrett, P.J., et al., 2001. Orbitally induced oscillations in the East Antarctic Ice Sheet at the Oligocene/Miocene boundary. Nature 413, 719–723.

Nawrocki, J., Pańczyk, M., Williams, I.S., 2011. Isotopic ages of selected magmatic rocks from King George Island (West Antarctica) controlled by magnetostratigraphy. Geological Quarterly 55 (4), 301–322.

Newsom, E.R., et al., 2016. Southern Ocean deep circulation and heat uptake in a high-resolution climate model. Journal of Climate 29 (7), 2597–2619.

Nong, G.T., Najjar, R.G., Seidov, D., Peterson, W., 2000. Simulation of ocean temperature change due to the opening of Drake Passage. Geophysical Research Letters 27, 2689–2692.

O'Brien, P.E., Cooper, A.K., Richter, C., et al., 2001. Proceedings of ODP, Init. Repts., 188 [CD-ROM]. Available from: Ocean Drilling Program, Texas A&M University, College Station, TX 77845-9547, United States.

Ohneiser, C., Florindo, F., Stocchi, P., Roberts, A.P., DeConto, R.M., Pollard, P., 2015. Antarctic glacio-eustatic contributions to late Miocene Mediterranean desiccation and reflooding. Nature Communications. Available from: https://doi.org/10.1038/ncomms9765.

Orsi, A.H., Whitworth III, T., Nowlin Jr., W.D., 1995. On the meridional extent and fronts of the Antarctic Circumpolar Current. Deep-Sea Research Part I 42 (5), 641–673. Available from: https://doi.org/10.1016/0967-0637(95)00021-W.

Pagani, M., Huber, M., Liu, Z., Bohaty, S.M., Henderiks, J., Sijp, W., et al., 2011. The role of carbon dioxide during the onset of Antarctic glaciation. Science (New York, N.Y.) 334 (6060), 1261–1264. Available from: https://doi.org/10.1126/science.1203909.

Pagani, M., Zachos, J.C., Freeman, K.H., Tipple, B., Bohaty, S., 2005. Marked decline in atmospheric carbon dioxide concentrations during the Paleogene. Science (New York, N.Y.) 309, 600–603.

Paleobiology and paleoenvironments of Eocene Rocks, McMurdo Sound, East Antarctica. In: Stilwell, J.D., Feldmann, R.M. (Eds.), Antarctic Research Series, vol. 76. American Geophysical Union, Washington, DC, p. 372.

Pälike, H., et al., 2012. A Cenozoic record of the equatorial Pacific carbonate compensation depth. Nature 488 (7413), 609–614. Available from: https://doi.org/10.1038/nature11360.

Passchier, S., Bohaty, S.M., Jiménez-Espejo, F., Pross, J., Röhl, U., Van De Flierdt, T., et al., 2013. Early eocene to middle miocene cooling and aridification of east Antarctica. Geochemistry, Geophysics, Geosystems 14 (5), 1399–1410. Available from: https://doi.org/10.1002/ggge.20106.

Passchier, S., Ciarletta, D.J., Miriagos, T.E., Bijl, P.K., Bohaty, S.M., 2016. An Antarctic stratigraphic record of stepwise ice growth through the Eocene-Oligocene transition. GSA Bulletin . Available from: https://doi.org/10.1130/B31482.1.

Passchier, S., Ciarletta, D.J., Miriagos, T.E., Bijl, P.K., Bohaty, S.M., 2017. An Antarctic stratigraphic record of stepwise ice growth through the Eocene-Oligocene transition. GSA Bulletin 129 (3–4), 318–330. Available from: https://doi.org/10.1130/B31482.1.

Paxman, G.J.G., Gasson, E.G.W., Jamieson, S.S.R., Bentley, M.J., Ferraccioli, F., 2021. Long-term increase in Antarctic Ice Sheet vulnerability driven by bed topography evolution. Geophysical Research Letters 47 (20), e2020GL090003. Available from: https://doi.org/10.1029/2020GL090003.

Paxman, G.J.G., Jamieson, S.S.R., Ferraccioli, F., Bentley, M.J., Ross, N., Armadillo, E., et al., 2018. Bedrock Erosion Surfaces Record Former East Antarctic Ice Sheet Extent. Geophysical Research Letters. Available from: https://doi.org/10.1029/2018GL077268.

Paxman, G.J.G., Jamieson, S.S.R., Hochmuth, K., Gohl, K., Bentley, M.J., Leitchenkov, G., et al., 2019. Reconstructions of Antarctic topography since the Eocene–Oligocene

boundary. Palaeogeography, Palaeoclimatology, Palaeoecology 535 (May), 109346. Available from: https://doi.org/10.1016/j.palaeo.2019.109346.

Pearson, P.N., Foster, G.L., Wade, B.S., 2009. Atmospheric carbon dioxide through the Eocene-Oligocene climate transition. Nature 461 (7267), 1110–1113. Available from: https://doi.org/10.1038/nature08447.

Pearson, P.N., McMillan, I.K., Wade, B.S., Jones, T.D., Coxall, H.K., Bown, P.R., Lear, C.H., 2008. Extinction and environmental change across the Eocene-Oligocene boundary in Tanzania. Geology 36 (2), 179–182. Available from: https://doi.org/10.1130/G24308A.1.

Pérez, L.F., Hernández-Molina, F.J., Lodolo, E., Bohoyo, F., Galindo-Zaldívar, J., Maldonado, A., 2019. Oceanographic and climatic consequences of the tectonic evolution of the southern scotia sea basins, Antarctica. Earth-Science Reviews 198. Available from: https://doi.org/10.1016/j.earscirev.2019.102922.

Persico, D., Fioroni, C., Villa, G., 2012. A refined calcareous nannofossil biostratigraphy for the middle Eocene-early Oligocene Southern Ocean ODP sites. Palaeogeography, Palaeoclimatology, Palaeoecology 335–336, 12–23. Available from: https://doi.org/10.1016/j.palaeo.2011.05.017.

Petersen, S.V., Schrag, D.P., 2015. Antarctic ice growth before and after the Eocene-Oligocene transition: new estimates from clumped isotope paleothermometry. Paleoceanography 30, 1305–1317. Available from: https://doi.org/10.1002/2014PA002769.

Pole, M., Hill, B., Harwood, D.M., 2000. In: Stilwell, J.D., Feldmann, R.M. (Eds.), Paleobiology and Paleoenvironments of Eocene Rocks, McMurdo Sound, East Antarctica. Antarctic Research Series, 76. American Geophysical Union, Washington, DC, pp. 243–251.

Poole, I., Cantrill, D.J., Utescher, T., 2005. A multi-proxy approach to determine Antarctic terrestrial palaeoclimate during the Late Cretaceous and Early Tertiary. Palaeogeography, Palaeoclimatology, Palaeoecology 222, 95–121.

Poole, I., Hunt, R., Cantrill, D., 2001. A fossil wood flora from King George Island: ecological implications for an Antarctic Eocene vegetation. Annals of Botany 88 (1), 33–54.

Poore, R.Z., Matthews, R.K., 1984. Oxygen isotope ranking of late Eocene and Oligocene planktonic foraminifers: implications for Oligocene sea-surface temperatures and global ice-volume. Marine Micropaleontology 9 (2), 111–134. Available from: https://doi.org/10.1016/0377-8398(84)90007-0.

Porebski, S.J., 1995. Facies architecture in a tectonically-controlled incised-valley estuary: La Meseta Formation (Eocene) of Seymour Island, Antarctic Peninsula. Studia Geologica Polonica 107, 7–97.

Pound, M.J., Salzmann, U., 2017. Heterogeneity in global vegetation and terrestrial climate change during the late Eocene to early Oligocene transition. Scientific Reports 7, 43386. Available from: https://doi.org/10.1038/srep43386.

Powell, R.D., Krissek, L.A., van der Meer, J.J.M., 2000. Preliminary depositional environmental analysis of CRP-2/2A, Victoria Land Basin, Antarctica: Palaeoglaciological and palaeoclimatic inferences. Terra Antartica 7, 313–322.

Powell, R., Naish, T.R., Fielding, C.R., Krissek, L.A., van der Meer, J.J.M., 2001. Depositional environments for strata cored in CRP-3 (Cape Roberts Project), Victoria Land Basin, Antarctica: Palaeoglaciological and palaeoclimatological inferences. Terra Antartica 8 (3), 207–216.

Prebble, J.G., Raine, J.I., Barrett, P.J., Hannah, M.J., 2006. Vegetation and climate from two Oligocene glacioeustatic sedimentary cycles (31 and 24 Ma) cored by the Cape Roberts Project, Victoria Land Basin, Antarctica. Palaeogeography, Palaeoclimatology, Palaeoecology 231, 41–57.

Prentice, M.L., Matthews, R.K., 1988. Cenozoic ice-volume history: development of a composite oxygen isotope record. Geology 16 (11), 963–966. Available from: https://doi.org/10.1130/0091-7613(1988)016(0963:CIVHDO)2.3.CO;2.

Pross, J., Contreras, L., Bijl, P.K., Greenwood, D.R., Bohaty, S.M., Schouten, S., et al., 2012. Persistent near-tropical warmth on the Antarctic continent during the early Eocene epoch. Nature 488, 73. Available from: https://doi.org/10.1038/nature11300.

Prothero, D.R., 1994. The late Eocene-Oligocene extinctions. Annual Review of Earth and Planetary Sciences 22, 145–165.

Raine, J.I., Askin, R.A., 2001. Terrestrial palynology of Cape Roberts Project Drillhole CRP-3, Victoria Land Basin, Antarctica. Terra Antartica 8 (4), 389–400.

Reguero, M.A., Marenssi, S.A., Santillana, S.N., 2002. Antarctic Peninsula and South America (Patagonia) Paleogene terrestrial environments: biotic and biogeographic relationships. Palaeogeography, Palaeoclimatology, Palaeobiology 179 (3–4), 189–210.

Reguero, M.A., Marenssi, S.A., Santillana, S.N., 2012. Weddellian marine/coastal vertebrates diversity from a basal horizon (Ypresian, Eocene) of the Cucullaea I Allomember, La Meseta formation, Seymour (Marambio) Island, Antarctica. Revista Peruana de Biología 19, 275–284.

Roberts, A.P., Wilson, G.S., Harwood, D.M., Verosub, K.L., 2003. Glaciation across the Oligocene–Miocene boundary in southern McMurdo Sound, Antarctica: new chronology from the CIROS-1 Drill-Hole. Palaeogeography, Palaeoclimatology, Palaeoecology 198 (1), 113–130.

Rose, K.C., Ferraccioli, F., Jamieson, S.S.R., Bell, R.E., Corr, H., Creyts, T.T., et al., 2013. Early East Antarctic Ice Sheet growth recorded in the landscape of the Gamburtsev Subglacial Mountains. Earth and Planetary Science Letters 375, 1–12. Available from: https://doi.org/10.1016/j.epsl.2013.03.05.

Rugenstein, M., Stocchi, P., von der Heydt, A., Dijkstra, H., Brinkhuis, H., 2014. Emplacement of Antarctic ice sheet mass affects circumpolar ocean flow. Global and Planetary Change . Available from: https://doi.org/10.1016/j.gloplacha.2014.03.011.

Sadler, P., 1988. Geometry and stratification of uppermost Cretaceous and Paleogene units on Seymour Island, Northern Antarctic Peninsula. In: Feldmann, R.M., Woodburne, M.O. (Eds.), Geology and Paleontology of Seymour Island, Antarctic Peninsula, vol. 169. Geological Society of America Memoir, pp. 303–320.

Sagnotti, L., Florindo, F., Verosub, K.L., Wilson, G.S., Roberts, A.P., 1998. Environmental magnetic record of Antarctic palaeoclimate from Eocene/Oligocene glaciomarine sediments, Victoria Land Basin. Geophysical Journal International 134, 653–662.

Salabarnada, A., Escutia, C., Röhl, U., Nelson, C.H., McKay, R., Jiménez-Espejo, F.J., et al., 2018. Paleoceanography and ice sheet variability offshore Wilkes Land, Antarctica – Part 1: Insights from late Oligocene astronomically paced contourite sedimentation. Climate of the Past 14, 991–1014. Available from: https://doi.org/10.5194/cp-14-991-2018.

Salamy, K.A., Zachos, J.C., 1999. Latest Eocene-early Oligocene climate change and Southern Ocean fertility: inferences from sediment accumulation and stable isotope data. Palaeogeography, Palaeoclimatology, Palaeoecology 145 (1–3), 61–77. Available from: https://doi.org/10.1016/S0031-0182(98)00093-5.

Sandroni, S., Talarico, F., 2001. Petrography and provenance of basement clasts and clast variability in CRP-3 drillcore (Victoria Land Basin, Antarctica). Terra Antarctica 8 (4), 449–467.

Sangiorgi, F., Bijl, P.K., Passchier, S., et al., 2018. Southern Ocean warming and Wilkes Land ice sheet retreat during the mid-Miocene. Nature Communications 9, 317. Available from: https://doi.org/10.1038/s41467-017-02609-7.

Sauermilch, I., Whittaker, J. M., Klocker, A., Munday, D. R., Hochmuth, K., LaCasce, J. H., Bijl, P., 2021. Gateway-driven weakening of ocean gyres leads to Southern Ocean cooling. Nature Communications, in press (manuscript number NCOMMS-20-23968B).

Savin, S.M., 1977. The history of the Earth's surface temperature during the past 100 million years. Annual Review of Earth and Planetary Sciences 5, 319–355.

Savin, S.M., Douglas, R.G., Stehli, F.G., 1975. Tertiary marine paleotemperatures. Bulletin of the Geological Society of America 86 (11), 1499–1510. Available from: https://doi.org/10.1130/0016-7606(1975)86(1499:TMP)2.0.CO;2.

Scher, H.D., Martin, E.E., 2006. Timing and climatic consequences of the opening of Drake Passage. Science (New York, N.Y.) 312, 428–430.

Scher, H.D., Martin, E.E., 2008. Oligocene deep water export from the north Atlantic and the development of the Antarctic circumpolar current examined with neodymium isotopes. Paleoceanography 23 (1). Available from: https://doi.org/10.1029/2006PA001400.

Scher, H.D., Bohaty, S.M., Smith, B.W., Munn, G.H., 2014. Isotopic interrogation of a suspected late Eocene glaciation. Paleoceanography 29 (6), 628–644. Available from: https://doi.org/10.1002/2014PA002648.

Scher, H.D., Bohaty, S.M., Zachos, J.C., Delaney, M.L., 2011. Two-stepping into the icehouse: East Antarctic weathering during progressive ice-sheet expansion at the Eocene-Oligocene transition. Geology 39 (4), 383–386. Available from: https://doi.org/10.1130/G31726.1.

Scher, H.D., Whittaker, J.M., Williams, S.E., Latimer, J.C., Kordesch, W.E.C., Delaney, M.L., 2015. Onset of Antarctic circumpolar current 30 million years ago as Tasmanian Gateway aligned with westerlies. Nature 523 (7562), 580.

Scotese, C.R., Wright, N., 2018. PALEOMAP Paleodigital Elevation Models (PaleoDEMS) for the Phanerozoic PALEOMAP Project. Available from: <https://www.earthbyte.org/paleo-dem-resource-scotese-and-wright-2018/>.

Shackleton, N., Kennett, J., 1976. Oxygen isotopic evidence for the development of the psychrosphere 38 Myr ago. Nature 260, 513–515. Available from: https://doi.org/10.1038/260513a0.

Shackleton, N.J., Backman, J., Zimmerman, H., Kent, D.V., Hall, M.A., Roberts, D.G., et al., 1984. Oxygen isotope calibration of the onset of ice-rafting and history of glaciation in the North Atlantic region. Nature 307 (5952), 620–623. Available from: https://doi.org/10.1038/307620a0.

Shackleton, N.J., Kennett, J.P., 1975. Paleotemperature history of the Cenozoic and the initiation of Antarctic glaciation: oxygen and carbon isotope analyses in DSDP sites 277, 279 and 281, Initial Reports Deep Sea Drilling Projects, vol. 29, 743.

Sheldon, N.D., Retallack, G.J., Tanaka, S., 2002. Geochemical climofunction from North American soils and application to paleosols across the Eocene-Oligocene boundary in Oregon. The Journal of Geology 110, 687–696.

Shen, Y., 1994. Subdivision and correlation of Cretaceous to Paleogene volcano-sedimentary sequence from Fildes Peninsula, King George Island, Antarctica. In: Shen, Y. (Ed.), Stratigraphy and Palaeontology of Fildes Peninsula, King George Island, Antarctica, State Antarctic Committee. Science Press, Beijing, pp. 1–36. Monograph 3.

Shipboard Scientific Party, 2001a. Leg 188 Summary: Prydz Bay-Co-Operation Sea, Antarctica. In: O'Brien, P. E., Cooper, A. K., Richter, C., et al. (Eds.), Proceedings of the Ocean Drilling Program, Initial Reports, vol. 188. Available from: <http://www-odp.tamu.edu/publications/188_IR/188TOC.HTM>.

Shipboard Scientific Party, 2001b. Leg summary. In: Exon, N.F., Kennett, J.P., Malone, M.J., et al. (Eds.), Proceedings of the Ocean Drilling Program, Initial Reports, vol. 189. Available from: <http://www-odp.tamu.edu/publications/189_IR/chap_01/chap_01.htm>.

Shipboard Scientific Party, 2001c. Site 1170. In: Exon, N.F., Kennett, J.P., Malone, M.J., et al. (Eds.), Proceedings of the Ocean Drilling Program, Initial Reports, vol. 189. Available from: <http://www-odp.tamu.edu/publications/189_IR/chap_05/chap_05.htm>.

Shipboard Scientific Party, 2001d. Site 1172. In: Exon, N.F., Kennett, J.P., Malone, M.J., et al. (Eds.), Proceedings of the Ocean Drilling Program, Initial Reports, vol. 189. Available from: <http://www-odp.tamu.edu/publications/189_IR/chap_06/chap_06.htm>.

Sijp, W.P., England, M.H., Huber, M., 2011. Effect of the deepening of the Tasman Gateway on the global ocean. Paleoceanography 26 (4), 1–18. Available from: https://doi.org/10.1029/2011PA002143.

Sloan, L.C., Rea, D.K., 1995. Atmospheric carbon dioxide and early Eocene climate: a general circulation modeling sensitivity study. Palaeogeography, Palaeoclimatology, Palaeoecology 119, 275–292.

Smellie, J.L., Pankhurst, R.J., Thomson, M.R.A., Davies, R.E.S., 1984. The Geology of the South Shetland Islands: VI. Stratigraphy, Geochemistry and Evolution. British Antarctic Survey, pp. 1–85, Scientific Report 87.

Spada, G., Stocchi, P., 2007. SELEN: a Fortran 90 program for solving the "sea level equation.". Computers & Geosciences 33. Available from: https://doi.org/10.1016/j.cageo.2006.08.006.

Spicer, R.A., Ahlberg, A., Herfort, A.B., Hofmann, C.-C., Raikevich, M., Valdes, P.J., et al., 2008. The Late Cretaceous continental interior of Siberia: A challenge for climate models. Earth and Planetary Science Letters 267, 228–235. Available from: https://doi.org/10.1016/j.epsl.2007.11.049.

Stickley, C.E., Brinkhuis, H., Schellenberg, S.A., Sluijs, A., Röhl, U., Fuller, M., et al., 2004. Timing and nature of the deepening of the Tasmanian Gateway. Paleoceanography 19 (4), PA4027. Available from: https://doi.org/10.1029/2004PA001022.

Stilwell, J., Zinsmeister, W., 1992. Molluscan systematics and biostratigraphy, lower tertiary La Meseta formation, Seymour Island, Antarctic Peninsula, Antarctic Research Series, vol. 55. American Geophysical Union, Washington, DC, p. 192.

Stocchi, P., Escutia, C., Houben, A.J.P., Vermeersen, B.L.A., Bijl, P.K., Brinkhuis, H., et al., 2013. Relative sea-level rise around East Antarctica during Oligocene glaciation. Nature Geoscience 6, 380. Available from: https://doi.org/10.1038/ngeo1783.

Strand, K., Passchier, S., Näsi, J., 2003. Implications of quartz grain microtextures for onset Eocene/Oligocene glaciation in Prydz Bay, ODP Site 1166, Antarctica. Palaeogeography, Palaeoclimatology, Palaeoecology 198 (1–2), 101–111.

Strother, S.L., Salzmann, U., Sangiorgi, F., Bijl, P.K., Pross, J., Escutia, C., et al., 2017. A new quatitative approach to identify reworking in Eocene to Miocene pollen records from offshore Antarctica using red fluorescence and digital imaging. Biogeosciences 14 (8), 2089–2100. Available from: https://doi.org/10.5194/bg-14-2089-2017.

Tambussi, C.P., Acosta Hospitaleche, C.I., Reguero, M.A., Marenssi, S.A., 2006. Late Eocene penguins from West Antarctica; systematics and biostratigraphy. In: Francis, J.E., Pirrie, D., Crame, J.A. (Eds.), Cretaceous-Tertiary High-Latitude Palaeoenvironments; James Ross Basin, Antarctica, 258. Geological Society Special Publications, pp. 145–161.

Tauxe, L., Stickley, C.E., Sugisaki, S., Bijl, P.K., Bohaty, S.M., Brinkhuis, H., et al., 2012. Chronostratigraphic framework for the IODP expedition 318 cores from the Wilkes Land margin: constraints for paleoceanographic reconstruction. Paleoceanography 27, PA2214. Available from: https://doi.org/10.1029/2012PA002308.

Tochilin, C.J., Reiners, P.W., Thomson, S.N., Gehrels, G.E., Hemming, S.R., Pierce, E.L., 2012. Erosional history of the Prydz Bay sector of East Antarctica from detrital apatite and zircon geo- and thermochronology multidating. Geochemistry, Geophysics, Geosystems 13 (11), Q1101.

Toggweiler, J.R., Bjornsson, H., 2000. Drake Passage and paleoclimate. Journal of Quaternary Science 15, 319–328. Available from: https://doi.org/10.1029/2012GC004364.

Torres, T., Marenssi, S.A., Santillana, S., 1994. Maderas Fósiles de la isla Seymour, Formación La Meseta, Antártica. Serie Científica del INACH, Santiago de Chile 44, 17–38.

Troedson, A., Smellie, J., 2002. The Polonez Cove formation of King George Island, Antarctica: stratigraphy, facies and implications for mid-Cenozoic cryosphere development. Sedimentology 49, 277–301.

Truswell, E.M., 1997. Palynomorph assemblages from marine Eocene sediments on the West Tasmanian continental margin and the South Tasman rise. Australian Journal of Earth Sciences 4, 633–654.

Vandenberghe, N., Hilgen, F.J., Speijer, R.P., Ogg, J.G., Gradstein, F.M., Hammer, O., et al., 2012. The Paleogene period. In: Gradstein, F.M., Ogg, J.G., Schmitz, M.D., Ogg, G.M., (Eds.), The Geological Time Scale 2012, Amsterdam, Netherlands, Elsevier, pp. 855–921.

Van Hinsbergen, D.J.J., De Groot, L.V., Van Schaik, S.J., Spakman, W., Bijl, P.K., Sluijs, A., et al., 2015. A paleolatitude calculator for paleoclimate studies. PLoS One 10 (6). Available from: https://doi.org/10.1371/journal.pone.0126946.

Viebahn, J.P., von der Heydt, Le Bars, D., Dijkstra, H.A., 2016. Effects of Drake Passage on a strongly eddying global ocean. Paleoceanography 31 (5), 564–581. Available from: https://doi.org/10.1002/2015PA002888.

Villa, G., Fioroni, C., Persico, D., Roberts, A.P., Florindo, F., 2013. Middle Eocene to late Oligocene Antarctic glaciation/deglaciation and Southern Ocean productivity. Paleoceanography 29, 223–237. Available from: https://doi.org/10.1002/2013PA002518.

Warny, S., Kymes, C.M., Askin, R., Krajewski, K.P., Tatur, A., 2018. Terrestrial and marine floral response to latest Eocene and Oligocene events on the Antarctic Peninsula. Palynology 43 (1), 4–21. Available from: https://doi.org/10.1080/01916122.2017.1418444.

Wei, W., Thierstein, H.R., 1991. Upper Cretaceous and Cenozoic calcareous nannofossils of the Kerguelen Plateau (southern Indian Ocean) and Prydz Bay (East Antarctica). In: Proceedings of the ODP, Scientific Results, J. Barron et al., (Eds.) (Ocean Drilling Program, College Station, TX, 1991), vol. 119, pp. 467–493.

Westerhold, T., Marwan, N., Drury, A.J., Liebrand, D., Agnini, C., Anagnostou, E., et al., 2020. An astronomically dated record of earth's climate and its predictability over the last 66 million years. Science (New York, N.Y.) 369 (6509), 1383–1387. Available from: https://doi.org/10.1126/science.aba6853.

Whitehead, J.M., Quilty, P.G., McKelvey, B.C., O'Brien, P.E., 2006. A review of the Cenozoic stratigraphy and glacial history of the Lambert Graben – Prydz Bay Region, East Antarctica. Antarctic Science 18, 83–99.

Whitehouse, P.L., Gomez, N., King, M.A., Wiens, D.A., 2019. Solid Earth change and the evolution of the Antarctic Ice Sheet. Nature Communications 10 (1), 503. Available from: https://doi.org/10.1038/s41467-018-08068-y.

Wilch, T.I., McIntosh, W.C., 2000. Eocene and Oligocene volcanism at Mount Petras, Marie Byrd land: implications for middle Cenozoic ice sheet reconstructions in West Antarctica. Antarctic Science 12, 477–491.

Williams, S.E., Whittaker, J.M., Halpin, J.A., Müller, R.D., 2019. Australian-antarctic breakup and seafloor spreading: balancing geological and geophysical constraints. Earth-Science Reviews 188, 41–58. Available from: https://doi.org/10.1016/j.earscirev.2018.10.011.

Willis, P.M.A., Stilwell, J.D., 2000. A possible piscivorous crocodile from Eocene deposits of McMurdo Sound, Antarctic. In: Stilwell, J.D., Feldmann, R.M. (Eds.), Paleobiology and

Palaeoenvironments of Eocene Rocks, McMurdo Sound, East Antarctica. Antarctic Research Series, vol. 76. American Geophysical Union, Washington, DC, pp. 355–358.

Wilson, D.S., Jamieson, S.S., Barrett, P.J., Leitchenkov, G., Gohl, K., Larter, R.D., 2012. Antarctic topography at the Eocene-Oligocene boundary. Palaeogeography, Palaeoclimatology, Palaeoecology 335–336, 24–34. Available from: https://doi.org/10.1016/j.palaeo.2011.05.028.

Wilson, D.S., Luyendyk, B.P., 2009. West antarctic paleotopography estimated at the Eocene-Oligocene climate transition. Geophysical Research Letters 36, L16302. Available from: https://doi.org/10.1029/2009GL039297.

Wilson, D.S., Pollard, D., Deconto, R.M., Jamieson, S.S.R., Luyendyk, B.P., 2013. Initiation of the West Antarctic Ice Sheet and estimates of total Antarctic ice volume in the earliest Oligocene. Geophysical Research Letters 40 (16), 4305–4309. Available from: https://doi.org/10.1002/grl.50797.

Wilson, G.S., 2000. Glacial geology and origin of fossiliferous-erratic-bearing moraines, southern McMurdo Sound, Antarctica – an alternative ice sheet hypothesis. In: Stilwell, J.D., Feldmann, R.M. (Eds.), Paleobiology and Paleoenvironments of Eocene Rocks, McMurdo Sound, East Antarctica. Antarctic Research Series, vol. 76. American Geophysical Union, Washington, DC, pp. 19–37.

Wilson, G.S., Naish, T.R., Aitken, A.R.A., Johnston, L.J., Damaske, D., Timms, C.J., et al., 2006. Basin development beneath the southern McMurdo Sound ice shelf (SMIS) – combined geophysical and glacial geological evidence for a potential Paleogene drilling target for ANDRILL. In: Open Science Conference, XXIX SCAR/COMNAP XVII, Hobart, Australia, Abstract.

Wilson, G.S., Roberts, A.P., Verosub, K.L., Florindo, F., Sagnotti, L., 1998. Magnetobiostratigraphic chronology of the Eocene–Oligocene transition in the CIROS-1 core, Victoria Land Margin, Antarctica: implications for Antarctic glacial history. Geological Society of America Bulletin 110, 35–47.

Wilson, T.J., 1999. Cenozoic structural segmentation of the Transantarctic Mountains rift flank in southern Victoria Land, Antarctica. In: Van der Wateren, F.M., Cloetingh, S. (Eds.), Lithosphere dynamics and environmental change of the Cenozoic West Antarctic rift system Global and Planetary Change 23, 105–127.

Yang, S., Galbraith, E., Palter, J., 2014. Coupled climate impacts of the Drake Passage and the Panama Seaway. Climate Dynamics 43, 37–52. Available from: https://doi.org/10.1007/s00382-013-1809-6.

Zachos, J., Pagani, M., Sloan, L., Thomas, E., Billups, K., 2001. Trends, rhythms, and aberrations in global climate 65 Ma to present. Science (New York, N.Y.) 292, 686–693.

Zachos, J.C., Breza, J.R., Wise, S.W., 1992. Early Oligocene ice-sheet expansion on Antarctica – stable isotope and sedimentological evidence from Kerguelen Plateau, Southern Indian Ocean. Geology 20, 569–573.

Zachos, J.C., Quinn, T.M., Salamy, K.A., 1996. High-resolution (104 years) deep-sea foraminiferal stable isotope records of the Eocene–Oligocene climate transition. Paleoceanography 11, 251–266.

Zachos, J.C., Stott, L.D., Lohmann, K.C., 1994. Evolution of early Cenozoic marine temperatures. Paleoceanography 9 (2), 353–387. Available from: https://doi.org/10.1029/93PA03266.

Zastawniak, E., Wrona, R., Gazdzicki, A.J., Birkenmajer, K., 1985. Plant remains from the top part of the Point Hennequin Group (Upper Oligocene), King George Island (South Shetland Islands, Antarctica). Studia Geologica Polonica 81, 143–164.

Zhang, Y.G., Pagani, M., Liu, Z., Bohaty, S.M., DeConto, R., 2013. A 40-million-year history of atmospheric CO2. Phil Trans R Soc A 371, 20130096. Available from: https://doi.org/10.1098/rsta.2013.0096.